

POLITECNICO DI TORINO

MASTER OF SCIENCE IN CIVIL ENGINEERING



Master's Thesis

**EVALUATION OF
THE AGEING EFFECTS ON
THE PERFORMANCE OF
NON-BITUMINOUS BINDER
FOR PAVING APPLICATIONS**

Candidate:
FEDERICA LA ROCCA

Supervisors:
Prof. EZIO SANTAGATA
Prof. DAVIDE DALMAZZO
Prof.ssa LUCIA TSANTILIS

ACADEMIC YEAR 2017-2018

To my family,
Mum, Dad, Fra and Paco,
for their endless love, support and patience.

ACKNOWLEDGEMENT

I would like to express my sincere gratitude to my professor, Ezio Santagata, who gave me the possibility to deepen such interesting topics and to live an extraordinary life experience.

I would also like to extend my heartfelt gratitude to Davide Dalmazzo and Lucia Tsantilis for offering their time and input in completing this thesis, despite the distance. Their opinions and contributions are gratefully appreciated.

A sincere thank you to my supervisors at the University of Nottingham, Davide Lo Presti and Ana Jimenez Del Barco Carrion, whose suggestions on both academic and professional side have been truly inspiring.

In addition, I want to give my special thanks to Juan and Lawrence and to everyone from Nottingham Transportation Engineering Centre of the University of Nottingham, from PhD students to the technicians, who helped me to accomplish this goal. Some of them by answering my questions or teaching me various aspects of binder testing; some others simply by making the work environment nice and friendly.

I would like to thank my childhood friends, my housemates and all my loved ones, to have been making these years easier and happier.

Thousands thanks to Martina and Gabriele for adopting me in their beautiful family. Endless thanks to Giuliana for her encouraging smiles, Giuseppe for his amazing personality, Federica for her sweetness and Martina for her jokes. Thanks to Sandra for her energy and colours and thank all my colleagues I met in Turin.

My gratitude goes to my uncle Tommaso and family for teaching me to always look beyond and to be ambitious.

Finally, my sincere gratitude goes to my real family and to the man with I'd like to build a new one: Pier Paolo. He has been a lighthouse in my decisions and he has always supported my choices, even with sacrifices. Thank you.

ABSTRACT

Sustainability has been the new global purpose from the last decades due to environmental concerns about the use of non-recoverable natural resources. The interest in using bio-materials in constructions and, in particular, in pavement engineering has grown significantly, heading us to concentrate on finding recoverable materials with the highest performances.

Roads are mainly composed of asphalt mixture, a combination of aggregates and bitumen, generally petroleum-based. Nowadays the tendency is to abandon these petrochemical products in a favour of environmental friendly materials, called BioBinders.

In this thesis, two different binders were studied and compared: a non-modified, neat and petroleum-based binder, defined as a target, and a bio-materials recently introduced in the market: BioPhalt®. The last is a non-bituminous binder, produced from pine derivatives and by-products of the papermaking industry.

As the common binders, these biomaterials are subjected to ageing: change in mechanical, physical and chemical properties with time due to traffic loads, environmental conditions (e. g. temperature) and UV radiation. The bitumen hardens and loses the initial viscoelastic properties, consequently the road become stiffer and more prone to deterioration: small cracks evolve in large cracks and potholes and other distresses start to form on the pavement. These effects undermine the lifetime of the infrastructure and the safety of the users.

Indeed, more investigation on this field are needed in order to govern this unpleasant effect of oxidation, polymerization and volatilization of bitumen.

This thesis presents the results from a laboratory study on the effects of aging on the properties of the two binders. Performance parameters and chemical characteristics were studied under several ageing conditions: neat, short term ageing and long-term ageing.

Both binders were aged artificially and then tested according different procedures that simulate performance characteristics (rutting, fatigue and cracking at low

temperature) and chemical ones. All the tests have been performed on both standard and bio bitumen to make the comparison between the two possible. All the collected data were analysed and compared, using the standard bitumen as guideline: in these ways it has been possible to clearly understand the differences between the two materials and to highlight the advantages and drawbacks of BioPhalt®.

It has been already proved that BioPhalt® has:

- greater rutting resistance than the target bitumen, but only for short term ageing, while for long term the situation is totally the opposite;
- excellent resistance to low temperature cracking and fatigue, since the material has greater viscous component;
- a strong inclination to oxidation.

This laboratory investigation states that aged BioPhalt® is a promising alternative to standard bitumen and, with further studies, it will be possible to replace the petroleum-based material with this renewable resource.

LIST OF CONTENTS

ACKNOWLEDGEMENT	V
ABSTRACT	VII
LIST OF CONTENTS	IX
LIST OF FIGURES	XI
LIST OF TABLES	XV
CHAPTER I INTRODUCTION	1
I.1 Background.....	1
I.2 Research Objectives	2
I.3 Thesis Outline.....	4
CHAPTER II LITERATURE REVIEW	7
II.1 Bitumen and Biomaterials.....	7
II.1.1 Petroleum- based bitumen	7
II.1.2 Biomaterials.....	10
II.2 Chemical Structure of bitumen	11
II.2.1 SARA test.....	14
II.2.2 FTIR test.....	17
II.3 Ageing.....	20
II.3.1 Short-term ageing	22
II.3.2 Long-term ageing	23
II.4 Rheology	23
II.5 Performance properties	28
II.5.1 Permanent deformation	28
II.5.2 Fatigue cracking	30
II.5.3 Low Temperature cracking.....	33
CHAPTER III MATERIALS AND METHODS.....	35
III.1 Materials	35
III.2 Ageing.....	37

III.3 Test Machines	42
III.3.1 Dynamic Shear Rheometer	42
III.3.2 Fourier Transform Infrared	46
III.3.3 SARA analysis	49
III.4 Rheology	53
III.4.1 Frequency Sweep	55
III.5 Performance	58
III.5.1 Rutting	58
III.5.2 Fatigue	60
III.5.3 Low Temperature Cracking	61
CHAPTER IV EVALUATION OF THE EFFECT OF AGEING	69
IV.1 Rheological parameters	70
IV.2 Performance related parameters	75
IV.2.1 Permanent Deformation	76
IV.2.2 Fatigue Cracking	84
IV.2.3 Low Temperature Cracking	88
IV.3 Chemical Properties	95
IV.3.1 SARA analysis	96
IV.3.2 FTIR Spectroscopy	101
CHAPTER V CONCLUSION AND RECOMMENDATIONS	111
V.1 Rheological Findings	111
V.2 Performance-related findings	112
V.3 Chemical findings	113
V.4 Summary of findings and recommendations	114
V.5 Future Works	115
REFERENCES	117

LIST OF FIGURES

Figure I-1. Research Objectives.....	2
Figure I-2. Experimental Programme	5
Figure II-1. General scheme for bitumen production	8
Figure II-2. Bitumen Uses.....	9
Figure II-3. Colloidal system of bitumen.....	12
Figure II-4. Typologies of colloidal structures of bitumen.....	16
Figure II-5. Example of FTIR-ATR Spectrum	18
Figure II-6. Viscoelastic Behaviour.....	24
Figure II-7. Sinusoidal wave forms for stress and strain functions	25
Figure II-8. Example of Mater Curve	26
Figure II-9. Black Diagram.....	26
Figure II-10. Rutting	28
Figure II-11. Fatigue Cracking.....	31
Figure II-12. Loading scheme of Amplitude Sweep for LAS test	32
Figure III-1. BioPhalt®.....	35
Figure III-2. Qualitative comparison between binders	36
Figure III-3. Top views BioPhalt®	36
Figure III-4. Top view 50/70 pen bitumen.....	37
Figure III-5. Example of RTFO test oven.....	38
Figure III-6. Oven and control binder in the cooling rank.....	39
Figure III-7. BioPhalt® in the cooling rank.....	39
Figure III-8. Example of PAV test machine	41
Figure III-9. Parallel Plate for DSR	43
Figure III-10. Rheometers.....	44
Figure III-11. Typologies of conditioning	45
Figure III-12. FTIR machine.....	46
Figure III-13. Details of FTIR machine	47
Figure III-14. Example of FTIR Spectrum	48

Figure III-15. Iatrosan	50
Figure III-16. Tools for SARA analysis.....	50
Figure III-17. Solvent container.....	51
Figure III-18. Plate and injector.....	52
Figure III-19. Example of AS plot.....	54
Figure III-20. Example of master curve.....	56
Figure III-21. Performance related test	58
Figure III-22. Example of MSCR's results.....	59
Figure III-23. Example of strains.....	60
Figure III-24. Bending Beam Rheometer	62
Figure III-25. Mould for beam specimen.....	64
Figure III-26. Specimens at room temperature	65
Figure III-27. Trimming.....	65
Figure III-28. BBR Specimen	66
Figure IV-1. Complex Modulus of C.....	71
Figure IV-2. Phase Angle of C.....	71
Figure IV-3. Complex Modulus of BP	72
Figure IV-4. Phase Angle of BP	73
Figure IV-5. Comparison of G^*	74
Figure IV-6. Black Diagram	75
Figure IV-7. Jnr of C.....	77
Figure IV-8. %R of C.....	78
Figure IV-9. Jnr of BP	79
Figure IV-10. %R of BP	80
Figure IV-11. Comparison of Jnr.....	81
Figure IV-12. Comparison of %R.....	82
Figure IV-13. Ageing Index of Jnr for C and BP	83
Figure IV-14. Ageing Index of %R of C and BP.....	83
Figure IV-15. Nf/ESALs for C	85
Figure IV-16. $G^*\sin\delta$ versus Damage Intensity of C.....	86
Figure IV-17. Nf/ESALs for BP	87
Figure IV-18. $G^*\sin\delta$ versus Damage Intensity of BP	87

Figure IV-19. Comparison of Traffic Volume indicator	88
Figure IV-20. Flexural Creep Stiffness.....	90
Figure IV-21. Ageing Index of Stiffness at -12°C	91
Figure IV-22. Ageing Index of Stiffness at -18°C.....	92
Figure IV-23. Ageing Index of Stiffness at -24°C	92
Figure IV-24. Critical Temperature for S	94
Figure IV-25. Critical Temperature for m-value	95
Figure IV-26. Example of SARA's results for standard bitumen	96
Figure IV-27. SARA analysis of 50/70 bitumen.....	97
Figure IV-28. Example of BioPhalt analysis.	98
Figure IV-29. SARA analysis of BioPhalt®.....	99
Figure IV-30. Comparison of SARA analysis	100
Figure IV-31. Spectrum of Control Binder at all ageing states	102
Figure IV-32. Spectrum of BioPhalt at all ageing states.....	103
Figure IV-33. Comparison of Ageing Index for sulphoxide group	105
Figure IV-34. Comparison of Ageing Index of Carbonyl group	106
Figure IV-35 Comparison of AI for Aliphatics	108
Figure IV-36. Comparison of AI for Aromatics	108

LIST OF TABLES

Table 1	42
Table 2. Amplitude Sweep Results	55
Table 3. Comparison of Rheological Index R	74
Table 4. Comparison of m-values	93
Table 5. Colloidal Index for C	98
Table 6. Colloidal Index of BP	99
Table 7. Comparison of Colloidal Index.....	100
Table 8. Ageing Index for SARA analysis	101
Table 9. FTIR indexes for C	104
Table 10. FTIR indexes for BP	104
Table 11. Aliphatics and Aromatics Index for C	107
Table 12. Aliphatics and Aromatics Index for BP	107

Chapter I

INTRODUCTION

I.1 Background

Bitumen is defined in the *Oxford English Reference Dictionary* as “a tarlike mixture of hydrocarbons derived from petroleum naturally or by distillation, and used for road surfacing and roofing”, and furthermore applications. Bitumen is mainly used in the production of asphalt, where it serves as an adhesive binding the aggregates and other materials together. The principal way of producing bitumen is through the refining of crude oil, extracted all over the Earth but mainly in United States, in the Middle East, Russia and in the countries around the Caribbean¹.

In the last centuries, the petroleum’s demand has been raising constantly but, on the other hand, resources of crude oil are limited and they are becoming poorer. If the market continues demanding with this rhythm, in very few years, petroleum won’t be enough to satisfy all the requests. For this reason, companies are moving to renewable resources, like natural or obtained from industries’ waste, in order to satisfy their needs without renouncing to environmental-friendly economic growth: this is the sustainable development.

Researchers has been studying new alternatives to tar, not only in terms of manufacturing, but also in terms of properties.

BioPhalt[®] is one of the first attempt of non-bituminous binder and it was certified as a promising bio-material for road surfacing. It was already used in bikeways, as rejuvenator for Reclaimed Asphalt (RA) and in paved roads, but the ones that are affected only by light traffic. Unfortunately, the utilisation of this material is still limited and further evaluations are needed. In fact, asphalt

¹ The Shell Bitumen Handbook, Great Britain, The University Press of Cambridge, 2003.

mixtures are subjected to ageing and the bitumen hardens and loses the initial viscoelastic properties: this is revealed by an increase of stiffness and elasticity and a lack of ductility.

The ageing effect is non-negligible and requires a deep investigation on the artificially-aged binders' behaviour in order to govern this unpleasant effect of oxidation, polymerization and volatilization of bitumen.

As shown later, this thesis presents an evaluation of the ageing effect on this renewable binder.

I.2 Research Objectives

The purpose of this project is to carefully study, characterise and analyse BioPhalt®'s behaviour under short and long-term ageing conditions, as shown in Figure I-1. All the data has been compared to 50/70 bitumen's one, in the same ageing conditions.

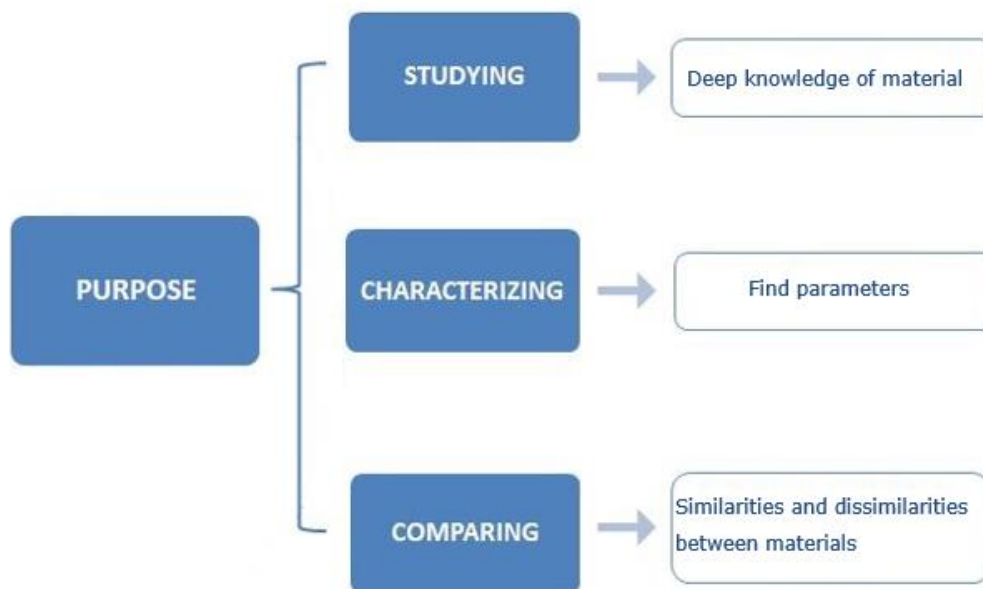


Figure I-1. Research Objectives

The investigation was structured as follow.

During the preliminary phase, a very deep knowledge on binders and bio-materials has been required, in order to understand which procedure should have been followed to have the best results, in terms of setting of tests machines and typologies of required data. In addition, it was being looked for the best parameter to represent the data. After that, all the tests were performed and data analysed and compared, plotting everything in graphs for a clear overview.

Data have been represented by parameters that concern three different aspects:

- Rheological;
- Performance-related;
- And chemical characteristics.

In particular, for the *rheological area*, a model capable to fit the master curve was adopted (CAM- WLF model) and it gave parameters as Complex Modulus G^* and Phase Angle δ .

For the *Performance-related*, three different sections were studied, that are resistance of materials to:

- Rutting: simulate the bitumen's behaviour at high temperature;
- Fatigue: representative of bitumen's behaviour at air temperature and repetitively loaded;
- Cracking at low temperature.

Chemical characteristics has been studied with two different

According to this procedure, the BioPhalt[®] will be characterize well-around.

I.3 Thesis Outline

This thesis is structured into five main sections with the following content:

- *Chapter I: Introduction* – This chapter includes a background on biomaterials for road's bitumen and on ageing. The background is followed by the problem statement and research objectives.
- *Chapter II: Literature Review* – This chapter is divided into five sections. The first section presents a literature review of biomaterials for paving applications. The second presents the chemical characteristics of these complex materials. The others present all the test that are needed to characterise binders and, respectively: the third part discusses the causes and effects of ageing of bitumens, the fourth is dedicated to rheological behaviour of binder and the last is related to performance properties, divided in other three sub-sections. For each of these sections, limitations and challenges of the tests are highlighted.
- *Chapter III: Materials and Methods* – This chapter reports a detailed description of the experimental programme. First of all, binders were aged, using the Rotational Thin Film Oven (RTFO) and the Pressure Ageing Vessel (PAV). The first test represents the ageing that happens during the mixing and compaction of asphalt mixture samples, whereas the second simulates the bitumen after several years from his implementation. To have a complete characterisation of these materials under several points of view, lots of tests were performed: rheological, performance-based and chemical. Dynamic Shear Rheometer (DSR) and Bending Beam Rheometer (BBR) were used to describe the first two, whereas for the chemical classification Fourier Transform Infrared Spectrometer (FTIR) and Iatrosan were chosen. Test methods such as Amplitude Sweep and Frequency Sweep will be used to characterise the rheological properties of the binders by observing Complex Modulus G^* and Phase Angle δ .

Binders' performances are related to three main pavement's distresses: rutting, fatigue and cracking at low temperature. Respectively, the tests and parameters that allow us to analyse these issues are: Multiple Stress Creep Recovery (MSCR) by calculating non-recoverable creep compliance J_{nr} and Percentage of recovery %R; Linear Amplitude Sweep by computing number of cycles to failure N_f ; Bending Beam Rheometer by observing the normal stiffness S_{60} and creep ratio m_{60} . For the chemical analysis, Fourier Transform Infrared and SARA analysis were performed, computing how much chemical bound indexes change with ageing. [Figure I-2]

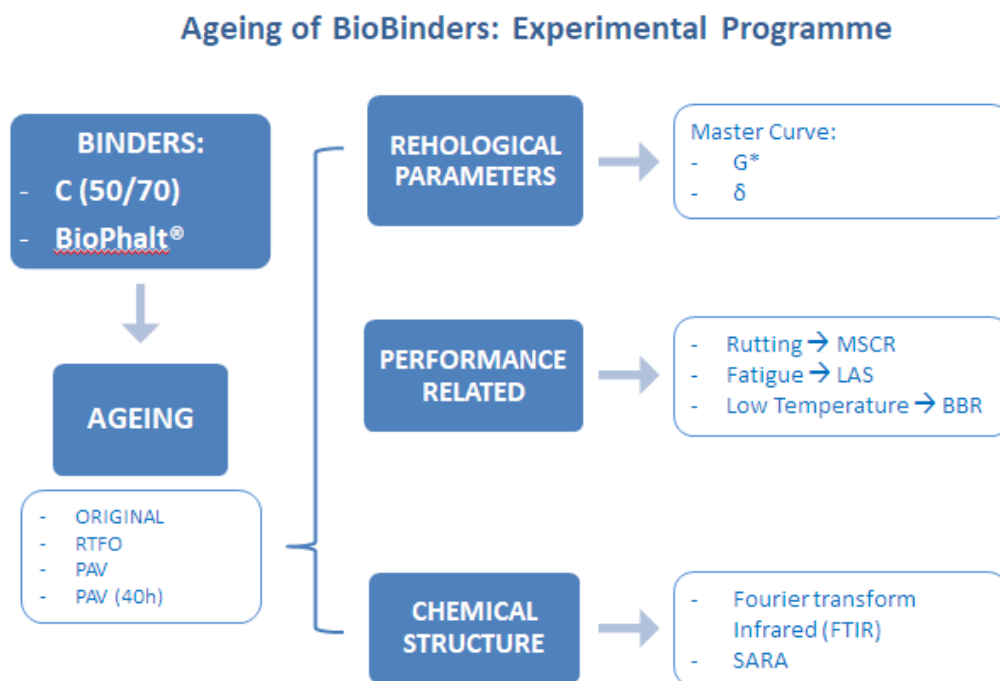


Figure I-2. Experimental Programme

- *Chapter IV: Evaluation of the effects of ageing* – This chapter presents a widespread assessment of the effect of ageing on a standard bitumen 50/70 and on BioPhalt®. The obtained results are plotted in several graphs that allow to individuate changes in trend of the curves due to ageing effect. As a support of the curves, Ageing

Indexes were introduced: they are able to represent how much a certain parameter changes with ageing and to draw a development. They were computed for every and each area (rheological, performance-related and chemical) in order to clearly distinguish the effect of time for each aspect of the bitumen. Thanks to this way of proceeding, a well-rounded evaluation for each binder will come up and an easy comparison between materials will be possible. This chapter will explain advantages and drawbacks of BioPhalt® as a binder for paving applications.

- *Chapter V: Conclusions and Recommendations* – Conclusions gathered from the most relevant testing results and recommendations based on these conclusions are offered in this section. Direction for future work is also provided in this section.

Chapter II

LITERATURE REVIEW

This chapter includes five sections to cover the topic of effect of ageing on biomaterials. These sections are as follows: definition of bitumen and biomaterials, causes and effects of ageing, background of rheology, test binder characterization for rutting, fatigue and low temperature cracking, background of chemical structure of binder. Limits and challenges of tests are also provided.

II.1 Bitumen and Biomaterials

II.1.1 *Petroleum- based bitumen*

Bitumen is an organic by-product of the refining of crude oil. It is generally agreed that crude oil originates from the accumulation over millions of years of the remains of marine organisms and vegetable matter deposited with mud and fragments of rock on the ocean bed. Due to the substantial weight of the upper layers of sediment and to the application of heat from within the Earth's crust, the organisms and vegetable matter convert into the hydrocarbons, that is the crude oil.² Once in the refinery, the crude is subjected to fractional distillation process at atmospheric pressure and high temperature, in which the volatiles will be collected by condensers, each at a slightly different temperature. The portion of the crude oil that doesn't volatilize is called "long crude" and is further refined in a vacuum distillation column. The remains from this second

² The Shell Bitumen Handbook, Great Britain, The University Press of Cambridge, 2003.

process is known as “short crude” and this is the base from which is possible to manufacture the bitumen. The whole process is shown in Figure II-1. A wide variety of process may be employed in order to produce bitumen that meets the requirements of the PG asphalt binders.³

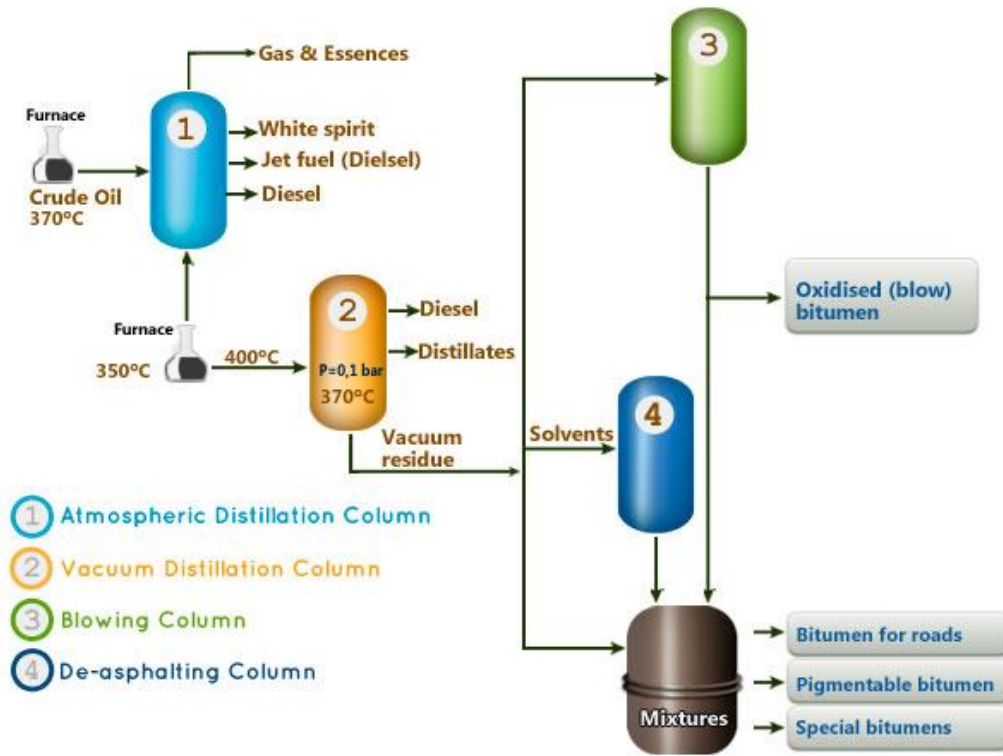


Figure II-1. General scheme for bitumen production

The global economic growth of the twentieth century and the copious availability of crude oil laid the basis for bitumen to be used in a wide range of modern applications beyond paving and roofing, as waterproofing in agriculture and buildings, hydraulic and erosion controller, paints, automotive and electrical. In that century, demand increased rapidly, reaching a peak of 2.4 million tonnes in 1973 only in the UK.⁴ Despite thousands typologies of applications, the most

³ Asphalt Binder Testing, Technician’s manual for Specification testing of Asphalht binders, USA, 2007

⁴ The Shell Bitumen Handbook, Great Britain, The University Press of Cambridge, 2003.

notably uses all over the world have always been for roofing and road surfaces, which accounts for approximately 85% of all bitumen use [Figure II-2].

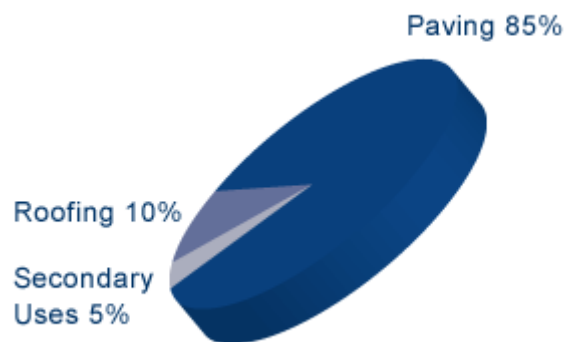


Figure II-2. Bitumen Uses

A confirmation of what just said comes from the United States, in which more than 90% of the pavements are made of asphalt and more than 550 million tons of asphalt mixtures are produced to satisfy the construction needs of the industry.⁵

The demanding growth of asphalt consumption for application in roadway is principally driven by construction of asphalt pavement and pavement maintenance and repair. The recent development of new technology in the refinery has degraded the quantity of asphalt, and thus resulted in an increased price of asphalt material⁶. In addition, asphalt binder production consumes great energy and releases greenhouse gases considering fuel energy used in manufacture, transportation, and application processes.⁷ Therefore, the rising cost of asphalt binder and the environmental concern encourage the use of alternative binders to replace petroleum-based asphalt binder or performance modifier to enhance the quality of asphalt binder.⁸

⁵ Xu Yang; Zhanping You et al., Asphalt Binders Blended with a High Percentage of Biobinders: Aging Mechanism Using FTIR and Rheology, in *J. Mater. Civ. Eng.*, 2015, 27(4)

⁶ J.Q. Zhu, B. Birgisson, N. Kringos, Polymer modification of bitumen: advances and challenges, *Eur. Polym. J.* 54 (2014) 18–38.

⁷ L.P. Thives, E. Ghisi, Asphalt mixtures emission and energy consumption: a review, *Renewable Sustainable Energy Rev.* 72 (2017) 473–484.

⁸ G. Xu, H. Wang et al., Rheological properties and anti-aging performance of asphalt binder modified with wood lignin, in *Construction and Building Materials* 151 (2017) 801–808

II.1.2 Biomaterials

In the last decades, copious researches have been conducted to develop alternative binder materials from sustainable resources, like biomass. In the literature, a great number of examples are provided. Shell Oil Company has produced a vegetable oil-based binder with fewer emissions and found that that material was less susceptible to temperature⁹. Ecopave Australia has used sugar and molasses to produce bio-asphalt product that showed the improved mechanical and rheological properties¹⁰. In addition, other renewable sources of materials to partially replace the traditional asphalt binder were found in microalgae¹¹ and from the waste of animals¹², agricultural industries¹³, cooking oil¹⁴ and wood¹⁵ (cedar¹⁶, lignin¹⁷).

One of this new environmental-friendly material is the BioPhalt®, a patented Eiffage's product, born in France in 2007.

BioPhalt® was developed to replace clear bitumen and it is mainly used in paving applications as surface coarse. It was manufactured from the distillation of tall oil, a derivative of pine trees. Eiffage chose that bio raw material because it is a local product, fully available in France. In addition, this by-product doesn't compete food industries, thus it has low environmental impact. The blend was defined with a design procedure in the laboratory.

It appears as a very clear brown pitch, almost transparent, so it doesn't hide the colour of the aggregates: this allows a better integration in the environment,

⁹ E. Andersen, J. Vasudevan, et al., Road trials with vegetable oil based binders in Norway, Shell Bitumen Technical Publications and Patents from 2005–2007, 2007.

¹⁰ D. Johnson, GEO320 Technology Improves Shell Bitumen. http://www.pressbox.co.uk/detailed/Technology/GEO320_Technology_improves_Shell_Bitumen_46855.html.

¹¹ E. Chailleux, M. Audo, B. Bujoli, C. Queffelec, J. Legrand, O. Lepine, Alternative binder from microalgae: algorith project, *Transp. Res. E-circ.* (2012) 7–14.

¹² E.H. Fini, E.W. Kalberer, et al, Chemical characterization of biobinder from swine manure: Sustainable modifier for asphalt binder, *J. Mater. Civ. Eng.* 23 (11) (2011) 1506–1513.

¹³ M.A. Raouf, C. Williams, Temperature and shear susceptibility of a nonpetroleum binder as a pavement material, *Transp. Res. Rec.* 2180 (2010) 9–18.

¹⁴ M.Z. Chen, B.B. Leng, S.P. Wu, Y. Sang, Physical, chemical and rheological properties of waste edible vegetable oil rejuvenated asphalt binders, *Constr. Build. Mater.* 66 (2014) 286–298.

¹⁵ X. Yang, Z. You, et al, Mechanical performance of asphalt mixtures modified by bio-oils derived from waste wood resources, *Constr. Build. Mater.* 51 (2014) 424–431.

¹⁶ S.H. Yang, T. Suciptan, Rheological behavior of Japanese cedar-based biobinder as partial replacement for bituminous binder, *Constr. Build. Mater.* 114 (2016) 127–133.

¹⁷ G. Xu, H. Wang et al., Rheological properties and anti-aging performance of asphalt binder modified with wood lignin, in *Construction and Building Materials* 151 (2017) 801–808.

especially in the countryside. In addition, there is the possibility to colour it with several tonalities, for an even better integration.

It can be used as the upper layer of the pavement¹⁸.

The temperatures at which the material is treated are slightly lower than the common bitumen, from 115° C to 130°C.

The problem of BioPhalt®, as bio-binder, is more susceptible to ageing compared to conventional binders. Some cracks during the first years were observed in some of the trial sections paved by Eiffage. In addition, this binder is quite expensive. These two reasons motivated the company to combine BioPhalt with Reclaimed Asphalt Pavement RAP to have a balanced composition:

- RAP stabilizes the ageing of BioPhalt®;
- RAP decreases the global cost of the mix;
- Because BioPhalt® is full of fatty acids, it acts as a rejuvenator of the RAP and then improves the quality of the final mix.

One of the purposes of the company is also to study and analyse the behaviour of original and aged BioPhalt® to improve its properties and make it a proper binder.

An in-depth analysis of the effect of ageing on this material is provided in this research.

II.2 Chemical Structure of bitumen

Bitumen is basically composed of long chains of hydrocarbon with different molecular weights. It is characterised by a wide range of compound types of differing molecular size, aromaticity and polarity, making the chemical composition of the asphalt binder exceedingly complex. In addition, the precise composition varies according to the source of the crude oil from which the bitumen originates.

¹⁸ Eiffage Travaux Publics, Brochure of BioPhalt®, July 2017, www.eiffagetravauxpublics.fr

Bitumen is traditionally regarded as a colloidal system¹⁹ in which it is possible to individuate two broad chemical groups: the high molecular weight called asphaltene or micelles that are dispersed or dissolved in the second chemical group, a lower molecular weight oily medium, called maltenes [Figure II-3 (a)]. The maltenes can be further subdivided into saturates, aromatics and resins [Figure II-3 (b)].

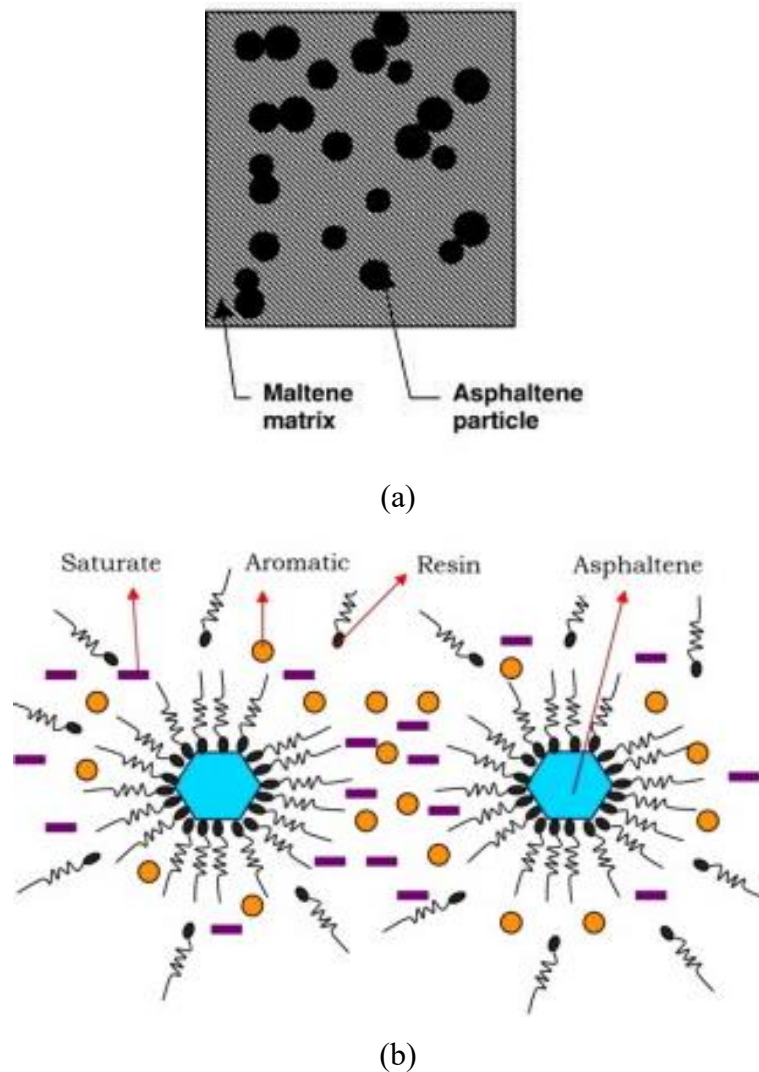


Figure II-3. Colloidal system of bitumen

Asphaltenes are n-heptane insoluble black or brown amorphous solids containing. Resins are dispersing agents or peptisers for the asphaltenes. Both resin and asphaltene have polar constituents but the difference between them depends on

¹⁹ Girdler R. B. Proc Assoc Asph Pav Tech, vol 34, p 45, 1965. Association Asphalt Paving Technologists, Seattle.

miscibility with n-heptane: asphaltene is insoluble, while resin is miscible.²⁰⁻²¹ Away from the centre of the micelle, there is a gradual transition to less polar aromatic resins, these layers extending outwards to the less aromatic oily dispersion medium.

Aromatics oils comprise the lowest molecular weight aromatic and non-polar compounds in the bitumen. They signify the major proportion of the dispersion medium for the peptised asphaltenes. In effect, they constitute 40 to 65% of the total bitumen.²²

Saturates consist of straight and branch chain aliphatic hydrocarbons and they are nonpolar viscous oils.

Studies on blending of saturates, aromatics, resins and asphaltene fractions separated from bitumen has demonstrated the effect that constitution has on rheology [23 24 25 26 27]. These chemical functional groups are responsible for intermolecular interactions that contribute to the behaviour of the asphalt. The viscosities of the saturates, aromatics and resins depend on the molecular weight distribution. The higher the molecular weight, the higher the viscosity.

Consequently, it is possible to deduce that the colloidal behaviour has a considerable influence on the resultant viscosity.

Furthermore, the colloidal system governs the response of bitumen to load also due to oxidative age hardening.²⁸

²⁰ M. Choiri, A.A. Hamouda, SPE-141329-MSSPE International Symposium on Oilfield Chemistry, 11–13 April, The Woodlands, Texas, US (2011)

²¹ S. Zendejboudi, A. Shafiei, A. Bahadori, L.A. James, A. Elkamel, A. Lohi, in *Chem. Eng. Res. Des.*, 92 (5) (2014), pp. 857-875

²² The Shell Bitumen Handbook, Great Britain, The University Press of Cambridge, 2003.

²³ MCKAY J R et al. Petroleum asphaltenes: Chemistry and composition, ACS advances in chemistry series no 170, Paper 9.

²⁴ REERINK H. Size and shape of asphaltene particles in relationship to high temperature viscosity, *Ind Eng Chem Prod Res Deve*, vol 12, no 1, 1973.

²⁵ GRIFFIN R L and T K MILES. Relationship of asphalt properties to chemical constitution, *J Chem Eng Data*, vol 6, Jul 1961.

²⁶ GRIFFIN R L et al. Influence of composition of paving asphalt on viscosity, Viscosity/temperature, susceptibility and durability, *J Chem Eng Data*, vol 4, no 4, Oct 1959.

²⁷ AMERICAN SOCIETY for TESTING and MATERIALS. The influence of asphalt composition on rheology, Papers on road and paving materials (bituminous), ASTM Special technical publication no 294, 1960. ASTM, Philadelphia.

²⁸I. Yut, A. Zofka, Attenuated Total Reflection (ATR) Fourier Transform Infrared (FT-IR) Spectroscopy of Oxidized Polymer-Modified Bitumens, in *Applied Spectroscopy*, July 2011

Bitumen is a widely used material, but its aging behaviour is only understood at a macroscopic level as hardening and embrittlement over time. Oxidation of the bitumen has not yet been understood on a molecular level²⁹.

One of the purpose of this research is to develop a chemical analysis on the aged bitumen, both bituminous and non-bituminous based. To accomplish this task, SARA test and Fourier Transform InfraRed test (FTIR) were performed on both BioPhalt® and control binder.

II.2.1 SARA test

Typically, crude oils consist of four solubility fractions: saturates, aromatics, resins, and asphaltenes, abbreviated as SARA³⁰. Consequently, SARA became the name of the chemical composition analysis of the bitumen.

SARA methods separate crude oil into its fractions according to their solubility in solvents of differing polarity. Gravimetric adsorption chromatography, HPLC, TLC-FID are the traditional methods to separate the SARA fractions, and have been employed widely for several decades (Jewell et al., 1972; Suatoni and Swab, 1975; Karlsen and Larter, 1991). In this research the TLC-FID, flame ionization detection method has been used.

A.B Brown and J.W. Sparks (1957) registered a variation of both chemical composition and colloidal structure after aging processes. Thus, it follows that the colloidal structure is straight connected with aging.

The evolution of the colloidal structure has a very large effect on viscoelastic properties of residues and asphalt.³¹

Researches attested that in the aged samples there is a shift of all the solubility classes (resins, saturates plus aromatics) towards the adjacent class, i.e. a part

²⁹ F. Handle, M. Harir, et al., Tracking Aging of Bitumen and Its Saturate, Aromatic, Resin, and Asphaltene Fractions Using High-Field Fourier Transform Ion Cyclotron Resonance Mass Spectrometry, in *Energy Fuels* 2017, 31, 4771–4779

³⁰ B.J. Fuhr, C. Hawrelechko, et al., Comparison of bitumen fractionation methods, *Energy & Fuels*, 2005; 19(4): 1327–1329.

³¹ Y. S. Kumbarger, K. P. Biligiri, Understanding Aging Behaviour of Conventional Asphalt Binders used in India, in *Transportation Research Procedia* 17 (2016) 282 – 290

of aromatics and saturates is converted to resins, and a part of resins to asphaltenes. This conversion leads to a light increase of the asphaltenes³².

It has also been shown that the rheological properties of bitumens depend strongly on the asphaltene content. At constant temperature, the viscosity of a bitumen increases as the concentration of the asphaltenes blended into the parent maltenes is increased.

Furthermore, an increase in asphaltenes means a hardening process of the bitumen, since asphaltenes have a great molecular weight and this means that they play a big role in the viscosity of the material. The more asphaltenes, the harder the material is. In addition, the most abundant compounds in asphaltenes appear to be more saturated and apolar.³³

Also, according to the study carried out by M.N. Siddiqui and M.F. Ali, (1999), it was found that asphaltene contents were higher in PAV aged asphalts than in RTFO aged asphalt binders, and so that the PAV test exerts the biggest impact on four components and functional group in bitumen.

During the years, it has been developed the necessity to represent the colloidal structure with a parameter, in order to make the studies and comparisons easier. Yen et al. introduced the colloidal instability index I_c , nowadays applied as a widely-recognised monitoring and comparing criterion. It is able to easily designate the behaviour of the material.

Originally, it was the ratio between asphaltenes and resins and it showed that: in the presence of sufficient quantities of resins, I_c is low and indicates a 'SOL' type bitumen [Figure II-4 A]; otherwise, if the resin is negligible with respect the asphaltenes, I_c is high and the bitumen is a 'GEL' type [Figure II-4 B].

³² D. Mastrofini, M. Scarsella, The application of rheology to the evaluation of bitumen aging, *Fuel* 2000; 79:1005–1015.

³³ F. Handle, M. Harir, et al., Tracking Aging of Bitumen and Its Saturate, Aromatic, Resin, and Asphaltene Fractions Using High-Field Fourier Transform Ion Cyclotron Resonance Mass Spectrometry, in *Energy Fuels* 2017, 31, 4771–4779

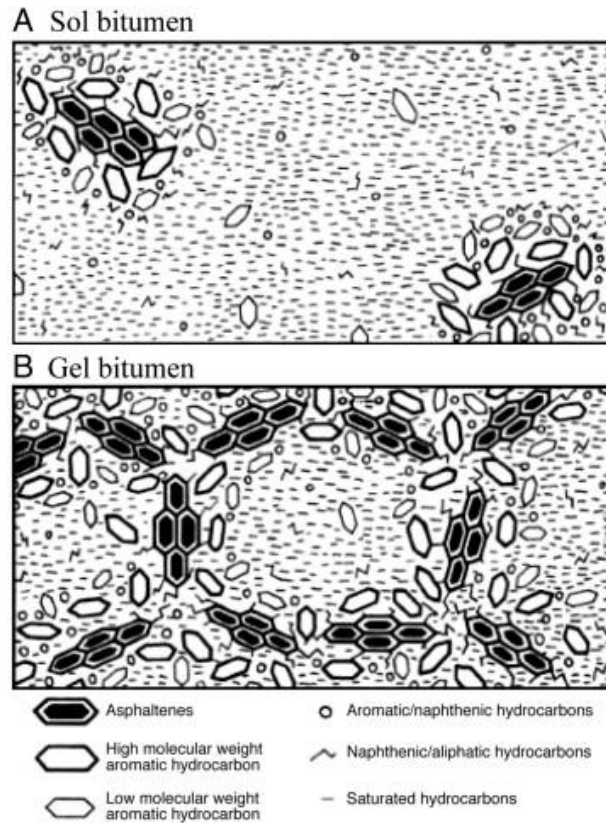


Figure II-4. Typologies of colloidal structures of bitumen

In the first case, ‘SOL’ type and low value of I_C , the asphaltenes are fully peptised and the resulting micelles have good mobility within the bitumen. This leads to a purely viscous material, whose flow speed is linearly proportioned to the tangential stress, also called Newtonian fluid.

If the aromatic/resin fraction is not present in sufficient quantities to peptise the micelles (high value of I_C , ‘GEL’ type), the asphaltenes can associate together further and there is a separation between the broad fractions. Bitumen shows a non-Newtonian behaviour, in which the viscosity depends on the tangential stress and strain.

In practice, most bitumens are of intermediate character.

Further studies proved that I_C depends also on the saturates and aromatics content. It has been demonstrated that, by keeping the asphaltenes constant and vary the content of the other three fractions:

- maintaining a constant ratio of resins to aromatics and increasing the saturates content softens the bitumen; and

- the addition of resins hardens the bitumen, thus increases the viscosity.³⁴

M. Wan and S.Wu et. Al. (2017) stated that the colloid structure is destroyed with ageing and so the index of colloid instability decreases.

II.2.2 FTIR test

Fourier transform infrared (FT-IR) spectroscopy enables evaluation of oxidation levels in bitumen by measuring the concentration of oxygen-containing chemical functionalities.

The evidence of the oxidative reaction sequence postulated by Petersen et al. has been supported by numerous studies employing Fourier transform infrared (FT-IR) spectroscopy. Recent research project titled “Evaluating Applications of Field Spectroscopy Devices to Fingerprint Commonly Used Construction Materials” indicated FT-IR as one of the most promising methods of spectroscopic analysis of bitumens.

Researchers have successfully identified chemical functional groups that formed during oxidative aging of bitumen, e.g., carboxylic acids, and sulfoxides³⁵.

In general, the objective of infrared spectroscopy, as in FTIR, is to gain information on how much a given sample absorbs light (i.e. infrared radiation) at a certain wavelength range. The sample is hit by the photons, which are absorbed and they produce the excitation of electrons, also called fundamental vibration. When the electrons return to their ground state, they release a part of the energy – and so photons. The difference between the initial energy and the released one represents the quantity of energy absorbed by the material. This way, transmission absorption spectra can be recorded. However, for materials with extremely high absorption coefficients like bitumen, there is the inherent problem that the transmission is very low or impossible and thus the signal is unacceptable low. Attenuated total reflectance (ATR) provides remedy, since the radiation is reflected at the outer surface of the sample. For ATR, an

³⁴ The Shell Bitumen Handbook, Great Britain, The University Press of Cambridge, 2003.

³⁵ I. Yut, A. Zofka, Attenuated Total Reflection (ATR) Fourier Transform Infrared (FT-IR) Spectroscopy of Oxidized Polymer-Modified Bitumens, in Applied Spectroscopy, July 2011

evanescent light wave is attenuated due to the resonances of molecular vibrations situated in the interface between the sample and a crystal of high refraction index (in this case a diamond).

With the FTIR-ATR, the software OPUS Data Collection Program®, used in this case, has been able to draw a spectrum of absorbance versus wavelength in cm^{-1} . An example is displayed in Figure II-5:

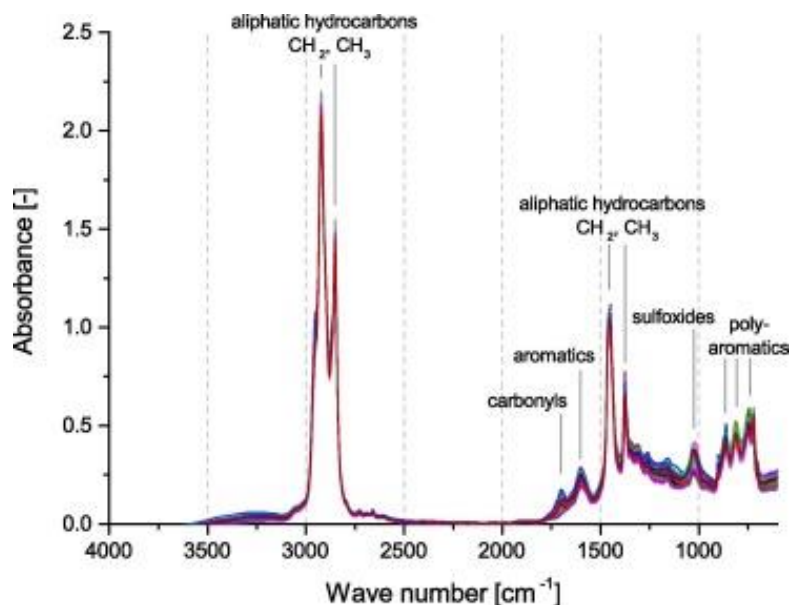


Figure II-5. Example of FTIR-ATR Spectrum

To analyse the obtained spectra, different approaches can be used: it's possible to either consider the original spectra or they can be normalized.

On the chosen spectra, it is possible to either look at single values from absorbance band maxima or to consider a range of wavenumbers by integrating the area below an absorbance spectrum around a certain band. In addition, the basis for obtaining the value can either be an absolute one (absorbance value of zero) or a relative one, i.e. a tangential base line. In this research, the spectra were normalized and then analysed with the integration method.

For spectra analysis derived from FTIR, several groups of molecular bounds can be unambiguously distinguished at different, well-defined wavelengths of an absorbance spectrum. The meaning of the peak has been individuated by J. C. Petersen (1986), J.F. Masson, L. Pelletier (2001), J. Lamontagne (2001) and E.

Pretsch, P. Buhlmann (2009). To represent these structures, qualitative indexes have been introduced.

To understand the effect of ageing on bitumen, those indexes that can reflect the changes of oxygen-containing functional groups have been in the focus of attention in this study.

The oxidation of hydrocarbons is associated, notably, with the increase of carbonyl group C=O (1700cm⁻¹) and sulphoxides S=O (at 1030cm⁻¹) bonds for laboratory aged asphalt (Mouillet et al., 2008; Siddiqui and Ali, 1999). This has been confirmed with in-situ aging on asphalt roads by Lamontagne et al. (2001a), Jung (2006) and Chávez-Valencia et al. (2007). More specifically, Mouillet et al. (2008) considers the S=O bands to represent the short-term aging during asphalt manufacturing, represented by the Sulphoxide Index:

$$I_S = \frac{A_{1030}}{\sum A}$$

On the other hand, C=O bands represents the long-term aging during the service life of the asphalt. Its index is:

$$I_C = \frac{A_{1700}}{\sum A}$$

Higher value indicates relatively more bonds. Researchers have shown in past investigations that higher oxidation rate (or ageing) leads to more carbonyl and sulphoxide groups at elevated temperatures (Cortizo et al. 2004).

Moreover, the changes of other molecular structures can also reflect the chemical modification of bitumen.

Aromaticity (at 1600 cm⁻¹) is the measure with FTIR of the relative contents of aromatic C=C bonds. This could include also volatile aromatics and heavier particles such as resins and asphaltenes as well. The Aromatic Index is:

$$I_{AR} = \frac{A_{1600}}{\sum A}$$

The bands around 1460 cm⁻¹ and 1376 cm⁻¹ are for the CH₂ and CH₃ groups, that are represented by the Aliphatics Index:

$$I_B = \frac{A_{1460} + A_{1376}}{\sum A}$$

Studies show that is difficult to draw a conclusion regarding the participation of these structures in the bitumen oxidation. In fact, the linear aliphatics (or “long chain” index) don’t evolve significantly with time during ageing process.³⁶

II.3 Ageing

The bitumen’s response to load depends mainly on three agents:

- Loading time/frequency;
- Temperature;
- Ageing state.

Loading time/frequency and temperature are governed by rheology, introduced in the following paragraph. The Ageing will be explained below.

In pavement applications, asphalts are exposed to aging processes during storage, mixing, transport, and construction, as well as in service life. Consequently, an in-depth analysis of the ageing process is necessary. In addition, the responsible of the viscous response in the asphalt mixture is the bitumen, thus the attention must be paid in testing this material.

Like organic substances, bitumen’s properties change with time since the material is affected by:

- **Volatilization**, that is the loss of volatile components, stronger at high temperatures. This phenomenon occurs mainly in the first stages of the mixture production.

³⁶ J. Lamontagne, P. Dumas et al., Comparison by FTIR spectroscopy different ageing techniques: application to road bitumen, in Fuel 80 (2001) 483-488.

- ***Oxidation***, that is a reaction between the molecules of the bitumen and oxygen. This results in an increase of stiffness due to the dimension of the oxygen's molecules.
- ***Polymerization***, that is a phenomenon in which the hydrocarbons tend to weld to each other in the presence of a source of energy, like heat or UV radiation. This makes the material brittle since it loses ductility.

Ageing effects involve chemical changes of hydrocarbons, which in turn has an impact on the rheological properties.

Several research studies have shown that the volatilization and oxidation are the biggest contributors to the hardening (aging) process of asphalt binders. Volatilization is the mainly responsible of the short-term aging phase, that occurs during the production stage at high temperatures, which are inclusive of blending, mixing and compaction processes of asphalt binders with aggregates. In fact, the volatilization concerns mainly the lighter aromatic fraction, that is the oil fraction, but the higher the temperature is, the more complex the components volatilize. In fact, rapid aging occurs at high temperatures on the surface of aggregates while mixing the bituminous mixture.³⁷

During the in-service life of the pavement, the principal cause of asphalt aging and embrittlement is the atmospheric oxidation of certain molecules with the formation of highly polar and strongly interacting functional groups containing oxygen.³⁸ This phenomenon occurs for the entire life of the pavement, from the mixing phase to the in-service life.

Generally higher temperature and longer exposure time to high temperature results in a greater degree of deterioration of asphalt binders and stiffening of asphalt mixtures.

All these factors cause an increase in elastic component of the bitumen and consequential stiffening of the asphalt mixture. Moderate levels of aging are generally accepted and can even enhance performance, but significant levels

³⁷J. F. Branthaver, J. C. Petersen, et al., "Binder Characterization And Evaluation: Volume 2-Chemistry", Report SHRP-A-368 (Strategic Highway Research Program, National Research Council of Academies, Washington, D.C., 1993).

³⁸ J. C. Petersen, Trans. Res. Rec., J. Trans. Res. Board 1096, 1 (1986).

result in embrittlement of the bitumen, considerably affecting the cracking resistance of the asphalt mixture, reducing it under repeated loading.³⁹ Nevertheless, increased fatigue susceptibility of bituminous mixtures reduces the service life of asphalt pavements.⁴⁰ While regular maintenance cycles can mitigate the aging effects, the long-term aging effects on the bitumen will eventually lead to surface cracks that require the pavement to be rehabilitated or replaced (Smith and Edwards, 2001).

The scope of this research is studying the ageing effects on biomaterials, this means that it's fundamental ageing the materials at both short and long term to make them representative of the binder characteristics inside the mixtures.

Despite the fact that studying the effect of ageing on just binder is insufficient to completely evaluate the effect of aging in an asphalt mixture because aging of asphalt mixture in the field is significantly influenced by the several factors relating to the mix, Brown et al show that binder testing is still important because it serves as a means to identify and eliminate binders that will age too quickly.

To age artificially the materials, a large number of laboratory methods have been used. This simulation of field ageing involves several conditions at which the sample must be subjected to be representative, like increasing the temperature, decreasing bitumen film thickness, increasing oxygen pressure, or using combinations of these factors.⁴¹

II.3.1 *Short-term ageing*

The effect of short term aging on asphalt binders in the laboratory is achieved by the Rolling Thin Film Oven Test (RTFO), which exposes the binder to continuous heat and air flow.

³⁹ J. Wu, G. Airey, The influence of aggregate interaction and aging procedure on bitumen aging, in Journal of Testing and Evaluation, Volume 37, Issue 5, September 2009, Pages 402-409.

⁴⁰ I. Yut, A. Zofka, Attenuated Total Reflection (ATR) Fourier Transform Infrared (FT-IR) Spectroscopy of Oxidized Polymer-Modified, in Applied Spectroscopy, July 2011

⁴¹ X. Lu, U. Isacson, Effect of ageing on bitumen chemistry and rheology, in Construction and Building Materials 16 (2002) 15-22

The rolling thin film oven test was first adopted in 1970 as ASTM D2872 (Airey and Brown, 1998). It simulates the hot mix process by bringing a heated asphalt film into contact with hot air, allowing the oxidation and the volatilization of the lighter component of the asphalt bitumen.

II.3.2 Long-term ageing

To make the binder similar to the field conditions after several years, the Pressure Ageing Vessel test (PAV) is used.

The current PAV test was developed during the SHRP program in the USA. The test consists of further ageing an already RTFO aged bitumen in a pressure vessel which is placed in an oven. To accelerate the ageing process, both temperature and pressure are increased in the oven. The aim is to achieve an amount of aging that is comparable to approximately several years of service life in a pavement.

II.4 Rheology

Rheology is the science that studies the scrolling and the deformation of matter due to an applied force. The rheological properties are fundamental in understanding the behaviour of complex materials, as asphalt bitumen.

In fact, several studies show that asphalt binder is characterized of a viscoelastic behaviour, time and temperature dependent. Their deformation depends not only on the materials themselves, but also on the intensity of load and speed and duration of loading.

The degree to which their behaviour is viscous and elastic is a function of both temperature and period of loading, or loading time. At high temperatures or long times of loading, they behave as viscous liquids whereas at very low temperatures or short times of loading they behave as elastic (brittle) solids. The intermediate range of temperature and loading times, more typical of

conditions in service, results in visco-elastic behaviour, that is a behaviour somewhere in-between the purely viscous and purely elastic one [Figure II-6]. In elastic materials, the response occurs simultaneously with the application of the force thus, if the load is removed, the deformation disappears simultaneously: in other words, there is no lag between force and response. On the other hand, in purely viscous materials the response doesn't occur simultaneously with the application of the force, but it needs a time lag to reveal itself. In addition, once the load is removed, the deformation isn't totally recovered but there is left a permanent deformation.

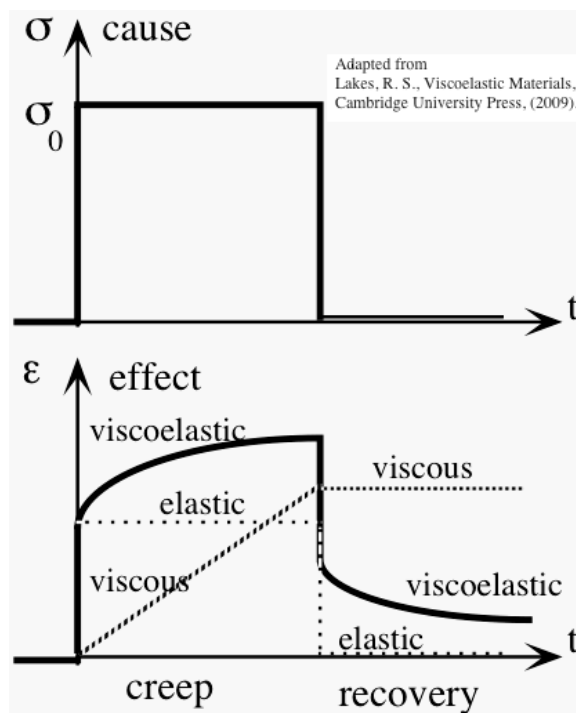


Figure II-6. Viscoelastic Behaviour

Viscoelasticity can be studied using dynamic mechanical analysis, where an oscillatory force (stress σ) is applied to a material and the resulting displacement (strain γ) is measured [Figure II-7].

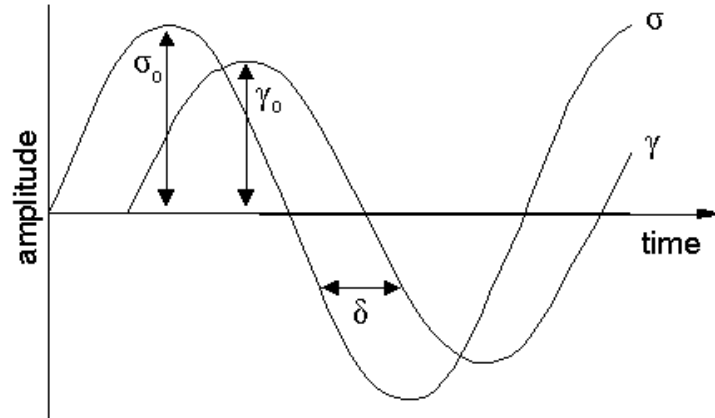


Figure II-7. Sinusoidal wave forms for stress and strain functions

In order to define the viscoelastic properties of bitumen, in 1954 Van der Poel introduced the concept of stiffness modulus as a fundamental parameter to describe the mechanical properties of bitumen by analogy with the elastic modulus of solids.

Complex Modulus G^* or dynamic modulus is the ratio of stress to strain at a certain frequency calculated from data obtained from either free or forced vibration tests, in shear, compression, or elongation. On the other hand, the phase angle δ represents the lag between the applied stress and the measured strain. The value of δ is in the range between 0° and 90° , in which 0° means elastic response, while 90° is the purely viscous response. Small phase angles are found at low temperature and high frequency and vice versa, indicating that, under these conditions, the bitumen approximates respectively to elastic and viscous behaviour.

These values are usually measured in shear condition at medium-high temperature by the dynamic shear rheometer. At low temperatures, sample are studied in flexural conditions. Creep stiffness S and the creep rate are studied by the bending beam rheometer.

The results are displayed by the Master Curve, that are the value of the G^* versus the frequency or time [Figure II-8] and the black diagram, G^* versus phase angle [Figure II-9].

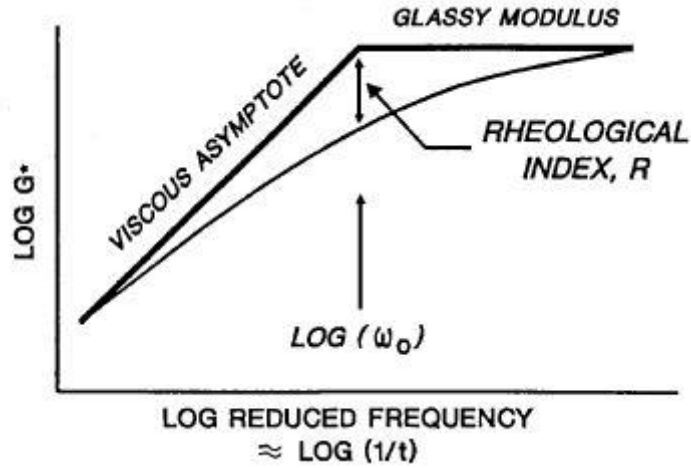


Figure II-8. Example of Master Curve

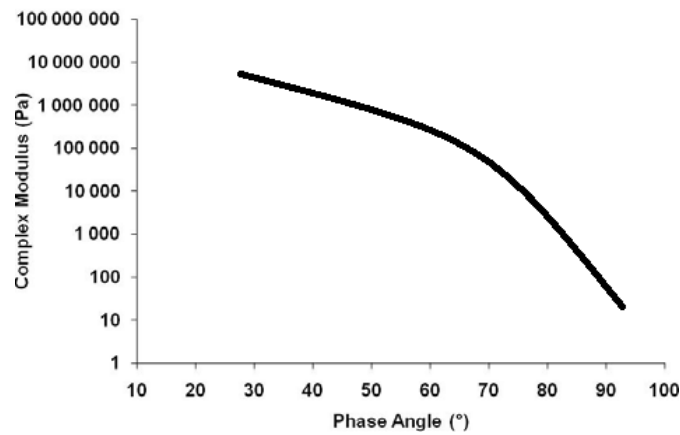


Figure II-9. Black Diagram

The rheological behaviour of bituminous binders is bounded by two main transitions.

At high frequencies and/or low temperatures, the elastic modulus approaches a limiting value, called a glassy modulus, G_g . At low frequencies and/or high temperatures, a material behaves as a Newtonian (viscous) fluid.⁴²

Both G^* and δ depend on frequency and temperature, thus to obtain the entire interval of values it is necessary to perform the test changing all the condition. Unfortunately, this is impossible due to the test machines' limits. Researchers found a solution to that issue: thanks the superimposition time-temperature principle, it's possible to perform the test keeping the frequency constant and

⁴² Herh PKW, Colo SM, Rudolph BKS. Dynamic shear rheometers pave the way for quality asphalt binders. Application Note. Rheo Logica Instruments; 1999.

varying the temperature. The superimposition principle takes into account the fact that the material behaves in the same way either at low temperature and high frequency or at high temperature and low frequency. Consequently, a master curve represents a binder's behaviour at a given temperature for a large range of frequencies. A good master curve should appear smooth and continuous.

The application of the principle typically involves the following steps:

- experimental determination of frequency-dependent curves of isothermal viscoelastic mechanical properties at several temperatures and for a small range of frequencies
- computation of a translation factor to correlate these properties for the temperature and frequency range
- experimental determination of a master curve showing the effect of frequency for a wide range of frequencies
- application of the translation factor to determine temperature-dependent moduli over the whole range of frequencies in the master curve.

In this thesis, the translation factors were computed using an empirical relation first established by Malcolm L. Williams, Robert F. Landel and John D. Ferry (also called the Williams-Landel-Ferry or WLF model).

The WLF equation is one of the best-known equations of polymer physics and for a long time it was believed to describe an approximately universal non-Arrhenius effect of temperature on viscosities and relaxation times in polymer systems.

Once all the curves merge in a unique one, as Figure II-8, it's possible to apply another model to obtain some meaningful parameters. The Christensen-Anderson- Marasteanu model (CAM) was adopted in the 1992 and it is an accurate and mathematically simple model, powerful enough to fit the curve at all frequencies. CAM model defines parameters that describe shape and position of the master curve: the rheological index is the difference between the glassy modulus and the modulus at the cross-over frequency. The latter is the frequency at which the two asymptotes of viscous and elastic behaviour meet each other.

II.5 Performance properties

II.5.1 Permanent deformation

Road construction materials are viscoelastic and they are not able to completely recover deformations, as an ideally elastic material does. This means that, as a result of every load application, bitumen will accumulate some amount of permanent deformation. The accumulation of deformations leads to a pavement's distresses called ruts.

A rut is a longitudinal surface depression in the wheel path [Figure II-10]. It may have associated transverse displacement.⁴³



Figure II-10. Rutting

This phenomenon is emphasized:

- when the pavement is subjected to high temperature during hot season;

⁴³ Federal Highway Administration, Distress identification manual for the Long-Term Pavement Performance Program, publication no. fhwa-rd-03-031, June 2003.

- In the first in-service life period, since the viscous components of the binder in the asphalt mixture are preponderant at the beginning rather than after several years;
- If there are very heavy static load applied on the pavement.

Lots of researches has focused on this topic to find parameters capable of representing and controlling permanent deformation.

During the SHRP programme in 1994, the SUPERPAVE performance grade system methods has identified the $G^*/\sin\delta$ value as an influential parameter useful to evaluate the permanent deformation (rutting) of asphalt mix. The complex shear modulus G^* and phase angle δ were measured from the Dynamic Shear Rheometer (DSR) test.

The increasing utilisation of modified bitumen has led to a general review of all the test protocol, in order to verify if they are applicable on modified bitumen. As a result of that, a copious number of researchers explained that the PG system was blind to modification. In fact, all asphalt binders of the same performance grade would be expected to perform the same in the same traffic/environmental conditions regardless of how they were produced. In fact, the $G^*/\sin\delta$ parameter captures viscous and elastic effects but it can't adequately capture the benefits of elastomeric modification because of the relatively small impact of phase angle δ on the overall value of $G^*/\sin\delta$.⁴⁴

Consequently, the Federal Highway Administration (FHWA) has developed a performance-based PG binder test, the Multiple Stress Creep and Recovery (MSCR) test, to supplement the conventional DSR high temperature test. Other studies confirm that the results from MSCR test are more reliable with respect the parameter $G^*/\sin\delta$: J. Z. Lubinda and F. Walubita et al. 2015; Anderson, Le Hir, et al., 2002; Bouldin, Dongré, & D'Angelo, 2001; D'Angelo & Dongré, 2002; Dongré & D'Angelo, 2003; Dongré, D'Angelo, Reinke, & Shenoy, 2004)".

This test is performed with the DSR at high temperature, presumably similar to the temperature that the pavement will experience along its life in the field.

⁴⁴ M. Anderson, J. D'Angelo et al., MSCR: A better tool for characterizing high temperature performance properties, <http://asphaltmagazine.com/mscr-a-better-tool-for-characterizing-high-temperature-performance-properties/>

According to the last ASTM D7405 – 15, the sample aged at RTFO or PAV is loaded at constant stress for 1 second then allowed to recover for 9 seconds. Twenty creep and recovery cycles are run at 0.1 kPa creep stress followed by ten creep and recovery cycles at 3.2 kPa creep stress. The first 10 cycles are for conditioning the specimen while the second 10 are for data collection and analysis. The two levels of creep stress provide response of the material in both presumably linear and non-linear viscoelastic region.

The MSCR covers the determination of non-recoverable creep compliance J_{nr} and the percent of recovery %R. J_{nr} is the residual strain in a specimen after a creep and recovery cycle divided by the stress applied in kPa. The percent recovery is intended to provide a means to determine the presence of elastic response and stress dependence.

II.5.2 Fatigue cracking

Another main type of distress in pavements is fatigue cracking.

It occurs in areas subjected to repeated traffic loadings (wheel paths). Can be a series of interconnected cracks in preliminary stages of development. Develops into many-sided, sharp-angled pieces, usually less than 0.3 meters (m) on the longest side, characteristically with a chicken wire/alligator pattern, in later stages⁴⁵ [**Errore. L'origine riferimento non è stata trovata.**].

⁴⁵ Federal Highway Administration, Distress identification manual for the Long-Term Pavement Performance Program, publication no. fhwa-rd-03-031, June 2003.



Figure II-11. Fatigue Cracking

In the existing Superpave specifications, the parameter $G^* \cdot \sin \delta$ has been defined as a fatigue parameter of asphalt binders (Anderson et al., 1994). Later, other studies demonstrate that this parameter could not characterise the actual fatigue damage resistance, because it is measured within the linear viscoelastic range before damage is expected to occur (Anderson & Kennedy, 1993; Bahia et al., 2001; Tsai & Monismith, 2005). To improve the Superpave specification, the time sweep test was proposed (Bahia et al., 2001). It has shown promising correlation with the mixture fatigue tests (Bahia et al., 2001), but it is not a practical method, because it is time consuming and often unrepeatable.

Thus, attempts have been made to find the accelerated fatigue test methods, and among them, one of the most promising is the linear amplitude sweep (LAS) test (Johnson, 2010), later modified by Hintz, Velasquez, Li, et al. (2011).

The procedure has been validated through comparison with mixture fatigue and field performance (Hintz, Velasquez, Johnson, et al., 2011; Safaei, Lee, Nascimento, Hintz, & Kim, 2014; Wang, Castorena, Zhang, & Kim, 2015; Zhou et al., 2013) and designated a provisional AASHTO standard procedure under AASHTO TP 101-1 (2012). The last version is the AASHTO TP 10112(2016).

LAS is an accelerated fatigue test that expresses fatigue life as a function of pavement strain. It consists of two steps. In the first step, the frequency sweep applies oscillatory shear loading at constant strain amplitude of 0.1% over a range of loading frequencies from 0.1 to 30 Hz to obtain the rheological

properties of the undamaged binders. In the second step, the amplitude sweep test applies incrementally increasing load amplitudes at the constant frequency of 10 Hz to obtain the damage characteristics of the binder. The step includes 10 intervals of constant strain amplitude where each interval is followed by another interval of increased strain amplitude beginning from 1% and ending at 30% with an increasing rate of 1% per round, as shown in Figure II-12:

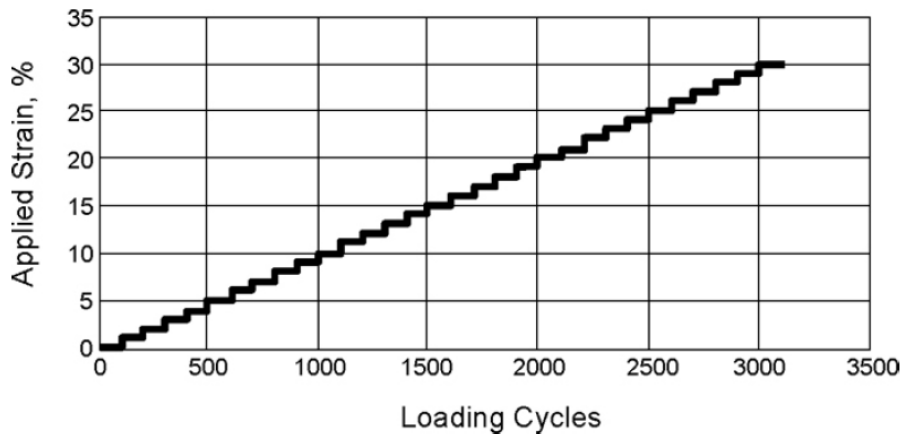


Figure II-12. Loading scheme of Amplitude Sweep for LAS test

Based on the AASHTO recommendation, the LAS test should be conducted at the intermediate pavement temperature. In this study, 20°C was selected as the test temperature, because it is generally recognized as an intermediate temperature for pavement. Based on the recommendation, at temperatures below about 20°C, the damage is almost due to pure fatigue, while at the higher temperatures, plastic deformation occurs to a considerable extent (Little et al.,2001).

Viscoelastic continuum damage (VECD) theory can be used to analyse the LAS test results (Johnson,2010). VECD modelling of asphalt binders or asphalt mixtures is based on Schapery's work potential theory and uses an internal state variable, D, to quantify damage due to stiffness reduction (Schapery, 1984). The primary benefit of using the VECD model is that it allows predicting fatigue damage under variable loading and temperature conditions as long as the viscoplastic strain is insignificant (Hintz, Velasquez, Johnson, et al.,2011;

Safaei et al.,2014; Wang et al.,2015). Further details regarding the VECD model and its application for LAS analysis may be found elsewhere (Hintz, Velasquez, Johnson, et al.,2011; Johnson,2010; Underwood, Kim, & Guddati,2010).

II.5.3 Low Temperature cracking

Pavement cracking can occur when the thermal stress inside the pavement, due to low temperature, is high enough to reach the tensile strength of pavements. In effect, as surrounding temperatures drop, pavements contract and build up internal stresses. If this contraction occurs fast enough the pavement may crack because it does not have time to relax these stresses. This type of crack is typically called “thermal crack”, or transverse crack because of the direction of cracking in relation to the direction of traffic. They can form during extreme cold or during repeated cycles of heating and cooling.

Daily temperature cycles also can propagate thermal cracking. Repeated heating and cooling will drive a crack across the road and down through the pavement structure. A major drop in temperature over a short period of time also can cause thermal cracking, even if the temperatures aren't extremely cold. Low-temperature cracking occur in pavements regardless of traffic volumes or loads because they are caused by environmental, not traffic, conditions.

In addition, the more the pavement is aged, the more sensitive the pavement is to thermal cracking since it becomes stiffer with time.

Preventing such kind of cracking is of great importance to ensure a long pavement lifetime.

Researches in this area has been conducted since the 1960s and, nearly a century ago, engineers began to recognize the link between low-temperature cracking in asphalt pavements and the asphalt binder's rheological properties.

One of the low temperature test method that can allow to govern the thermal cracking is the Bending Beam Rheometer (BBR) (Bahia et al, 1991).

The BBR applies a static stress to a bitumen beam and measures creep stiffness and the rate of stress relaxation. Asphalt binders that are not too stiff at low temperatures and able to relax built up stresses are desirable.

This test contemplates the preparation of an asphalt beam with a proper mould and, during the test, the beam is immersed in a cold liquid bath, capable of maintaining the desired test temperature. The static load is applied to the centre of the beam and its deflection is measured against time with a Linear Variable Displacement Transducers, LVDT. The test is largely software controlled.

Stiffness S is calculated based on measured deflection thanks the standard elastic beam properties. This way of proceeding is validated by the fact that the asphalt bitumen at low temperature behaves as an elastic material.

BBR test measures also how the asphalt binder relaxes the load induced stresses, thanks the stiffness ratio parameter m . BBR tests are conducted on PAV aged asphalt binder samples since the PAV is the most sever condition for pavement. In fact, samples subjected to long term aging would break at warmer temperatures than those that had been short term aged [Jung and Vinson, 1994].

Chapter III

MATERIALS AND METHODS

III.1 Materials

In this study, two binders were analysed and compared:

- BioPhalt®;
- 50/70 pen. bitumen.

The first is a patented material produced by Eiffage, a French multinational company. It is basically made of 60% of pitch from by-product of papermaking industry, 32% of rosin and 8% of SBS, mixed at 130°C for six hours. The company reserves the right to keep the mixing procedure confidential, thus further information are forbidden.

BioPhalt® appears as a clear brown material, difficult to handle since it is very sticky, so quite different from the common binders, as shown in Figure III-1.



Figure III-1. BioPhalt®

On the other hand, the 50/70 penetration bitumen is a dark bitumen characterized by a “medium stiffness”, not too much soft neither thick, a softening point between 46°C and 54°C and all the conditions that are provided by the Penetration Grade Specification, distributed by the Shell Bitumen Specifications, under the column of 50/70 penetration. During the laboratory tests, to distinguish the two materials, two codes were applied:

- 16-3181 for 50/70 pen bitumen, called also Control;
- 16-3182 for BioPhalt®.

In the following images, it's possible to appreciate the differences between the materials.



Figure III-2. Qualitative comparison between binders



Figure III-3. Top views BioPhalt®



Figure III-4. Top view 50/70 pen bitumen

III.2 Ageing

To conduct this study, it was necessary to age the binders to make them representative of the binder characteristics inside the mixtures. Since the rheological, physical and chemical properties of asphalt binders change with time because of oxidation, characterization is needed at different stages of the binder life. Current asphalt binder specifications consider three stages in the life of the material: a) original binder, which represents the asphalt stored before mixing with aggregates; b) primary-aged binder, or binder aged during the mixing and compaction process; and c) secondary-aged binder, which is the binder aged after several years of service life in the pavement. By aging the binder, conditions closer to those seen in situ are achieved.

The primary ageing is realized thanks the Rolling Thin Film Oven Test (RTFO), where ageing is enhanced by rotating eight containers in which 35 ± 0.5 g of asphalt binder are poured. This quantity guarantees a continuously renewal of the surface so that the film of asphalt coating inside the containers is able to react with oxygen.

The apparatus consists in an oven with a carriage, used to support the eight containers characterized by standard size, and an air jet that passes through copper tubing on the bottom of the oven in order to heat the air up [Figure III-5].

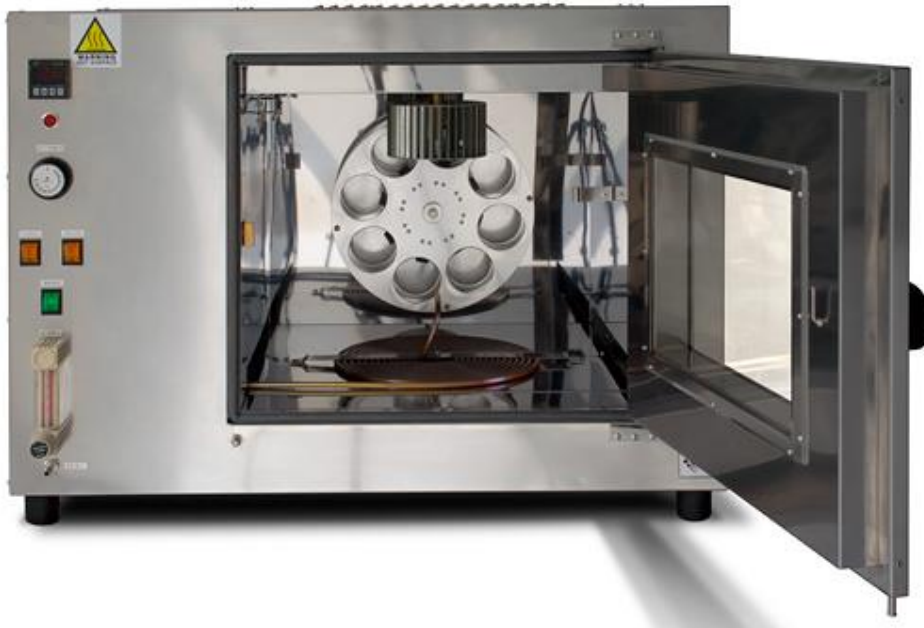


Figure III-5. Example of RTFO test oven

Calibration is needed to perfectly orientate the air jet position, to check the speed of the air flow and his inclination with respect to the containers. *AASHTO T240-6* is the standard that prescribes the procedure: the temperature inside the oven must be $163^{\circ}\pm 1^{\circ}\text{C}$, the carriage's speed must be 15 ± 0.2 revolutions per minute.

The first step of this test is to pour 35 ± 0.5 g of hot bitumen in each container (the 50/70 pen was pre-heated at 150°C , while the BioPhalt® at 140°C), immediately after the container must be turned to a horizontal position and rotated till the binder covers his walls, leaving a gap from the vertical face on the open end of the container itself. Once the container has been rotated it must be transferred immediately to the cooling rack and leave it there for 70 minutes [Figure III-6 and Figure III-7].



Figure III-6. Oven and control binder in the cooling rank



Figure III-7. BioPhalt® in the cooling rank

After that, it's possible to insert all the cylinders in the oven at 163°C. Once the door is closed, the containers must stay inside the oven (with carriage's rotation and air flow turned on) for 85 minutes. The last step is to remove the containers from the oven and scrape the binder for at least the 90% of the initial weight, pouring all the aged binder in a single tin. Finally, it's possible to perform all the desired tests on the aged binder.

To simulate the actual in-service behaviour of the material after several years in the field, another step is needed: on the bitumen already aged with RTFO, the application of elevated pressure and temperature simulates an accelerated oxidation ageing. This test is called Pressure Ageing Vessel (PAV). Studies show that five to ten years of long-term field ageing can be simulated in 20 hours under a pressure of 2.1 MPa.⁴⁶ Elevated pressure forces air into the asphalt binder which increases the amount of oxygen that is available for reacting with materials and elevating temperature increases the rate at which the oxidation reaction can occur.

The main components of the PAV are the pressure vessel and its environmental chamber, electronics to control and measure temperature and pressure and a vacuum oven for degassing the PAV residue, as shown in Figure III-8.

⁴⁶ Bahia, Hussain U., Anderson, David A., Pressure aging vessel (PAV): A test to simulate rheological changes due to field aging, Proceedings of the Conference on Physical Properties of Asphalt Cement Binders; Dallas, TX, USA; 7 December 1993 through 7 December 1993; Issue 1241, 1995, Pages 67-88.



Figure III-8. Example of PAV test machine

The temperature was chosen depending on the PG grades of binders, that are 64°C for the Control and 76°C for BioPhalt®. According to *ASTM D6373-13*, the temperature was selected equal to 100°C for both materials.

In the PAV procedure, firstly it is needed to pour 50 ± 0.5 g in the pans, that represent a thickness equal to approximately 3.2 mm. In this case, only 5 pans over 10 were used since it depends on the quantities required by each test. When the vessel was at 100°C, the pan older was removed and all the pans were placed in the older, finally the holder was returned to the vessel. When the temperature was reached again, the conditioning pressure equal to 2.1 MPa was applied and started the count of 20 hours. At the end of this time, the pressure was released over a period of 9 ± 1 minute, at a linear rate: a slow release tends to minimize the creation of air bubbles inside the samples. After that, all the pans were inserted individually in an oven set at 163°C for 15 minutes in order to pour the sample in a single little container. Subsequently, the container was inserted in the vacuum oven, following this order:

- 10 minutes without vacuum applied;
- 30 minutes with vacuum at 15 KPa;
- 30 minutes releasing the vacuum.

Now, the sample in the container was ready to pour in the little vials for the tests.

The purpose of this thesis is to study the effect of *ageing* on the performance of BioPhalt[®], compared to ones of a standard bitumen, that provides guidelines.

To make even more valuable this experimental programme, a second cycle of PAV was performed to simulate a further ageing of the samples. The same procedure described before was followed and, after this second cycle, the materials and the results were labelled as PAVx2.

The following table is to summarise which are the material and the different ageing phases:

Table 1

Name + Ageing phase	Label	Name + Ageing phase	Label
Control Original	C_Orig	BioPhalt [®] Original	BP_Orig
Control RTFO	C_RTFO	BioPhalt [®] RTFO	BP_RTFO
Control PAV	C_PAV	BioPhalt [®] PAV	BP_PAV
Control PAVx2	C_PAVx2	BioPhalt [®] PAVx2	BP_AVx2

III.3 Test Machines

III.3.1 Dynamic Shear Rheometer

Since asphalt binders are isotropic incompressible materials, the extensional properties at medium-high temperatures can be calculated from the shear properties.

Dynamic Shear Rheometer is the device that provides a means for measuring the complex shear modulus, the phase angle and other parameters by applying sinusoidal, oscillatory stresses or strains over a range of temperatures and loading frequencies to a thin disc of bitumen, sandwiched between two plates, the lower fixed and the upper oscillating [Figure III-9 **Errore. L'origine riferimento non è stata trovata.**]. The sinusoidal or oscillatory loading is

applied to two plates repeatedly rotating the top plate in an alternating clockwise and counter-clockwise position with respect to zero position.

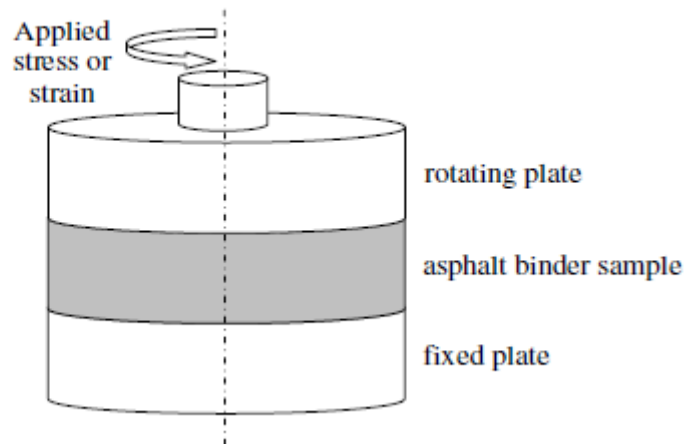


Figure III-9. Parallel Plate for DSR

A lot of type of plate are used, but, usually, parallel plates geometry is applicable to asphalt binders that behave as a linear viscoelastic material. The height of the cylinder, equal to the gap between the plates, depends on their geometry and affects the estimation of the Complex Modulus G^* . In fact, this value is computed by dividing the peak-to-peak that occurs during a DSR loading cycle by the peak-to-peak shear strain that occurs during the same cycle:

$$G^* = \frac{\text{stress } \sigma}{\text{strain } \gamma} = \frac{8Th}{\pi d^4 \varphi}$$

Where:

- T = torque applied to the test specimen [Nm];
- h = thickness of the specimen [mm];
- d = diameter of the trimmed specimen [mm], equal to the diameter of the plates;
- φ = angular deflection [rad].

Two sets of metal parallel plate were used, depending on the operational conditions: 8 mm for low-intermediate temperatures (-5 – 34°C) with a gap of 2 mm and 25 mm for intermediate and high temperatures (30 – 90°C) with a gap of 1 mm. Since the properties of asphalt change with temperature, the testing temperature for characterizing the binder must be the same temperature as the temperature experienced by the binder in the field, thus, depending on the test, several values were chosen.

Two typologies of DSR were used, one at “Politecnico of Turin” and the other at NTEC. They are respectively: the MCR301 and MCR302 models produced by Anton-Paar, shown in Figure III-10 (a) and the other the Gemini model produced by Bohlin, in Figure III-10 (b).

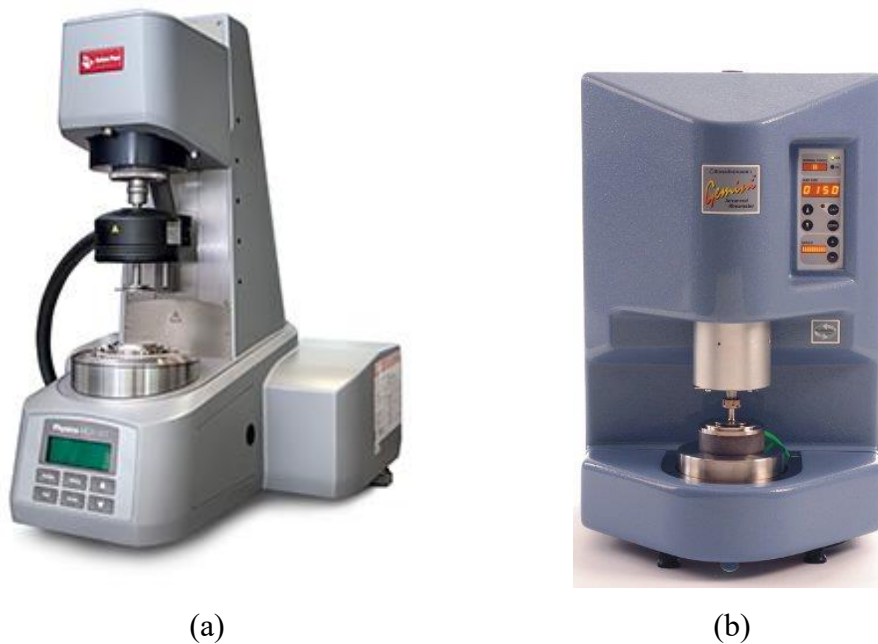


Figure III-10. Rheometers

First of all, it is necessary to set the zero gap between the spindles at the midrange of the anticipated test temperatures. Subsequently, the specimen is poured directly from the vials or disassembled from a mould and put on the pre-heated lower plate, being careful that adhesion between plates and samples is ensured. Immediately after mounting the test specimen on one of the plates and closing

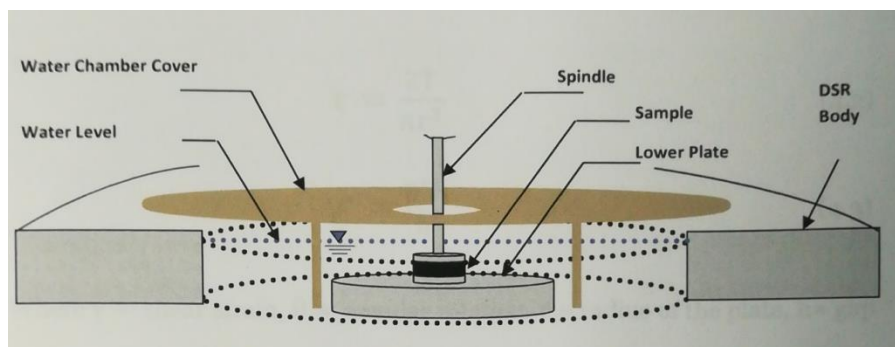
them, a trimming operation with a spatula is necessary to remove any excess binder and to guarantee that the diameter of the cylinder is the same of the one of the plates. It is worth to highlight that, according to equation of G^* , the thickness of the specimen affects the measured modulus in a linear manner while the diameter affects the measured modulus to the fourth power.

After that, it's possible to close the plates at the desirable gap and taking care that the sample forms a proper bulge.

This system must be surrounded by an environmental chamber that conditions the samples and plates by either air or water. The Anton-Paar rheometer follows the first method [Figure III-11 **Errore. L'origine riferimento non è stata trovata.**(a)] whereas the Bohlin the second one [Figure III-11 (b)].



(a)



(b)

Figure III-11. Typologies of conditioning

In this experimental programme, the vials have been in the oven at 150°C for 15 minutes, then the 25mm sample were poured in the mould and leaved in the fridge for 15 minutes to guarantee the disassembling, whereas the 8mm sample were poured either directly on the plate or on the mould, depending on the laboratory operational procedure.

All the details of the tests conducted with the DSR were illustrated below, in specific sections. The analysis of the data was conducted by Excel, as in all the other cases, if not specified.

III.3.2 *Fourier Transform Infrared*

One of the principal effect of the ageing of bitumen is the change in chemical bounds that can be reflected in change of rheological, physical and mechanical properties. Analysing the change in chemical composition allows for a better understanding of the behaviour of the asphalt bitumen. In particular, oxidation, volatilization and polymerization are the main causes of the ageing and thus a chemical inspection is due.

A Bruker Tensor 27 FT-IR was used, with OPUS Data Collection Program (V 1.1) [Figure III-12 **Errore. L'origine riferimento non è stata trovata.**].



Figure III-12. FTIR machine

The software collects a FT-IR Spectrum using attenuated total reflectance ATR, that allows analysing the bitumen sample directly applied on a crystal (diamond).

The procedure consists on: firstly verify if the crystal is clean performing a scansion without sample, after that spread a very little amount of material on the surface of the crystal with a spatula and then scan the sample. The rays go through the bitumen [Figure III-13] with different wavelengths and the software immediately draws the spectrum of absorbance over the wavelength. This corresponds to vibrations of various chemical bonds: the higher is the absorbance, the higher is the number of that type of bond in the material. Peaks are recorded where the bound is more excited.

Two replicates for both BioPhalt® and Control binder at all levels of ageing were performed.

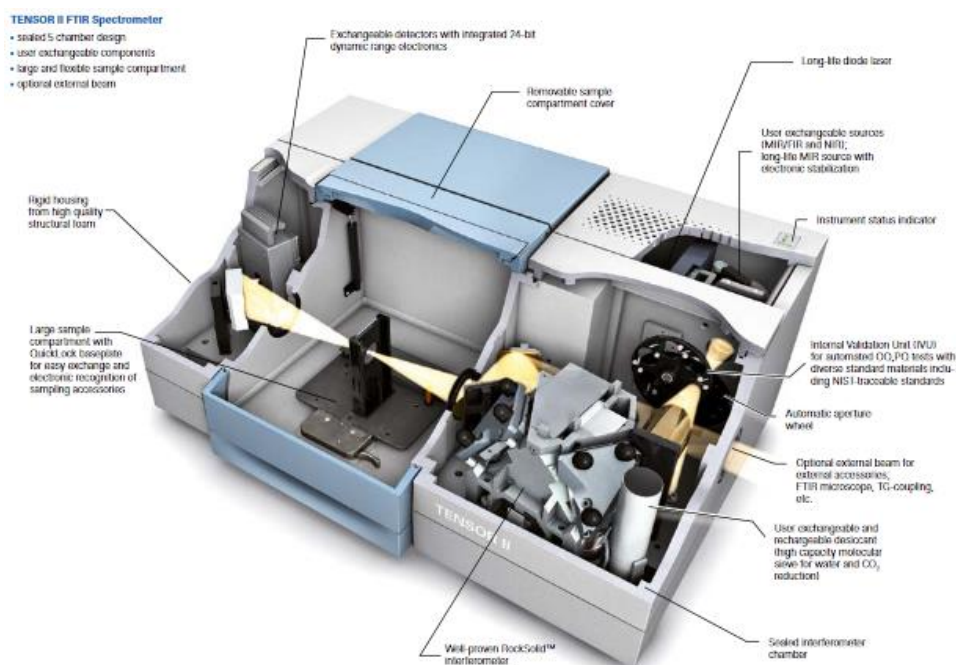


Figure III-13. Details of FTIR machine

For spectra analysis derived from FTIR, different groups of molecular bounds can be unambiguously distinguished at different, well-defined wavelengths of an absorbance spectrum. For bituminous binders, especially those structures associated with oxidative aging, i.e. uptake of oxygen, have been in the focus of attention in this research: carbonyl and sulphoxide group are the most

representative for the ageing, whereas asphaltenes as aliphatics and aromatics were investigated to compare with the SARA results.

The considered structural groups can be either looked at by band maxima or integration analysis: in this study, the integration analysis was used. The area below the absorbance spectrum around a peak is considered, normalized by the sum of the areas under all the peaks. A general spectrum with details for each peak is shown below:

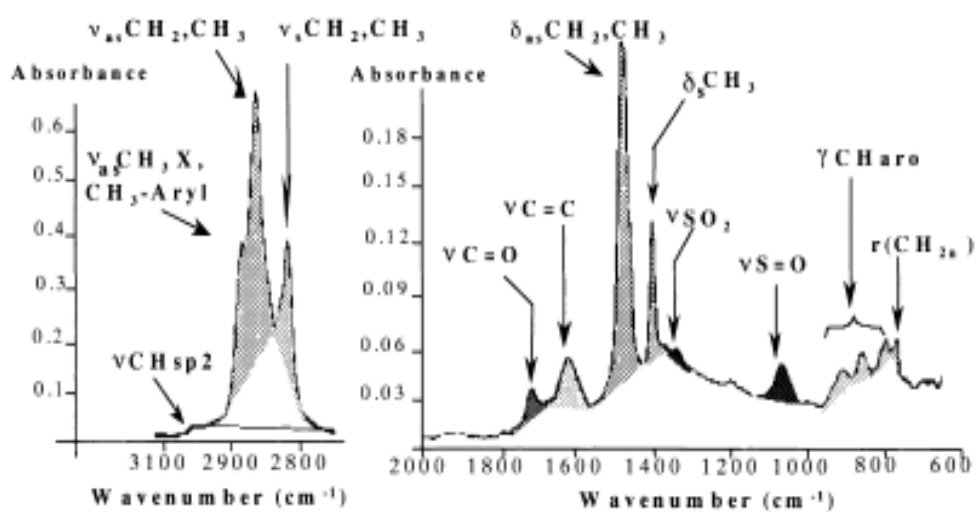


Figure III-14. Example of FTIR Spectrum

The oxygenated functions are identified at a wavelength equal to:

- 1700 cm^{-1} for the Carbonyl group $\text{C}=\text{O}$, that should increase in long-term ageing;
- 1030 cm^{-1} for the Sulphoxide group $\text{S}=\text{O}$ which should increase in short-term ageing⁴⁷.

The structural functions are:

- aromatic structures at 1600 cm^{-1} ($\text{C}=\text{C}$);
- Aliphatics (CH_2 , CH_3) at 1460 cm^{-1} and 1376 cm^{-1} .

⁴⁷ P. Mikhailenko, A. Berton et al, Method for analyzing the chemical mechanisms of bitumen ageing and rejuvenation with FTIR spectroscopy, Conference paper in rilem bookseries, October 2015

The data were analysed thanks the software Essential FTIR[®] that integrates the peaks from valley to valley around a peak. Then, the following indexes were estimated:

- Carbonyl Index: $I_C = \frac{A_{1700}}{\Sigma A}$;
- Sulphoxide Index: $I_S = \frac{A_{1030}}{\Sigma A}$;
- Aliphatic Index: $I_B = \frac{(A_{1460}+A_{1376})}{\Sigma A}$;
- Aromatic Index: $I_{Ar} = \frac{A_{1600}}{\Sigma A}$.

Where $\Sigma A = (A_{2950} + A_{2920} + A_{2850}) + A_{1700} + A_{1600} + A_{1460} + A_{1377} + A_{1030} + A_{870} + A_{810} + A_{743} + A_{723}$.

These values have been calculated twice for each material at all level of ageing: one for the first repetition and one for the second. Average among those two values has been used as a final parameter.

III.3.3 SARA analysis

A valuable contribute to this research is the analysis of the ageing effect on the chemical fractions of the samples. The SARA analysis allows to separate crude oil into fractions of saturate hydrocarbon (saturates), aromatic hydrocarbon (aromatics), resins, and asphaltenes (SARA). In this case, Iatroscan TLC-FID, that combines TLC with flame ionization detection was used. According to this method, four devices works together to produce results: Hydrogen Generator, Iatroscan [Figure III-15], Software Connector (PowerChrom) and the PC, and another machine that is the rods' dryer.

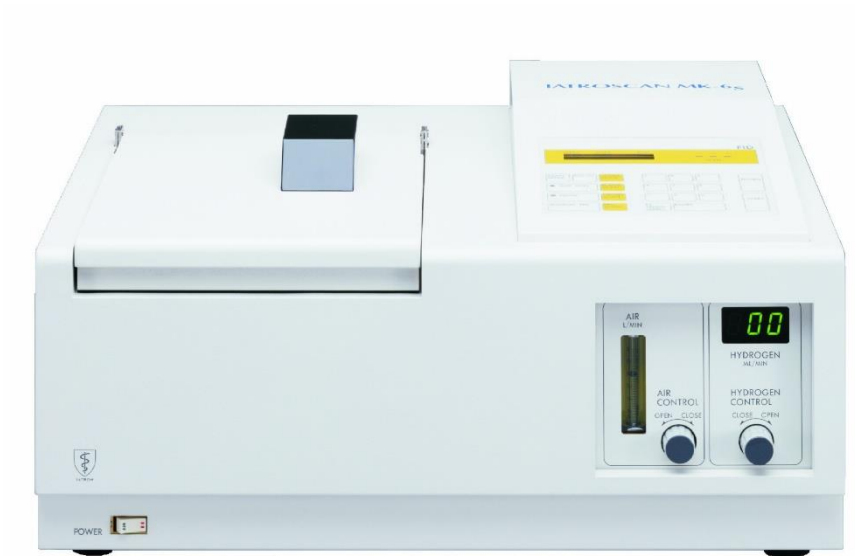


Figure III-15. Iatroscan

In addition, the tools used to develop this test are shown in Figure III-16: ten rods [A] with their supporting frame called shablon [B], forcipes [C], a locker [D]. It is important to hold the rods with forcipes from the transparent part in order to avoid contamination of the rods [E].

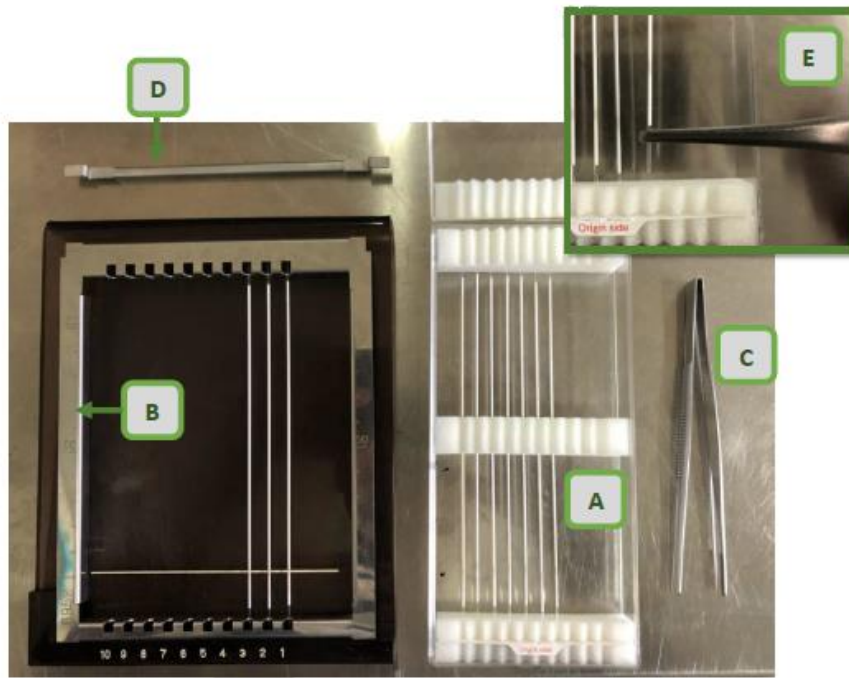


Figure III-16. Tools for SARA analysis

Four types of solvents are needed: n-Hexane, Toluene, Dichloromethane DCM and Methane MeOH. Each of them dissolves only one fraction of the bitumen.

Once all the machines are turned on, the hydrogen flows from the hydrogen generator and goes to the Iatroscan, in which it's possible to turn the hydrogen flame on with a lighter. Before each test, all the rods, placed in the shablon with the forcipes, must be cleaned by the blank scan several times till the spectrum drawn by the software is flat.

For the preparation of the samples, it needs to prepare 0,01 g of bitumen that will be dissolved in 10 ml of DCM for 30 minutes, stirred and shook sporadically. In the meanwhile, it's possible to prepare the containers in which the shablon will be put: preparing the paper that will cover one side of the container [Figure III-17] and measure 70 ml of all the solvent listed before.

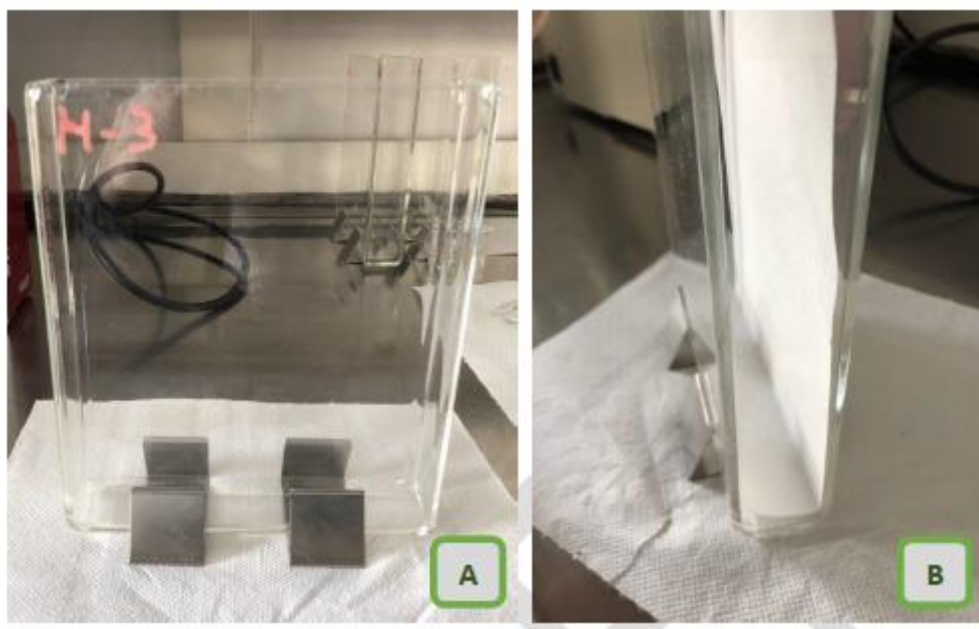


Figure III-17. Solvent container

At the end of this step, there will be the first container with n-Hexane, the second with Toluene and the third filled by 70 ml of a combination of DCM and MeOH in a proportion of 95:5. All the containers must be cover with the proper lid since the solvent evaporates very quickly.

The next step will be putting our sample on the rods. To do that, firstly the shablon should be placed on a plate which indicates with a horizontal line the precise point of the rod in which the sample should be located [Figure III-18- A].

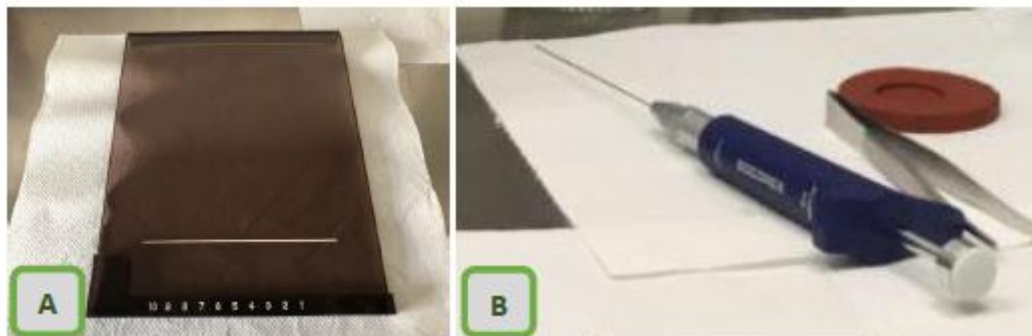


Figure III-18. Plate and injector

To transfer a drop of 1 microliter of sample from the cylinder to the rods, an accurate injector was used [Figure III-18 -B]: by clicking on its handle, it absorbs exactly 1 microliter and then, with another pressure on the handle, the sample drop should be poured on the specific location on rod, indicated by the white horizontal line. During the pouring operation, the rod must be rotated to be evenly distributed. This action should be repeated for all the ten rods.

As just said in the literature review, one of the most important phase of this test is the soaking of the shablon in order to allow the solvent to go through the rod and bring with it the particles. This capillarity effect is highlighted by a graduated frame, in the sense that the rods will stay:

- in the first solvent till the height of the column will reach 90 to 100 mm, that is the maximum height possible for that frame;
- in the second solvent till the column will reach 50 to 60 mm;
- and in the third solvent till 25 to 30 mm.

This technique is controlled by the time the column reaches the proper height, checked it turning a light on the back of the container. Thus, the sequence that must be followed is:

- put the shablon in the n-Hexane (first solvent) for 24 minutes;
- leave the shablon for 2 minutes at room temperature under the fan;

- put the shablon in the Toluene for 8 minutes and 30 seconds;
- insert it in the rods' dryer at 110°C for 2 minutes;
- leave it for 7 minutes at room temperature under the fan;
- put the shablon in the blend of DMC and MeOH for 2 minutes;
- insert it in the rods' dryer at 110°C for 2 minutes;
- and keep it under the fan for 5 minutes at room temperature.

Finally, now it's possible to transfer the rods' container in the Iatroscan, checking if the flame is on, the air flow is 2 l/min and the hydrogen pressure 160 ml/min and to start the flame ionization detection.

The software automatically integrates the areas under the four peaks and so it gives four values for each rod. At this point, the average and the standard deviation of each peak must be estimated. Comparing the results of each peak with the average and standard deviation allow to choose five over ten rods. The last step is to calculate the average of the areas of the selected rods. Finally, a Gaestel Index is evaluated, that is the colloidal index I_C .

III.4 Rheology

Investigating the rheological characteristics of BioPhalt® and the standard bitumen means analysing their master curve and black diagram, obtained with the Dynamic Shear Rheometer, DSR.

To better understand their behaviour, it is worth analysing the materials in their linear viscoelastic field, that is the range of strains in which the Complex Modulus G^* is constant. A primary Amplitude Sweep is needed in order to find the values of strain with those characteristics required in the second step: the Frequency Sweep.

The Amplitude Sweep is an oscillatory test in which the samples are subjected to a load – in this case strain – with oscillation in the amplitude but constant in the frequency. A typical plot of the Amplitude Sweep results represents the trend

of G^* versus the strain in a bi-logarithm scale, as shown in the Figure III-19. **Error. L'origine riferimento non è stata trovata.** as an example:

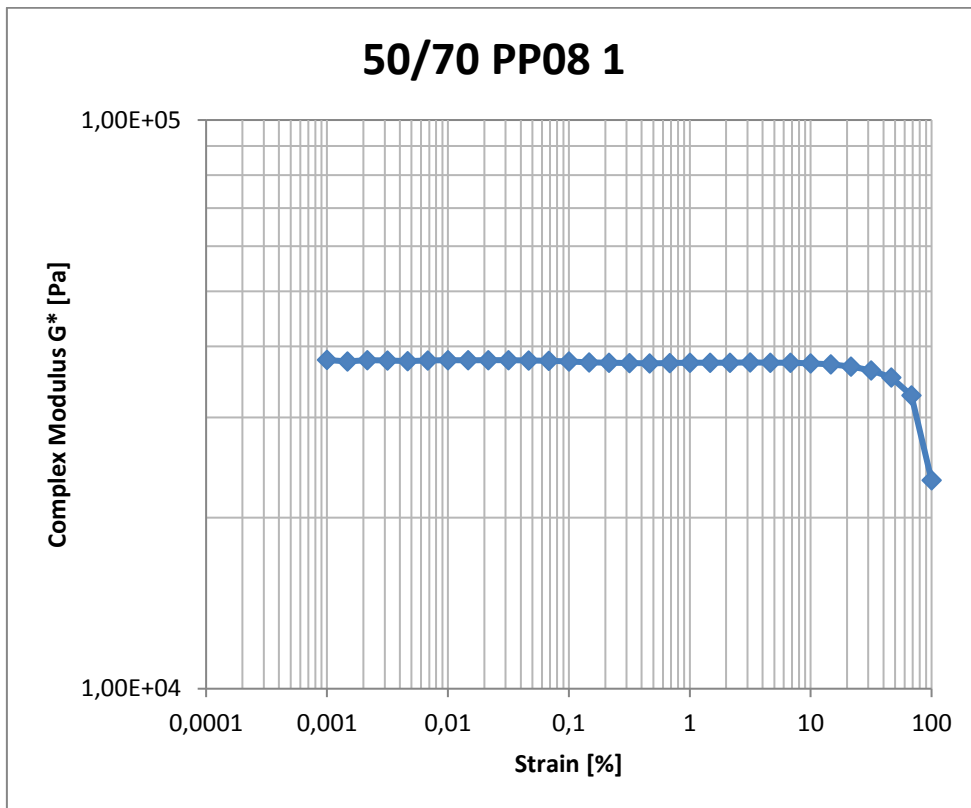


Figure III-19. Example of AS plot

The range of the strain is composed of the first γ value without noise, thus greater than 0.1% and the correspondent value to 95% of G^* . In that interval, G^* should be constant and so it's possible to select the strain that will ensure the linear viscoelastic response of the Frequency Sweep.

The following table summarise the values of strain, called γ_{LVE} , later used for the Frequency Sweep [**Error. L'origine riferimento non è stata trovata.**].

Table 2. Amplitude Sweep Results

Frequency [rad/s]	T [°C]	C	C RTFO	BP	BP RTFO
		γ_{LVE} (%)	γ_{LVE} (%)	γ_{LVE} (%)	γ_{LVE} (%)
1	4.00	2.7E-01	2.2E-01	3.7E-01	3.2E-01
100	4.00	1.4E-01	1.3E-01	2.1E-01	1.8E-01
1	10.00	3.8E-01	3.1E-01	5.7E-01	5.0E-01
100	10.00	1.8E-01	1.7E-01	2.7E-01	2.4E-01
1	16.00	5.2E-01	4.2E-01	8.4E-01	7.4E-01
100	16.00	2.4E-01	2.2E-01	3.6E-01	3.2E-01
1	22.00	7.3E-01	5.8E-01	1.2E+00	1.1E+00
100	22.00	3.1E-01	2.8E-01	4.7E-01	4.2E-01
1	28.00	1.0E+00	7.9E-01	1.7E+00	1.6E+00
100	28.00	4.0E-01	3.5E-01	6.2E-01	5.6E-01
1	34.00	1.4E+00	1.1E+00	2.4E+00	2.2E+00
100	34.00	5.1E-01	4.5E-01	8.2E-01	7.5E-01
1	40.00	1.9E+00	1.5E+00	3.4E+00	3.1E+00
100	40.00	6.7E-01	5.7E-01	1.1E+00	9.9E-01
1	46.00	2.7E+00	2.0E+00	4.7E+00	4.3E+00
100	46.00	8.6E-01	7.2E-01	1.4E+00	1.3E+00
1	52.00	3.7E+00	2.8E+00	6.4E+00	6.0E+00
100	52.00	1.1E+00	9.2E-01	1.9E+00	1.8E+00
1	58.00	5.2E+00	3.8E+00	8.7E+00	8.2E+00
100	58.00	1.4E+00	1.2E+00	2.5E+00	2.3E+00
1	64.00	7.2E+00	5.2E+00	1.2E+01	1.1E+01
100	64.00	1.9E+00	1.5E+00	3.3E+00	3.1E+00
1	70.00	1.0E+01	7.2E+00	1.6E+01	1.5E+01
100	70.00	2.4E+00	1.9E+00	4.3E+00	4.1E+00
1	76.00	1.4E+01	9.8E+00	2.1E+01	2.0E+01
100	76.00	3.2E+00	2.4E+00	5.7E+00	5.5E+00

For the binders aged at PAV and analysed in Nottingham, after having performed the Amplitude Sweep, a unique value of γ equal to 0.4% was selected.

III.4.1 Frequency Sweep

A Frequency Sweep is an oscillatory test method for the determination of the Complex Shear Modulus G^* and Phase Angle δ of binders over a range of temperatures and frequencies. In addition, the value of the load – the strain – ensures that this test is developed in the linear viscoelastic region of the material.

After collecting the data, it's necessary to model them in order to provide G^* , δ and the parameters useful to explain and/or predict the ageing behaviour of the materials, as the Glassy Modulus G_g , the crossover frequency ω_c and the rheological index R , as shown in Figure III-20.

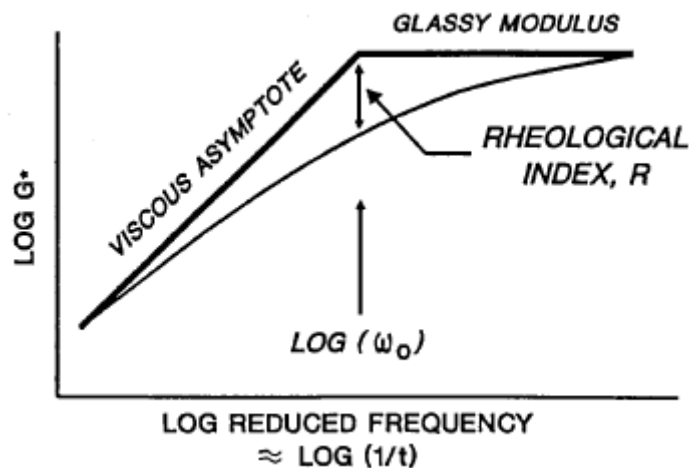


Figure III-20. Example of master curve⁴⁸

The results from the Frequency Sweep test are plotted in a bi-logarithmic scale where on the y axis there is the G^* and on the x-axis there is the frequency. For the limitation of the test machines, it is possible to investigate the material only in a very restrict interval of the frequency. To overcome this problem, the principle of time-temperature superimposition principle is used. It dictates that the results from the investigation at low frequency are identical to the one at high temperature and vice versa. Therefore, took one curve as a reference, it's

⁴⁸ D. W. Christensen, D.A. Anderson, Interpretation of dynamic mechanical test data for paving grade asphalt cements, 1992

possible to shift the other curves with respect to the reference one toward right if the test temperature is lower, whereas to left if the test temperature is higher. From the mathematical point of view, every single point of the curve is individuated by two coordinates: the $\log G^*$ as y and the $\log \omega$ as x. The principle of time-temperature superimposition principle, or method of reduced variables, dictates that the curves preserve the y but they will be shifted along the x axis according to shift factors, until the curves merge into a single, smooth curve. To shift the curve, shift factors are provided by viscoelastic functions for all the test temperatures: the equation of William Landel Ferry model will be used, at 4, 10, 16, 22, 28, 34, 40, 46, 52, 58, 64, 70, 76°C:

$$\log(a_T) = \frac{-C_1(T - T_r)}{C_2 + (T - T_r)}$$

T_r is the reference temperature equal to 34°C and C_1 and C_2 are two coefficients respectively equal to 12 and 110. Obviously, at 34°C the shift factor $a_t = 0$. Once plotted the value, it is possible to change manually the value of a_t and then minimize the sum of the squared difference: with the latter operation, the coefficient will change according to the characteristics of the materials. Now, the reference frequency ω_r can be estimated and it's possible to apply the Christensen Anderson Marasteanu model CAM, with the equations:

$$|G^*| = G_g \left[1 + \left(\frac{\omega_r}{\omega} \right)^{\frac{\log 2}{R}} \right]^{\frac{mR}{\log 2}}$$

$$\delta = \frac{90m}{\left[1 + \left(\frac{\omega}{\omega_r} \right)^{\frac{\log 2}{R}} \right]}$$

Therefore, the sum of the squared difference between the experimental value and the one from the CAM model will be computed for both G^* and δ . In the next chapter the result will be analysed and compared among the ageing level.

III.5 Performance

In this section, all the representative tests of the main roads' distress will be elucidated. Here a summary of the following paragraph:

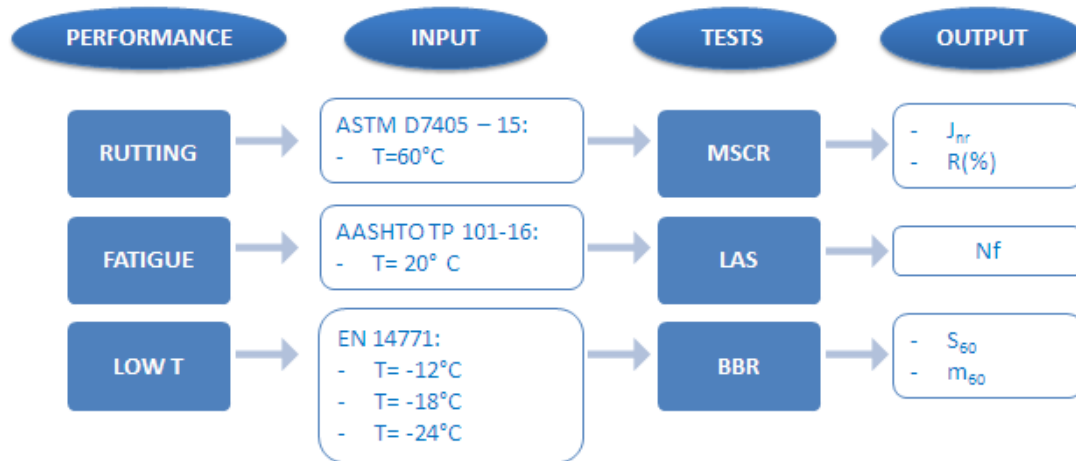


Figure III-21. Performance related test

III.5.1 Rutting

To studying the anomalies of the pavement due to permanent deformation at high temperature is possible to perform the Multi-stress Creep and Recovery (MSCR) Test, which is currently being considered as a replacement for the Superpave high temperature binder criteria $G^*/\sin\delta$.⁴⁹

The MSCR is a creep and recovery test that is conducted using a DSR and 25 mm parallel plate geometry, following the standard ASTM D7405 – 15. The test protocol requires 10 cycles of a creep load of 1 second duration followed by recovery at zero load maintained for 9 seconds, for two stress levels: 0.1 KPa and 3.2 KPa [Figure III-22 **Errore. L'origine riferimento non è stata trovata.**].

⁴⁹ J. A. D'Angelo, The Relationship of the MSCR Test to Rutting, in Journal Road Materials and Pavement Design, Volume 10, 2009.

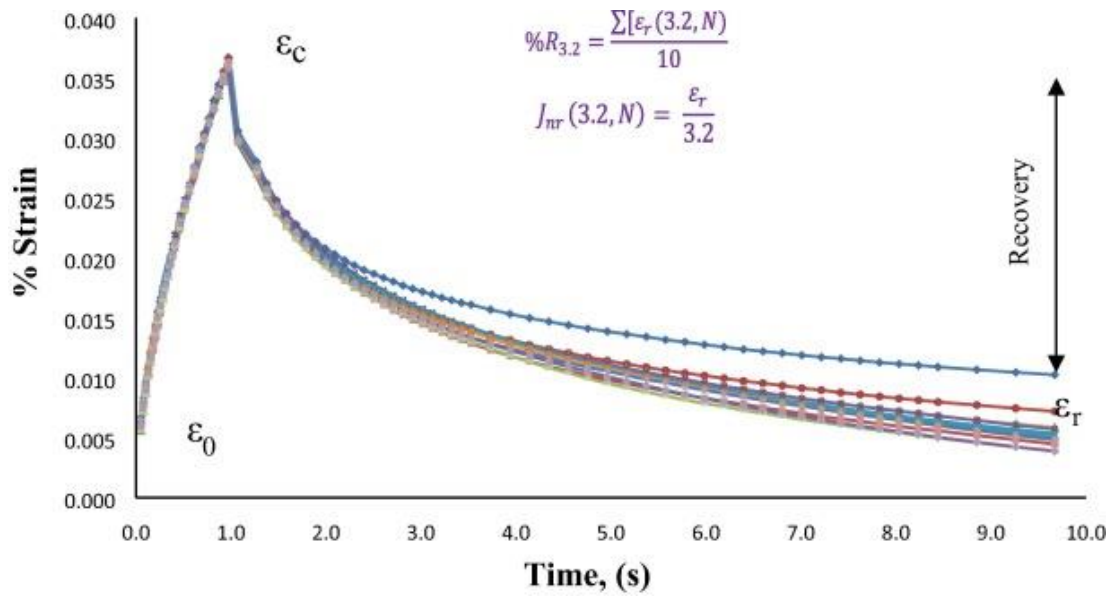


Figure III-22. Example of MSCR's results

Permanent deformation is more critical when the asphalt is softer due to high temperatures. For this test a representative value of temperature at which the rutting distress could start was chosen, equal to 60°C.

The MSCR test provides two principal parameters: the non-recoverable creep compliance (J_{nr}), that is the residual strain in a specimen after a creep and recovery cycle divided by the stress applied in KPa and the percentage of recovery %R, that is the ratio between the recovered strain in a cycle over the accumulated strain in the same cycle.

To evaluate them, the following values are needed: the strain at the beginning of the cycle ϵ_0 , the value of the strain at the end of the creep ϵ_c , their difference ϵ_1 that is the strain accumulated during the load time, the residual strain after one cycle ϵ_{10} and the accumulated residual strain ϵ_r .

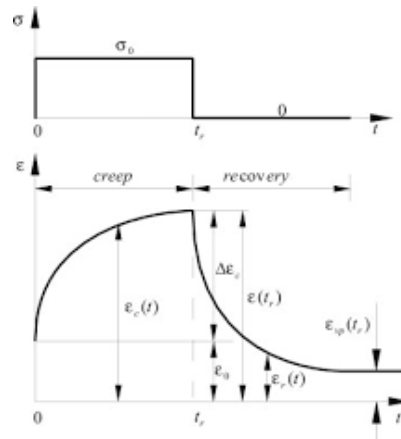


Figure III-23. Example of strains

Having those values, the %R and the J_{nr} are easily computed for both level of stress, thanks to:

$$J_{nr} = \frac{\varepsilon_{10}}{\text{level of stress}} \cdot 100$$

$$\%R = \frac{\varepsilon_1 - \varepsilon_{10}}{\varepsilon_1} \cdot 100$$

Two replicates per material at each level of ageing were performed.

III.5.2 Fatigue

The fatigue damage is more frequently among pavements that has been in the field for several years. Nevertheless, for the purpose of this research fatigue test will be conducted for all the level of ageing. The determination of the asphalt binder resistance to fatigue damage is provided by the Linear Amplitude Sweep LAS that applies a cyclic loading with linearly increasing amplitudes at a constant frequency on the samples. This causes an accelerated fatigue damage.

The test is run by the DSR following the standard *AASHTO TP 101-12 (2016)*, that considers the utilisation of the 8 mm spindle.

Two types of testing are performed in succession. The first is a frequency sweep in which the rheological properties of asphalt sample were tested: a strain load

with amplitude equal to 0.1% is applied on the asphalt sample at a frequency range of 0.2–30 Hz. At each frequency, the dynamic shear modulus and phase angle of the non-damaged binders were measured and recorded. The second test consist of an amplitude sweep: at 10 Hz frequency, continuous oscillatory loading cycles with linearly increasing strain amplitudes from 0 to 30% were applied to cause accelerated fatigue damage.

Based on the AASHTO recommendation, the test must be performed at the intermediate temperature of the pavement, thus 20°C was chosen. The fatigue resistance was then calculated from rheological properties and the amplitude sweep results. The parameters provided by this test are the number of cycles to failure and the accumulation of damage.

Based on the VECD theory, damage accumulation at each data point is calculated using the following equation (Hintz, Velasquez, Johnson, et al.,2011):

$$D(t) \cong \sum_{i=1}^N [\pi I_D \gamma_0^2 (|G^*| \sin \delta_{i-1} - |G^*| \sin \delta_i)]^{\frac{\alpha}{1+\alpha}} (t_i - t_{i-1})^{\frac{1}{1+\alpha}}$$

For the fatigue performance parameter N_f , the following equation was used:

$$N_f = A_{35}(\gamma)^{-B}$$

Where A_{35} depends on the Damage at failure D_f and other coefficients.

For each material at each level of ageing, two replicates were performed.

III.5.3 Low Temperature Cracking

The low temperature cracking of the asphalt bitumen is governed by the flexural stiffness S and the creep ratio m , provided by the Bending Beam Rheometer test machine. In fact, at low temperature, the bitumen's stiffness is very high and becomes almost comparable to the machines' one: performing shear test can result in measuring the strain of the machines. To solve this inconvenient, bitumen's properties at low temperatures are investigated measuring the

flexural creep stiffness of a bending beam: the name of the test is Bending Beam Rheometer.

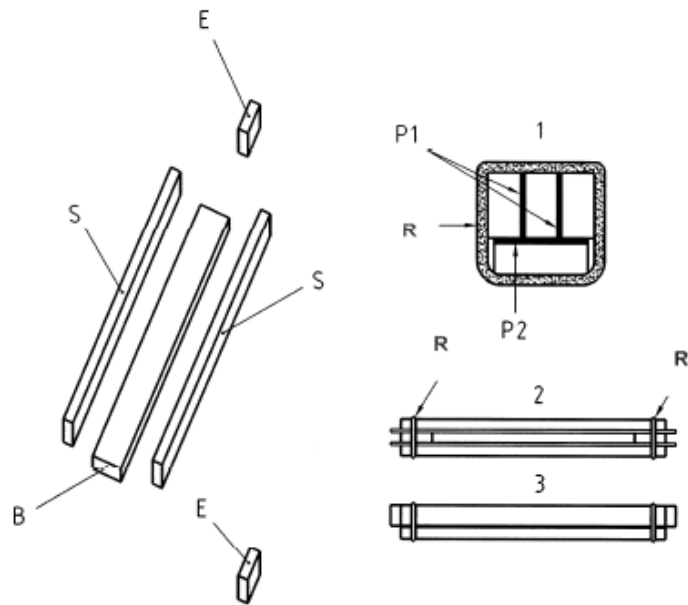
The test machine consists of: loading frame, controlled temperature bath; computer-based acquisition and test control system; calibration and verifications items; moulds for forming test specimens. [Figure III-24 **Errore. L'origine riferimento non è stata trovata.**]. A low temperature liquid bath is used to control the temperature.



Figure III-24. Bending Beam Rheometer

The preparation of the specimen requires a lot of caution and, at the end, the specimen must be carefully inspected before using.

According to *BS EN 14771:2012*, firstly it is necessary assembling the mould, which are composed of 5 pieces of steel, plastic strips and two o-rings, as shown in Figure III-25 from (a) to (c).



Key

- | | | | |
|----|--|---|---------------------------|
| B | metal base bar 6,4 mm × 19,1 mm × 165,0 mm | 1 | enlarged end view |
| S | metal side bar 6,4 mm × (12,7 mm ± 0,1 mm) × 165,0 mm | 2 | top view assembled mould |
| E | metal end pieces (6,4 mm ± 0,1 mm) × 12,7 mm × 19,0 mm | 3 | side view assembled mould |
| P1 | plastic strips 12,7 mm × 178,0 mm | R | O-ring |
| P2 | plastic strips 19,1 mm × 165,0 mm | | |

NOTE Approximate dimensions are shown if a tolerance is not given.

(a)



(b)



(c)

Figure III-25. Mould for beam specimen

All the steel pieces must be spread of glycerol-talc blend to avoid adhesion between bitumen and the mould. Once the asphalt binder is hot enough to be poured, the mould must be slightly overfilled by the material and then leaved at room temperature for 60 minutes to cool down. [Figure III-26].



Figure III-26. Specimens at room temperature

After that, it's possible to trim the excess of binder [Figure III-27], put the mould in the bath for less than 5 minutes and then demould them [Figure III-28].



Figure III-27. Trimming

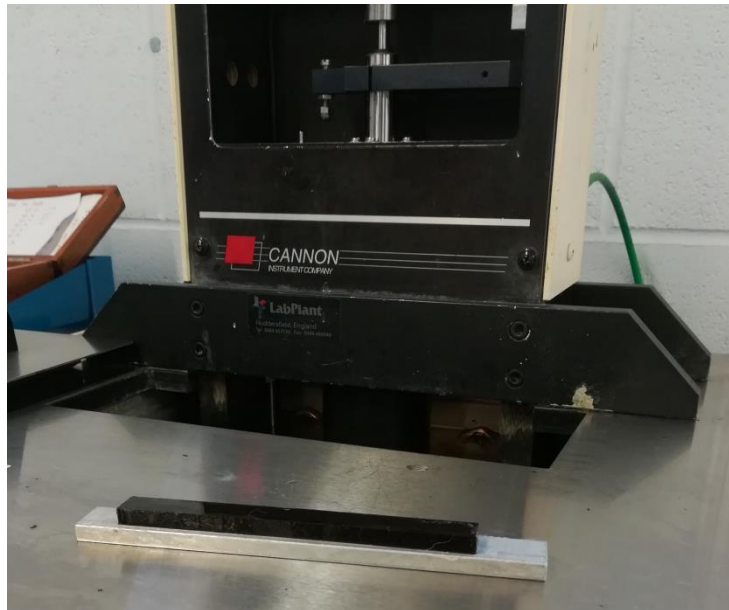


Figure III-28. BBR Specimen

The test procedure is based upon the measurement of the deflection of the midpoint, in three-point deflection, of the specimen during the application of a constant load for a specific duration. The load and deflection are used to calculate the maximum stress and strain in the beam and the stiffness is computed by dividing the maximum stress, that could be at the top of the beam (compression) or at the bottom (tension), by the maximum strain. For the stress:

$$\sigma = \frac{3PL}{2bh^2}$$

Where:

- σ = maximum stress at the top or bottom of beam, Pa;
- P = constant load, N;
- L = distance between supports, m;
- B = width of the beam, m;
- H = thickness of the beam, m.

For the strain:

$$\varepsilon = \frac{6\delta h}{L^2}$$

With:

- ε = maximum strain;
- δ = Deflection at 8, 15, 30, 60, 120 seconds, mm.

The modulus of the stiffness S , in MPa, is the fraction:

$$S = \frac{\sigma}{\varepsilon} = \frac{PL^3}{4b\delta h^3}$$

In addition, the plot of the Stiffness on a logarithm scale versus the time in seconds gives further information, as the m -value that is the absolute value of the slope of the curve and represents the time in which the stress in a certain material relaxes. Greater is m , less susceptible the pavement is to low temperature cracking.

In this experimental programme three test temperatures were chosen in order to be able to build a trend of the low-temperature behaviour of the binder.: -12°C, -18°C and -24°C Two repetition for all the materials were performed.

In the following chapter, all the result will be presented, explained and compared in order to understand the effect of ageing on the non-bituminous binder with respect the effect on the standard bitumen.

Chapter IV

EVALUATION OF THE EFFECT OF AGEING

This chapter develops the core of this research project: the evaluation of the ageing effect on non-petroleum based bitumen for paving application.

The evaluation is based on several aspects. First of all, an in-depth analysis of the aged BioPhalt® under the rheological, mechanical and chemical point of view. Moreover, the assessment is enriched by the comparison between the BioPhalt® and the control bitumen properties, aged at short and long term. Finally, a brief valuation of which is the material that behaves better under each condition is provided.

To allow an easy and clear analysis of the bitumens' properties, the Ageing Index has been introduced. It indicates the percentage of increase or decrease of parameters with respect ones at not-aged state. The Ageing Index is the ratio between the difference of the value of a certain parameter at aged state minus the parameter of the neat bitumen, and the value of the parameter at not-aged state.

For example, to monitor the evolution in time of the non-recoverable creep compliance, the following Ageing Index is used:

$$AI_{Jnr} = (Jnr_i - Jnr_{ORIG}) / (Jnr_{ORIG})$$

Where *i* could be either RTFO, PAV or the second cycle of PAV, called 2PAV.

The results are presented below.

IV.1 Rheological parameters

The rheological behaviour of the material is represented by its Master Curve, in which it is possible to observe the trend of the Complex Modulus G^* and the phase angle δ versus the frequency ω .

On neat binders, the effect of ageing is hardening them and makes them brittle. This is translated into an increase of G^* and elastic components of the bitumen, with a consequent decrease of phase angle δ . Therefore, the complex modulus moves close to the asymptote of the elastic behaviour that is independent from the frequency. The rheological index R increases since the curves become flatter with ageing process. The phase angle moves from higher values (maximum 90°) towards lower value (minimum 0°), since the elastic response to load prevails with respect to the viscous behaviour. Consequently, the lag in deformation represented by δ decreases. In addition, with ageing the values of phase angle are shifted to lower frequencies and this means that higher temperatures are needed to reach that value of δ .

The results of these changes are that the non-modified bitumens approach to solid-like behaviour. The confirmation of what just discussed is given by the plots of the 50/70 pen. bitumen, that is considered the referent material in this study. From now this control binder will be identified with “C”.

The following plots, Figure IV-1 and Figure IV-2, show the master curve and the phase angle of control binder at not aged, RTFO, PAV and 2PAV ageing state.

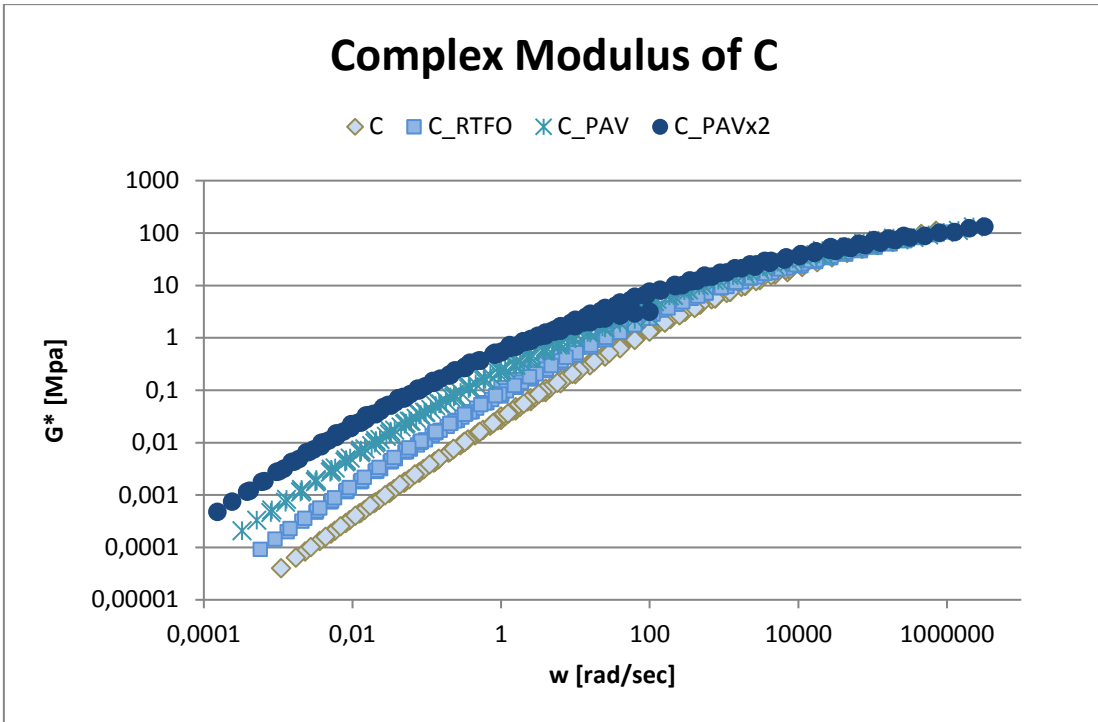


Figure IV-1. Complex Modulus of C

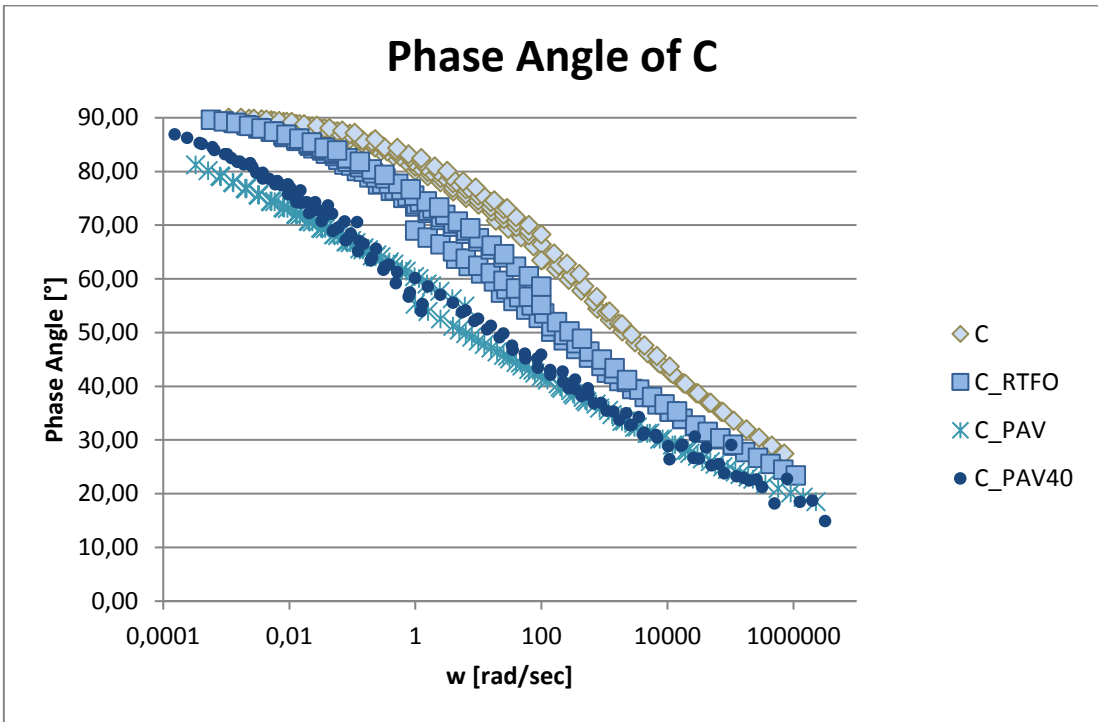


Figure IV-2. Phase Angle of C

Regarding the effect of ageing on BioPhalt®, from now individuated by BP, its master curve follows the trend just described, that is flattening and increasing of G^* , for the vast majority of frequencies apart from the low ones.

Therefore, more attention is paid to the values of G^* and δ at low ω , that, for the time-temperature superimposition principle, correspond to high temperature. The Figure IV-3 shows an inversion of the behaviour from the value of frequency equal to 100 rad/sec. This means that the response of BioPhalt® to load applied at low ω or at high temperature becomes more viscous with ageing. In fact, as G^* is more aged, it moves closer to the viscous asymptote. Therefore, an unusual behaviour of BioPhalt® at high temperature is expected.

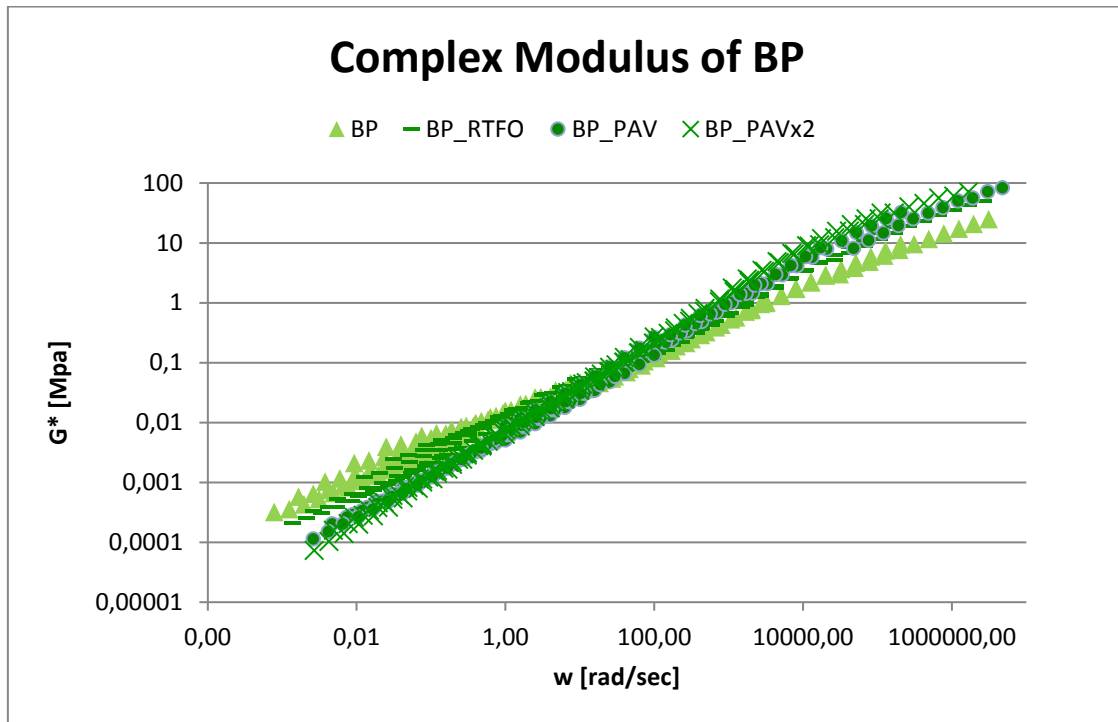


Figure IV-3. Complex Modulus of BP

The same aspect can be evaluated also looking at the plot of the Phase Angle δ versus the frequency [Figure IV-4]

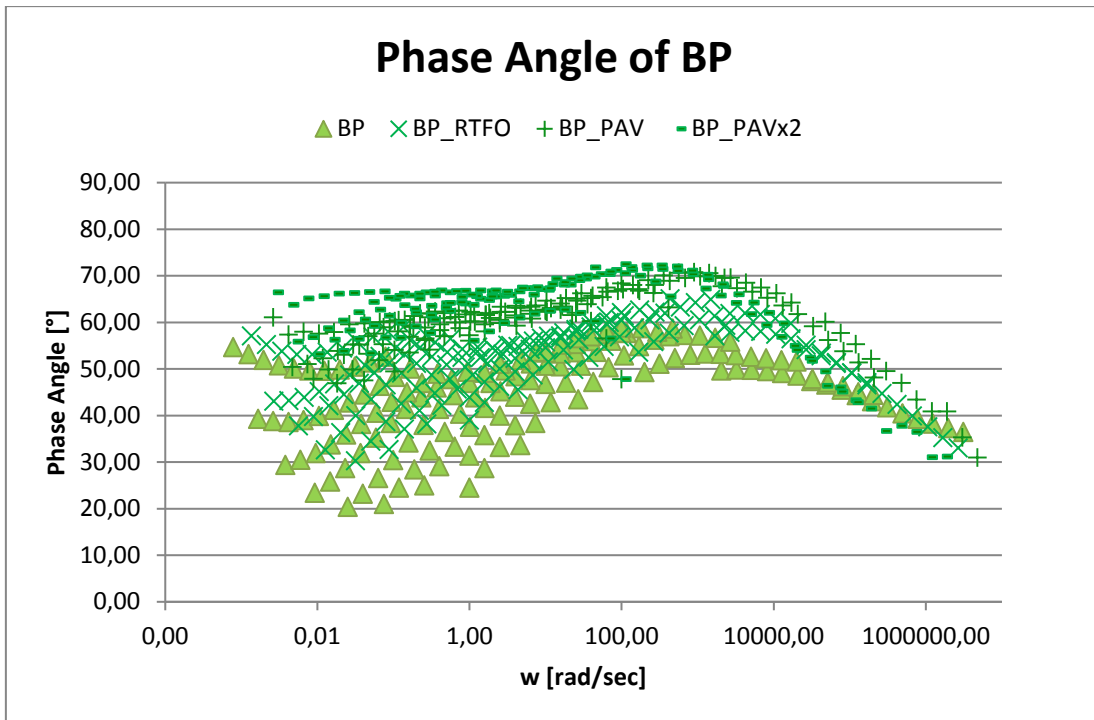


Figure IV-4. Phase Angle of BP

The unusual shape of the plot is typical of a strongly modified bitumen. The implication of this is that it wasn't possible to model the phase angle of BioPhalt® with CAM model.

It is worth focusing on the fact that δ increases with ageing to understand the behaviour of the material. When a load is applied to BP, especially at low ω , its deformation appears after a bigger lag than C. In other words, the more aged the BioPhalt® is, the more viscous component there are.

An easier representation that allow to make the comparison between the material is provided below, in Figure IV-5.

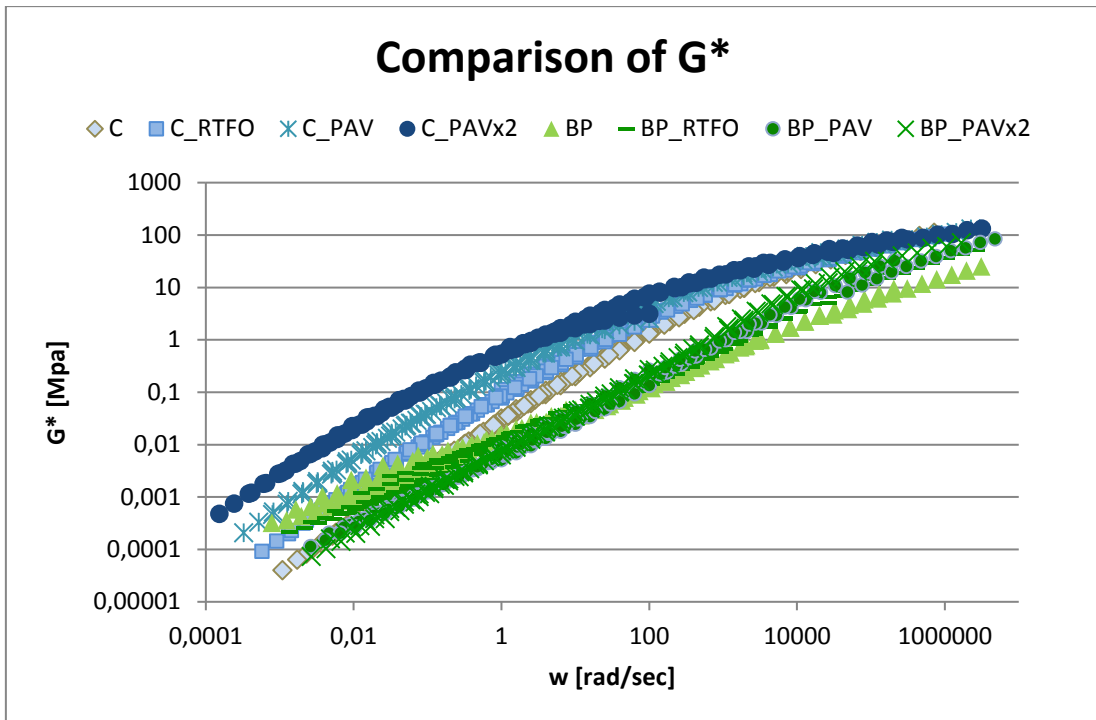


Figure IV-5. Comparison of G^*

Thank to Figure IV-5, it is possible to state: firstly, that G^* of C is generally greater than G^* of BP apart from the lower ω . This involves that the vegetable pitch is a softer bitumen.

In addition, the R index of C increases changing the ageing state whereas the BioPhalt®'s one doesn't follow a trend, as displayed in Table 3.

Table 3. Comparison of Rheological Index R

	C	BP
Orig	1.45	0.22
RTFO	1.71	0.19
PAV	2.38	0.49
PAVx2	2.47	0.36

Another graph from which it is possible to extrapolate information is the Black Diagram: G^* versus δ .

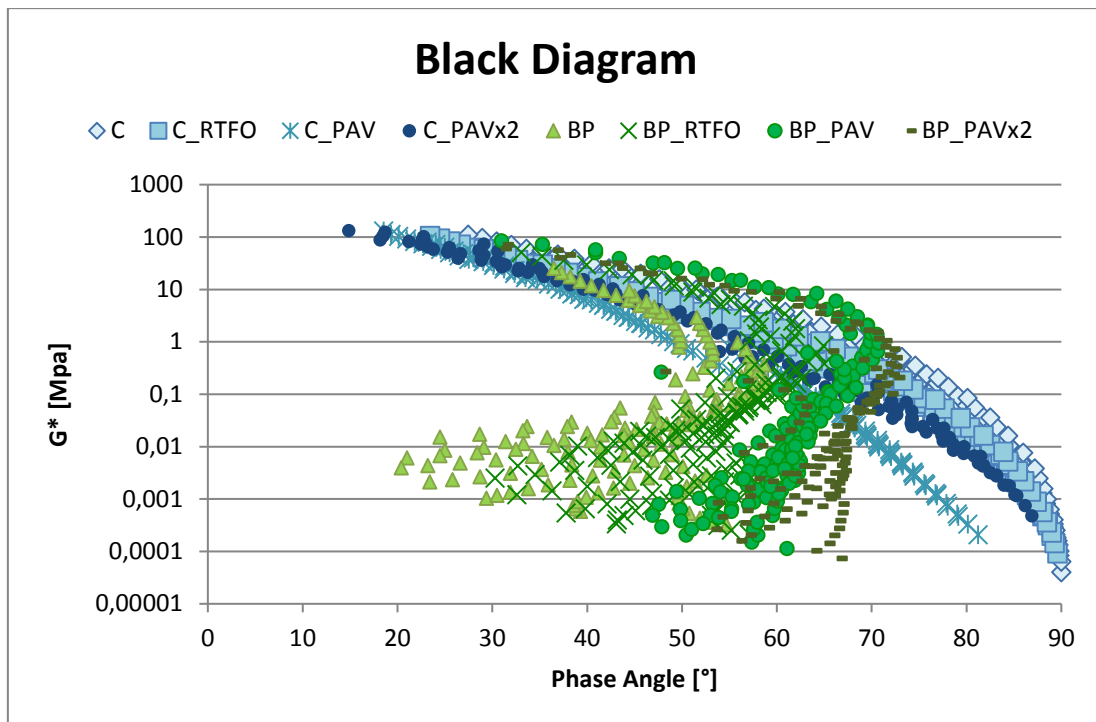


Figure IV-6. Black Diagram

This diagram clearly illustrates that the viscous component of aged BP is prevalent over the elastic one since the curve is shifted to the right, moving close to higher values of δ .

Moreover, at lower values of G^* , usually related to high temperature, there is a very important inversion in the behaviour of BP, that is the one seen previously.

This uncommon behaviour will be discussed later on, with the comments on the MSCR's results.

IV.2 Performance related parameters

The service life of asphalt pavement can depend on many factors including the traffic loading, the environment, the ageing state, the drainage and the quality of construction.

It is generally recognised that, among the materials which compose the asphalt mixture, the contribution of the bitumen plays a leading role in viscous response of pavements.

In the laboratory, bitumens are treated in order to represent the “in-field” conditions. For example: traffic load=loading time/frequency, environment=temperatures, ageing state=ageing level. In the laboratory tests, they are represented by changing the loading time/frequency condition,

This section presents the results of the evolution with ageing of the representative parameters for pavement distress: rutting at high temperature, fatigue cracking at medium temperature and low temperature cracking.

IV.2.1 *Permanent Deformation*

It is well recognised that the non-recovered deformation of binders has a considerable influence on pavement rutting performance. The multiple stress creep-recovery (MSCR) test was introduced to study this aspect: it provides parameter such as the non-recoverable creep compliance J_{nr} and the percent of recovery %R.

J_{nr} is the average of the residual strain in a specimen after 10 creep and recovery cycles divided by the stress applied in KPa that can be either 0.1 KPa to remain in the linear viscoelastic field and 3.2 KPa for the non-linear behaviour. The equations are:

$$J_{nr \text{ at } 100\text{Pa}} \text{ (1/KPa)} = \frac{1}{10} \left(\sum_{i=1}^{10} \frac{Y_{(nr)i}}{0.1} \right)$$

$$J_{nr \text{ at } 3200 \text{ Pa}} \text{ (1/KPa)} = \frac{1}{10} \left(\sum_{i=1}^{10} \frac{Y_{(nr)i}}{3.2} \right)$$

The lower is J_{nr} , the less prone to rutting the material is and so the longer the pavement’s life is.

Several studies proved that this factor tends to decrease with ageing. In fact, rutting is more severe during the preliminary stage of pavements since bitumen is still

soft and more viscous. On the other hand, ageing hardens the binders and so the residual strain decreases during this process.

Furthermore, in neat and original bitumen there is no differences between the two level of stresses.

The results obtained from the MSCR of bitumen C regarding the Jnr confirm what anticipated:

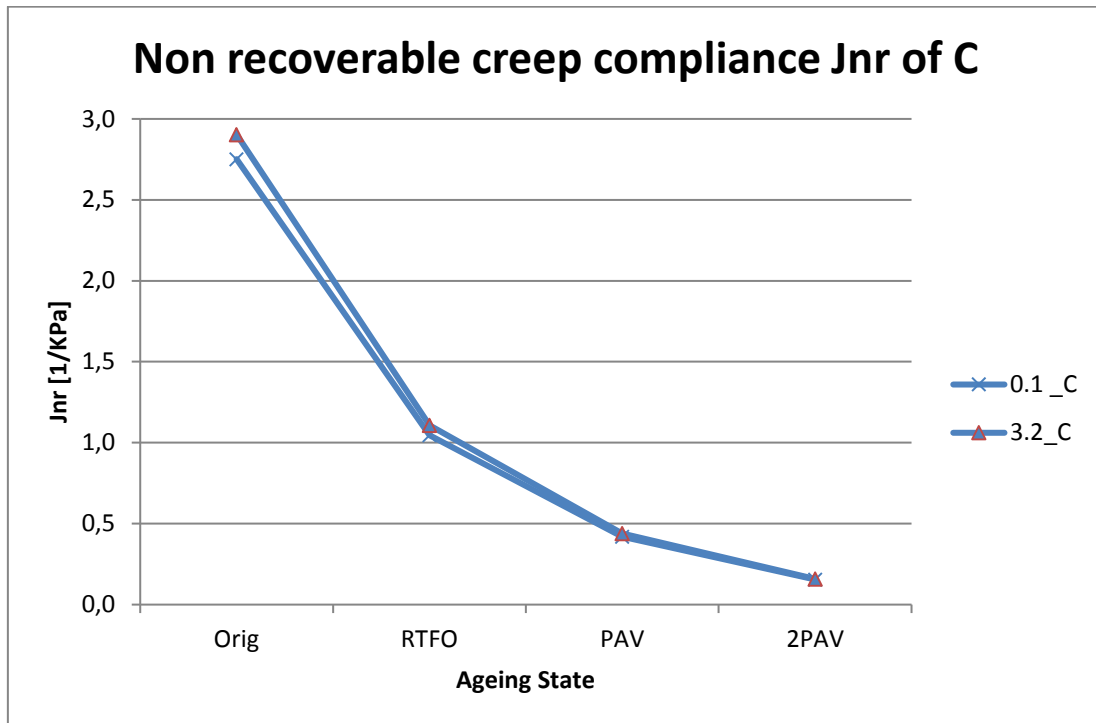


Figure IV-7. Jnr of C

On the other hand, the percent of recovery %R is intended to provide a means to determine the presence of elastic response and stress dependence of polymer modified and unmodified asphalt binders. In fact, %R represents the ability the material has to recover the impressed deformation. The question is:

$$\text{Recovery \% at 100 Pa or 3200 Pa} = \frac{1}{10} \left\{ \sum_{i=1}^{10} \frac{Y_{(r)i}}{Y_{(t)i}} \right\} * 100$$

In this case, the more the binder is aged, the more the %R is. So %R tends to increase with ageing. In addition, in common binders, %R isn't sensitive to level of stress.

As a proof of that, Figure IV-8 shows that the binders become more elastic with time and so they are able to recover more deformation.

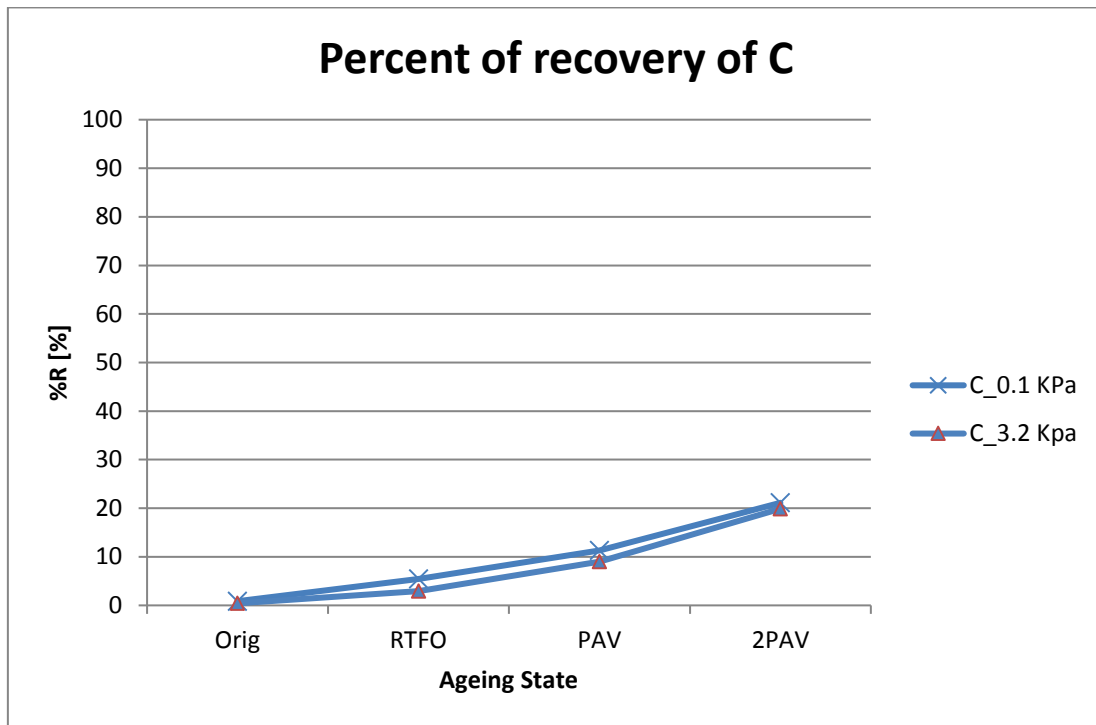


Figure IV-8. %R of C

As expected from the master curve's results, BioPhalt® behaves in a totally different way with respect to the common binders.

The first difference is that Jnr of BP increases with ageing [Figure IV-9]. In this way, the problem of rutting gets worse with time and it is not anymore only a short-term problem: the most severe conditions are shifted to the long term ageing.

This weird behaviour is confirmed by the BP's phase angle trend. Its plot reveals an increase in δ with time and so a liquid-like behaviour of this material.

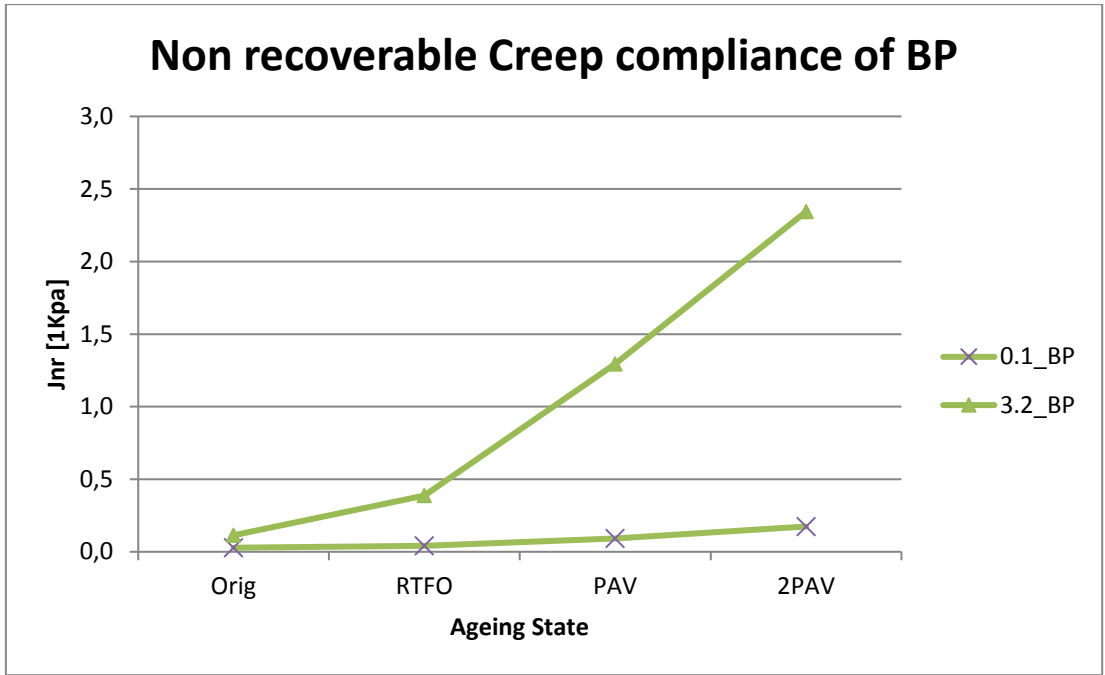


Figure IV-9. Jnr of BP

Regarding the %R results of BioPhalt®, it is possible to state that BioPhalt® has a great capacity to recover deformation, with peak also equal to 97.73% at 0.1 KPa in the original state. Unfortunately, %R of BP follows an opposite trend with respect the one that is appropriate: it decreases with ageing [Figure IV-10]. Also here, the materials loose his elasticity with time and the viscous component is predominant.

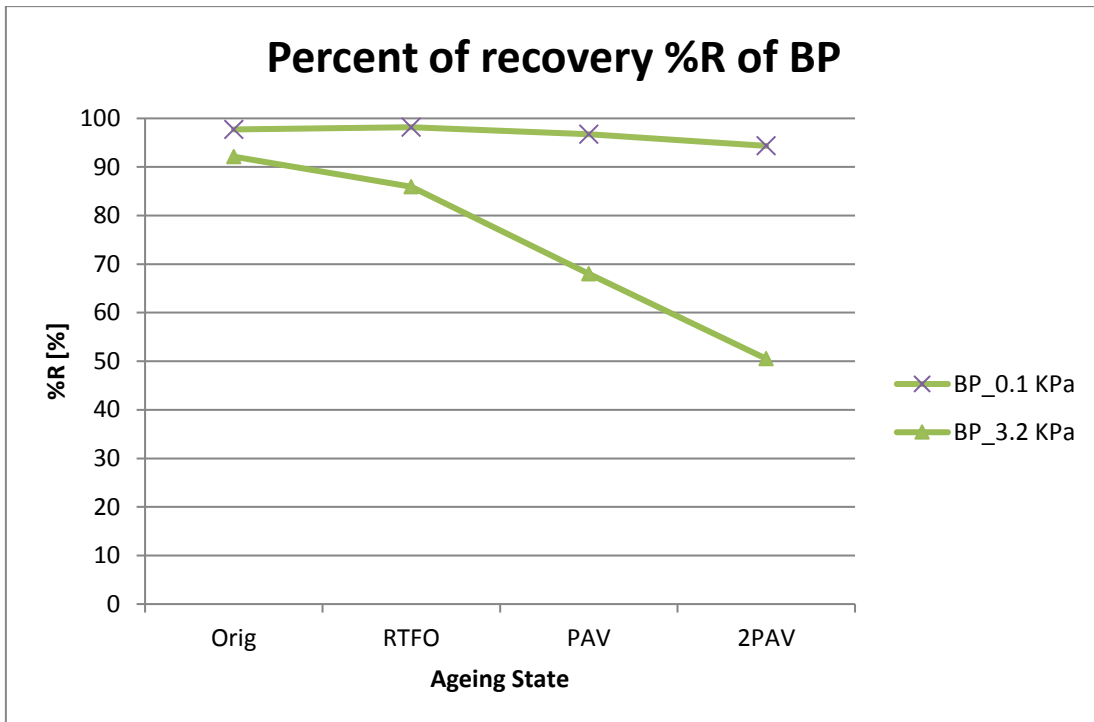


Figure IV-10. %R of BP

Another observation is that BP is strongly dependent on the stress level, that is related to non-linear viscoelastic field. This means that BP gives different results if tested under non-linear conditions. Despite the alterations, it is possible to state that the trends are the same in both conditions.

The comparison among the two materials allow to have a clear idea of both behaviours and, eventually, to choose one of them according to the requirements.

Regarding the Jnr:

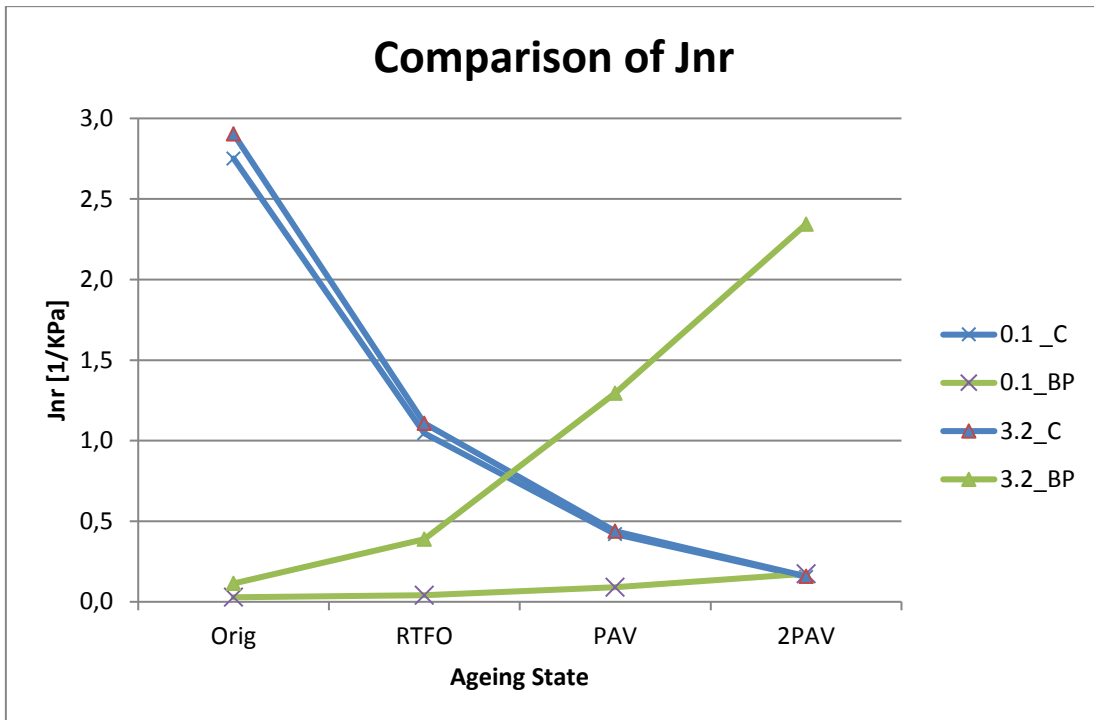


Figure IV-11. Comparison of Jnr

BioPhalt® showed a strong dependency to stress level. From Figure IV-11, it is noticed that, at 0.1 KPa the BioPhalt has lower Jnr and so, in linear viscoelastic field, BP is preferable. For 3.2 KPa, the BioPhalt behaves better only at short term ageing but, from the PAV, the control binder is better.

Regarding the %R:

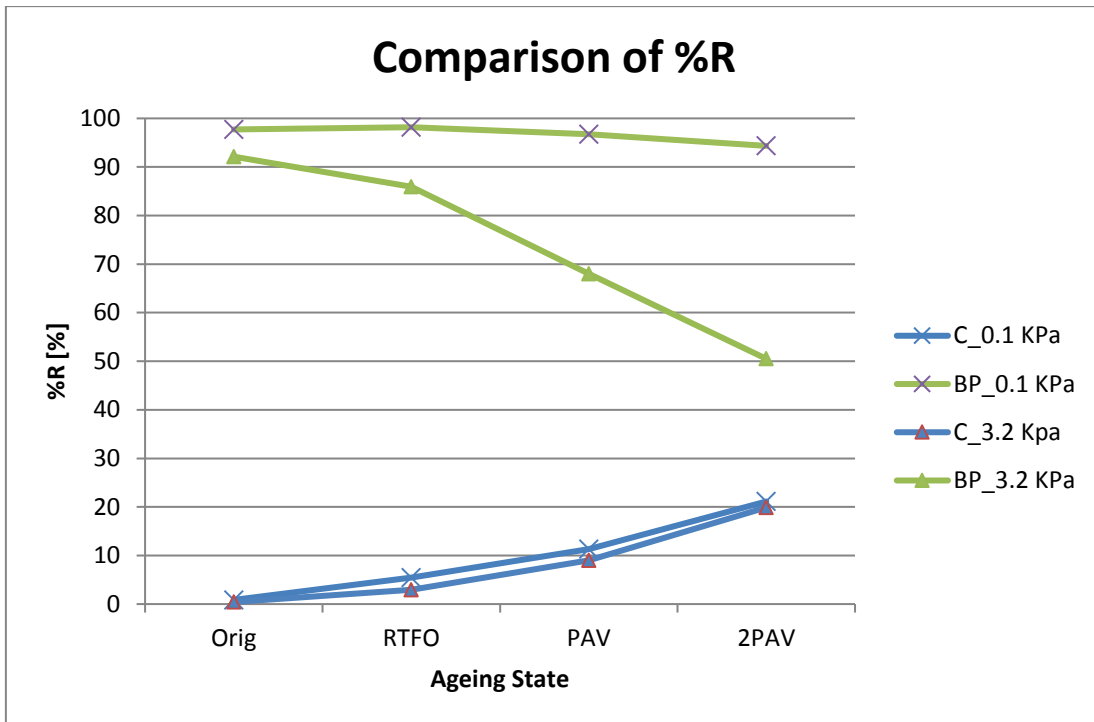


Figure IV-12. Comparison of %R

The single values of %R of BP is always better compared to the C ones: the material recover the majority part of the deformation at both levels of stress. In fact, the phase angle's plot, at high temperature and so low frequency, shows that BP has lower value of δ and so it is more elastic than C.

The problem is that this characteristic decreases with time, and so the material tends to recover less, thus to accumulate more.

In this research another mean was studied to represent and then display the results: the Ageing Indexes. They allow to see how the parameters develop with ageing and to understand the susceptibility of factors to ageing.

In the case of Jnr, the values of BioPhalt® are susceptible to ageing and they change a lot. In particular, they increase with time/ageing.

On the other hand, the values of C are more stable and decreasing.

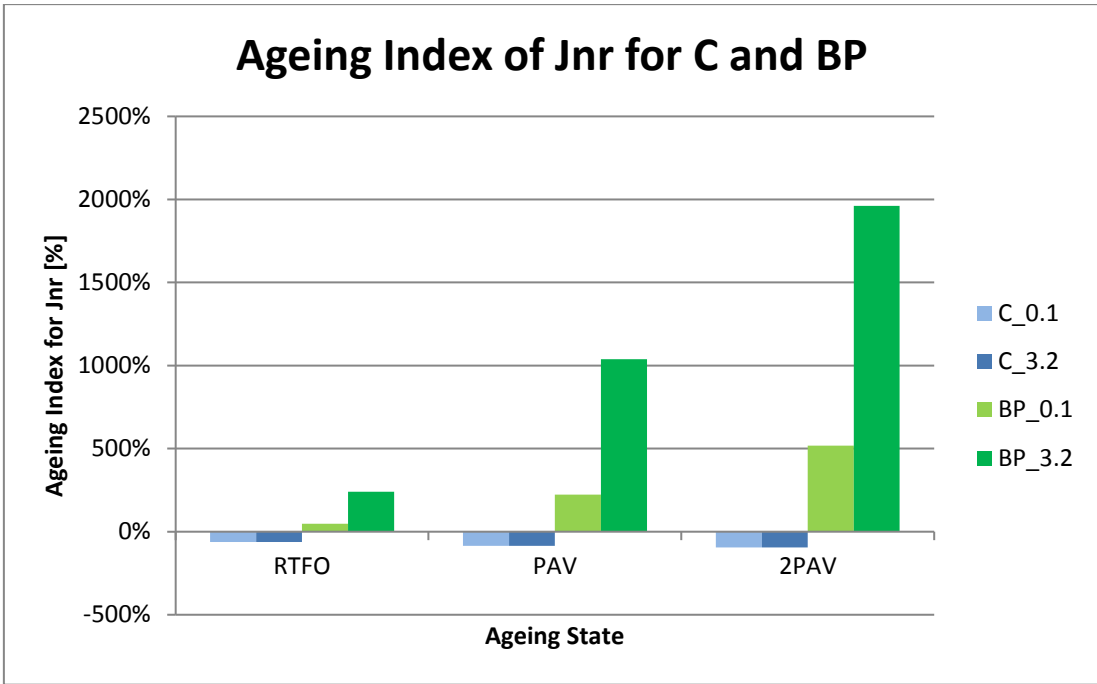


Figure IV-13. Ageing Index of Jnr for C and BP

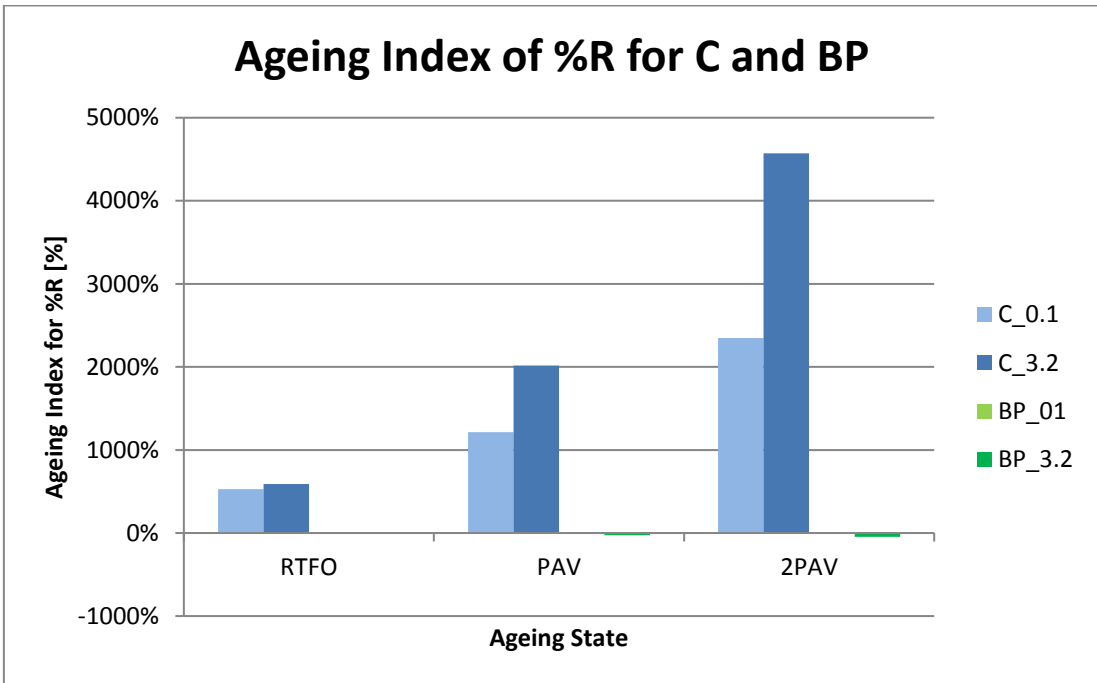


Figure IV-14. Ageing Index of %R of C and BP

Here it seems that the %R of BP is more stable with ageing, but it will decrease rather than increase.

IV.2.2 *Fatigue Cracking*

The pavement is subjected to continuous loads and it could fail due to intensive traffic. It has been proved that this failure can be represented by the number of cycles to failure N_f obtained with the LAS test.

This method is intended to evaluate the ability of an asphalt binder to resist fatigue damage by employing cyclic loading at increasing amplitudes in order to accelerate damage.

The test is represented by a traffic volume indicator that is the number of cycles to failure, called N_f , normalized to 1 million ESALs, that is the acronym for Equivalent Single Axle Load. According to the American Association of State Highway Officials (AASHO), its value is 18,000-lb. for a single axle with dual tires.

The higher N_f , the more resistant the material is.

Generally, this value decreases with ageing since pavement has already experienced several loads previously and so it becomes brittle with time. **Errore. L'origine riferimento non è stata trovata.** shows the 50/70 bitumen's results.

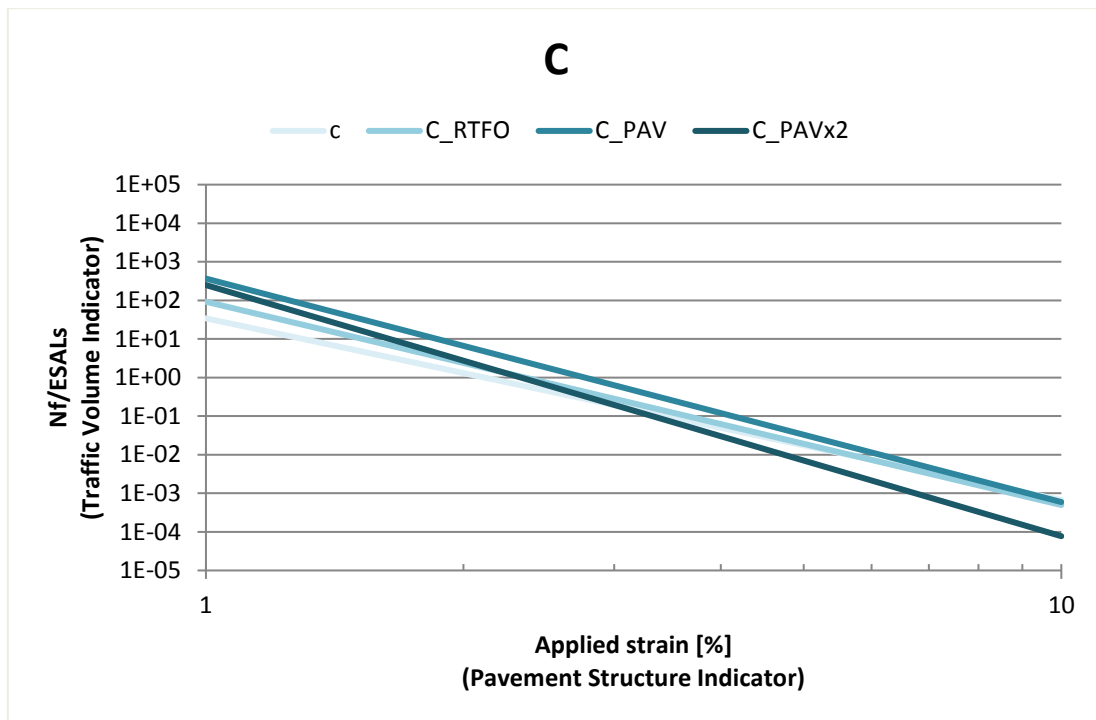


Figure IV-15. *Nf/ESALs for C*

As expected, $N_f/ESALs$ decreases with ageing. It is worth remembering that ageing process make the bitumen more brittle.

Moreover, the curve become more inclined: this means that little difference of strain in a long-term aged material correspond to bigger change of N_f .

It is noticeable that there is a dependence of $N_f/ESALs$ to strain since the curves rotate slightly. The slope of Wohler curves increases with ageing and this means that: for high level of strain N_f decreases with ageing and vice versa for low levels of strain.

These plots are also quite useful since it's possible to find the allowable fatigue life for a given strain amplitudes.

Another way of visualizing the results is the plot of $G \cdot \sin \delta$ over the Damage Intensity. $G \cdot \sin \delta$ represents the viscous component of the bitumen and the plot show how it changes under an increasing intensity of damage. $G \cdot \sin \delta$ is supposed to decrease, due to the embrittlement.

For the 50/70 bitumen, the plot is the one in Figure IV-16.

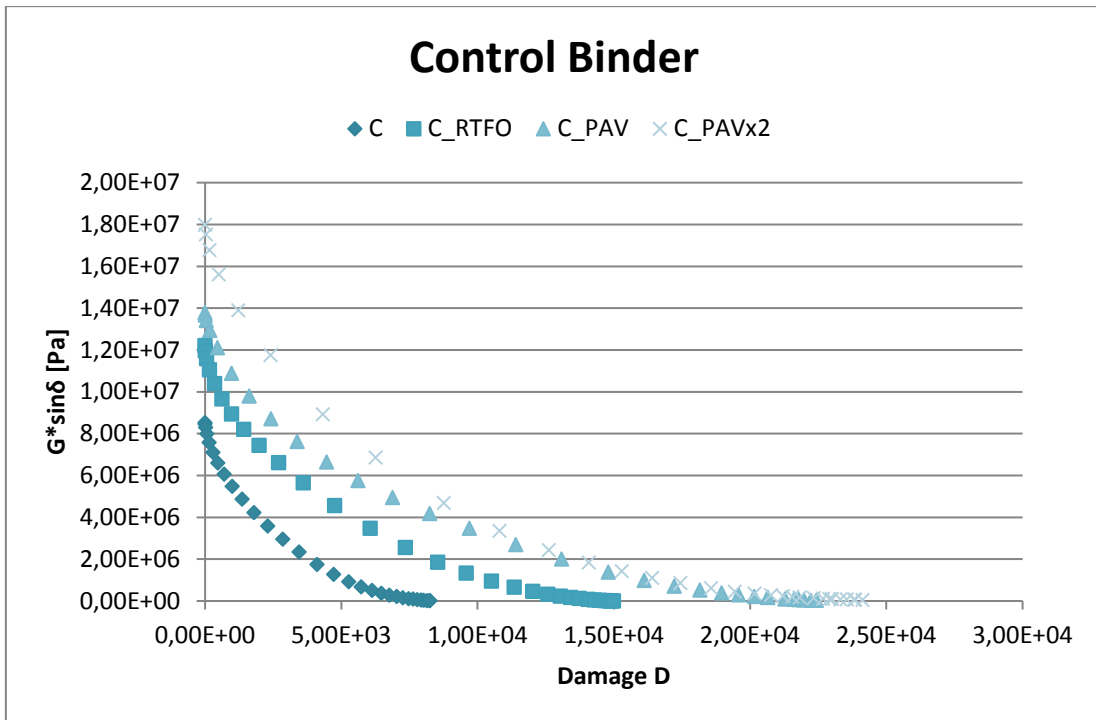


Figure IV-16. $G \cdot \sin \delta$ versus Damage Intensity of C

Also for the BioPhalt® the number of cycles to failure decrease with ageing. It is worth highlighting that the fatigue indicator of BP decreases more rapidly with respect the C's ones: the differences of Nf/ESALs for BP are bigger than the control binder.

Nf/ESALs decreases as the material is aged, thus aged BP reaches failure earlier than not-aged BP.

Here, the dependency on strain is weaker. In this case BP is not strongly dependent to strains since the curves are more or less parallel one to each other. [Figure IV-17]

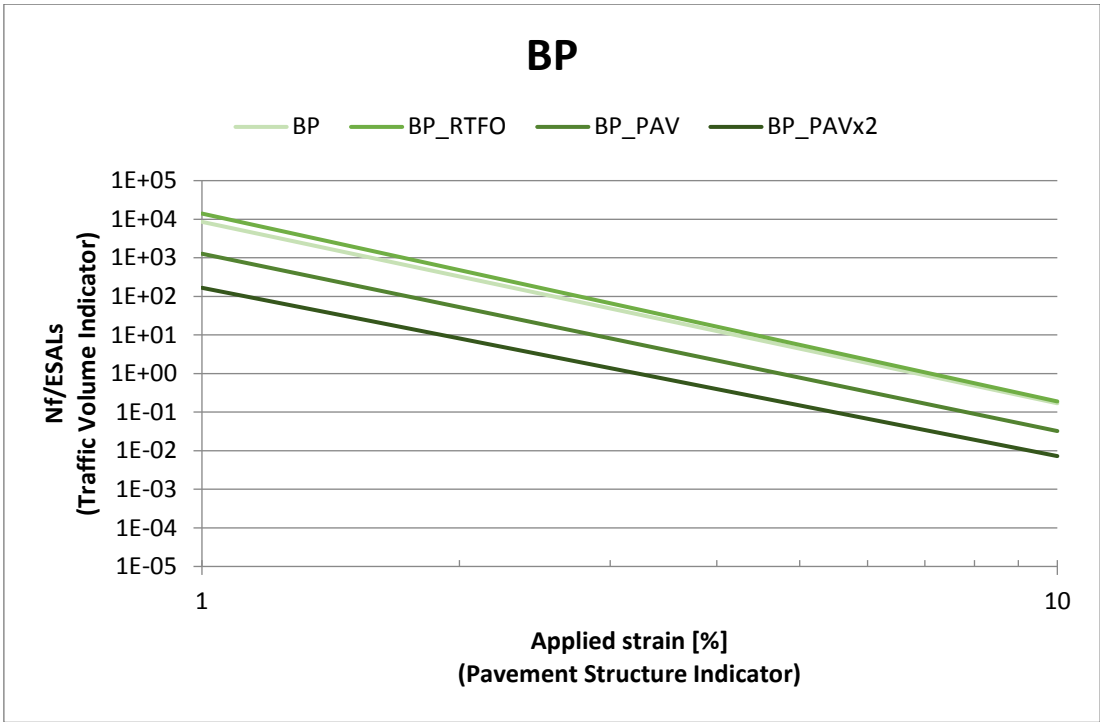


Figure IV-17. Nf/ESALS for BP

Also in this case $G^* \sin \delta$ decreases [Figure IV-18].

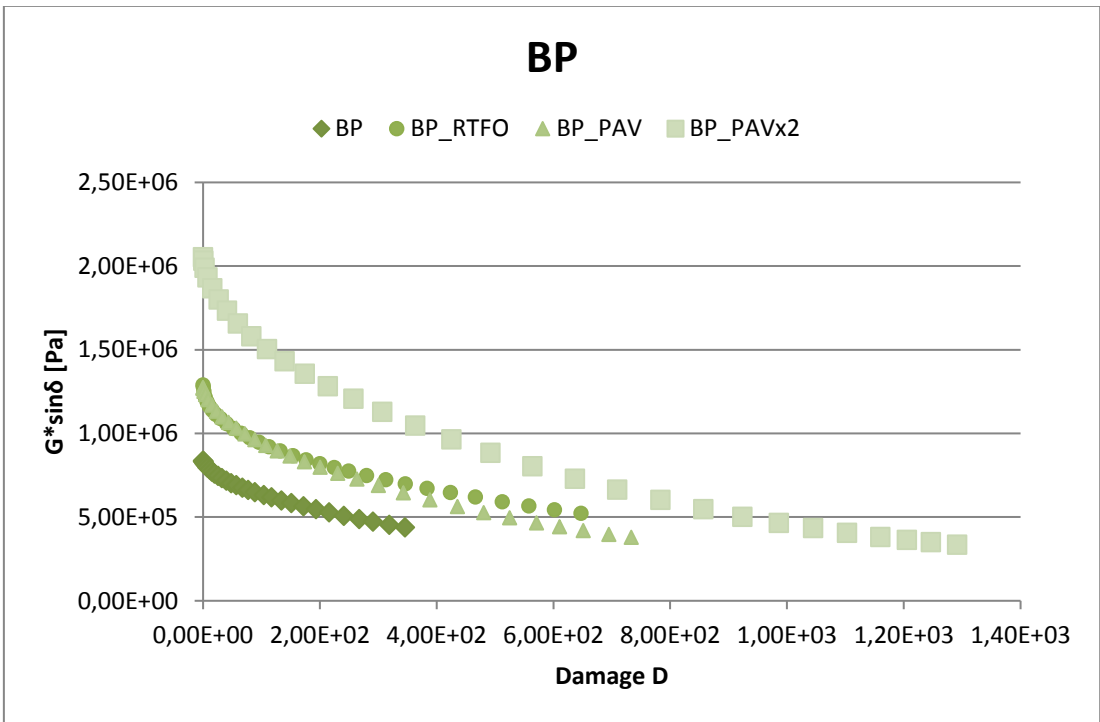


Figure IV-18. $G^* \sin \delta$ versus Damage Intensity of BP

The comparison and comments are provided below.

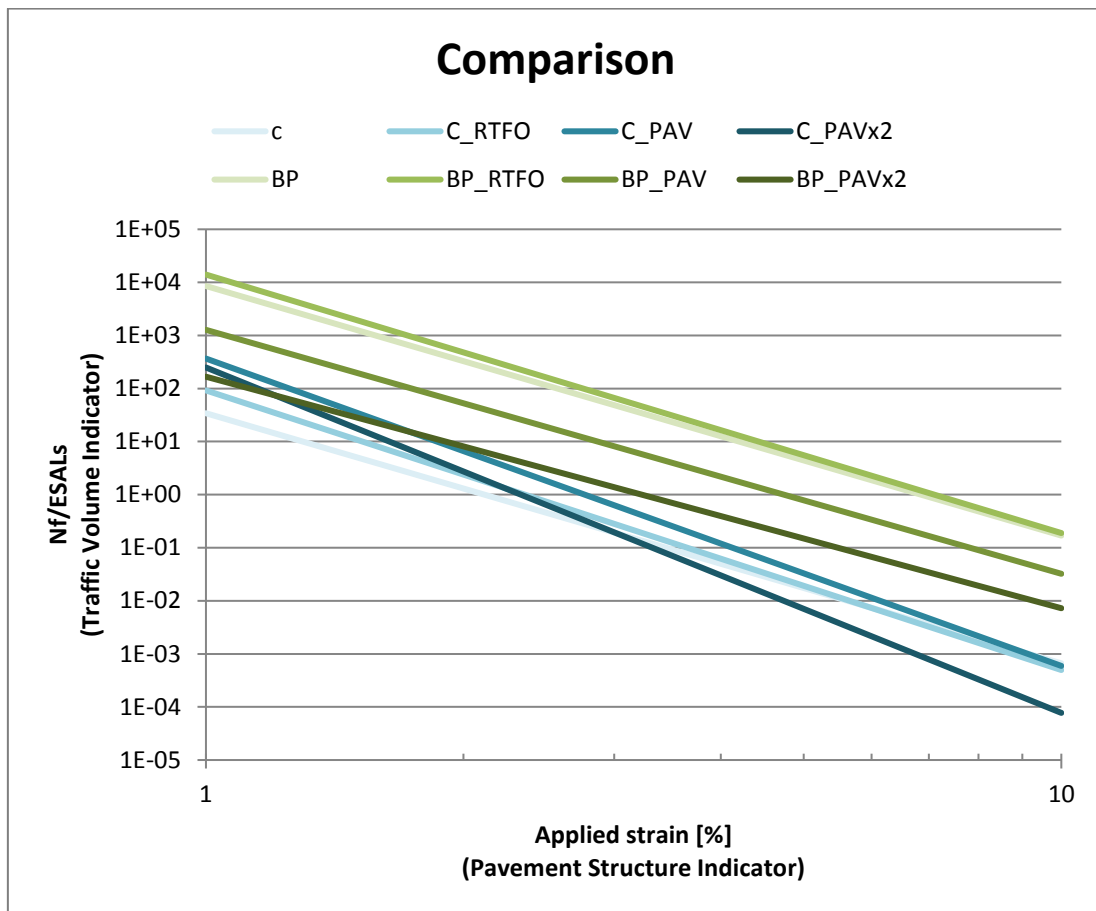


Figure IV-19. Comparison of Traffic Volume indicator

Nf of BP is mostly greater than Nf of C at all levels of ageing, apart from very few values of Nf aged at 2 PAV of BP at low strains.

Consequently, it's easy to declare that, at the same conditions, BP stands more than C during in-service life.

IV.2.3 Low Temperature Cracking

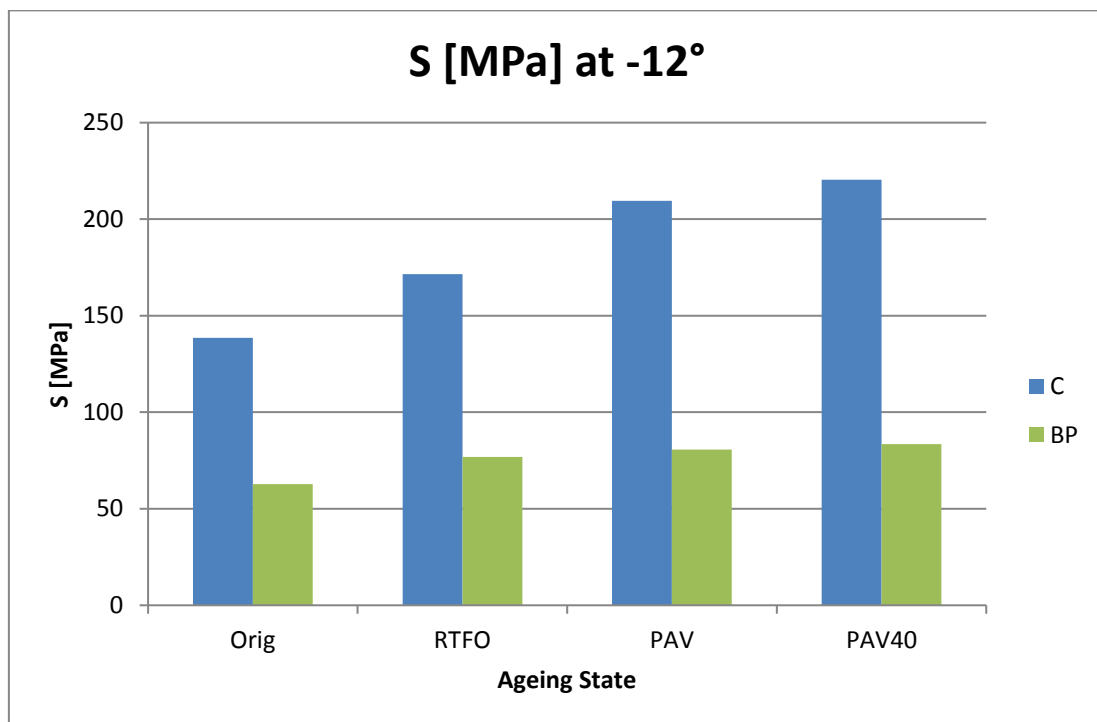
When temperatures dip well below freezing, pavements tend to shrink. As this shrinking occurs, stresses build in the pavement since it cannot shrink along the length of the roadway. When tensile stresses reach the tensile strength of pavements, they pull apart and cracks form.

The BBR test provides a mean for measuring the stress and strain in the sample along time. The ratio of stress and strain gives the flexural creep stiffness S along time as well. The absolute value of the slope of the stiffness curve plotted versus the logarithm of time is the stiffness ratio, or m -value.

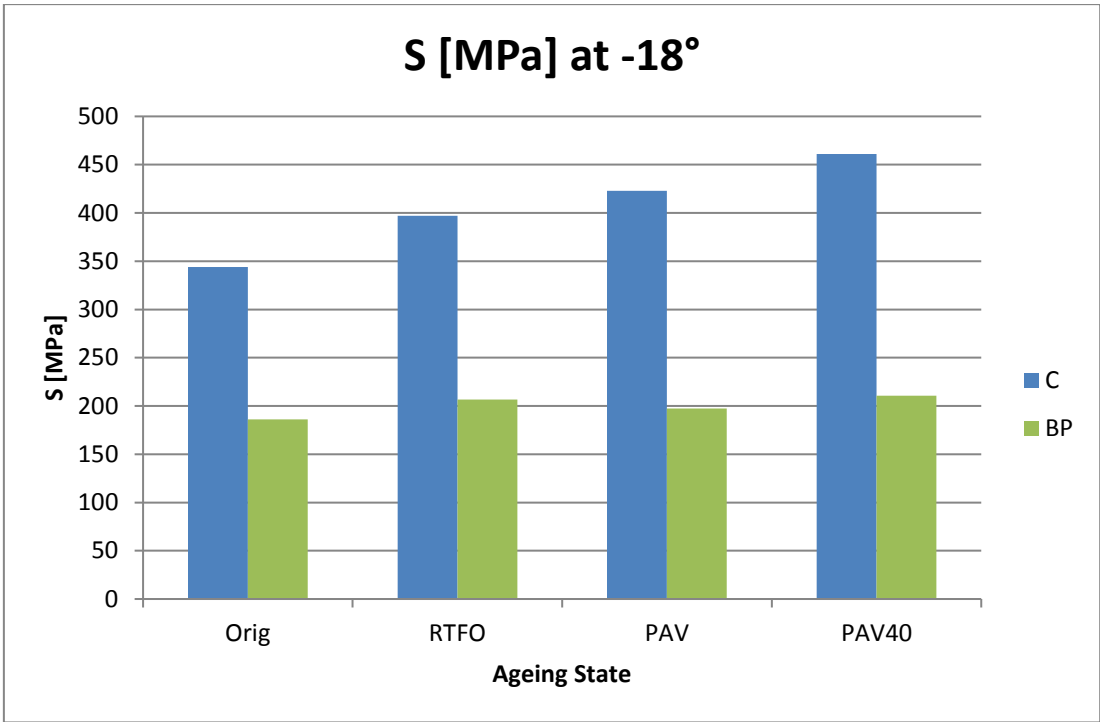
In this research three temperatures has been investigated to build a trend: -12°C , -18°C and -24°C .

The stiffness is supposed to increase with ageing due to the hardening of bitumen. The lower is the stiffness, the longer will be the resistance to low temperature cracking. In fact, lower stiffness leads to softer material, less elastic and so less brittle.

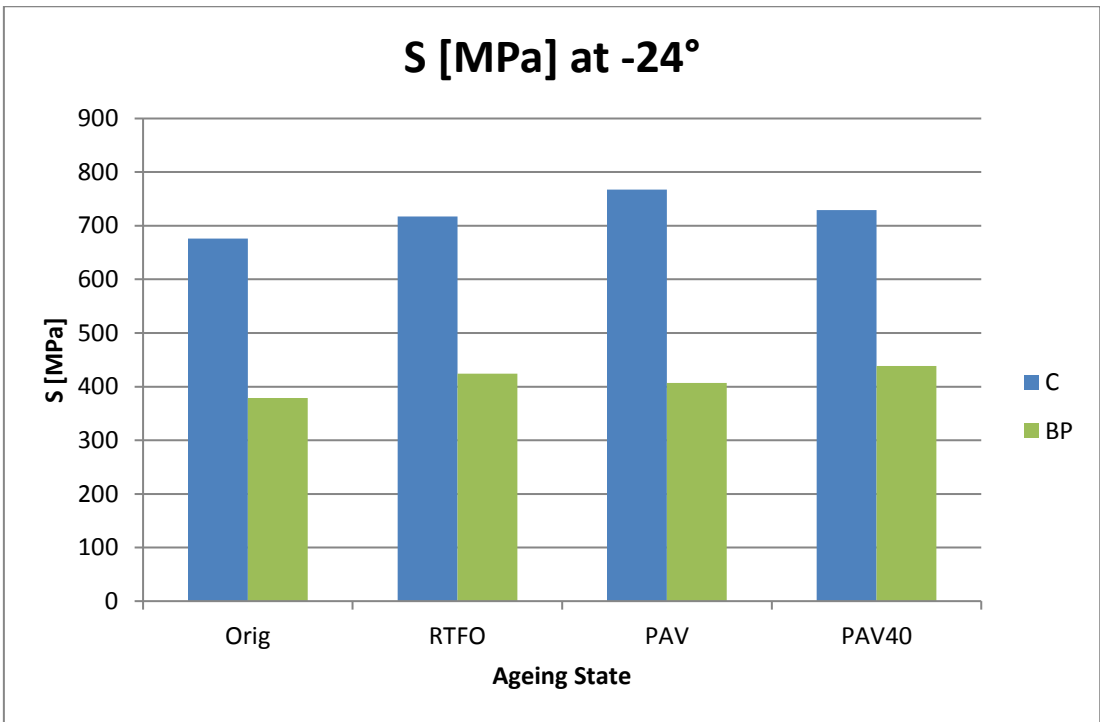
In this research, the stiffness and the stiffness ratio at 60 seconds have been analysed. The BBR's results are coherent with the hypothesis of increasing stiffness for both material, as shown in Figure IV-20 from a to c. The Control binder is displayed in blue, whereas the BioPhalt® in green.



(a)



(b)



(c)

Figure IV-20. Flexural Creep Stiffness

It is worth highlighting that the BioPhalt®'s flexural creep stiffness is more or less half the control's stiffness in all the test. More precisely, S of BP is 55% less than S of C at -12°C; is ≈50% of Stiffness of BP at -18°C and at -24°C the difference is 45%.

Another good point is that the stiffness of BP is less susceptible to ageing. This is revealed by ageing index AI of the stiffness at different temperatures [Figure IV-21, Figure IV-22, Figure IV-23].

Ageing Index of Stiffness for BP, or AI_S(BP), is generally lower than AI_S(C), thus BP is less susceptible to ageing at low temperatures. The lower is the temperature, the less noticeable is this effect. Briefly, at low temperatures BP behaves better than C since is less stiff and the risk of cracking is weaker.

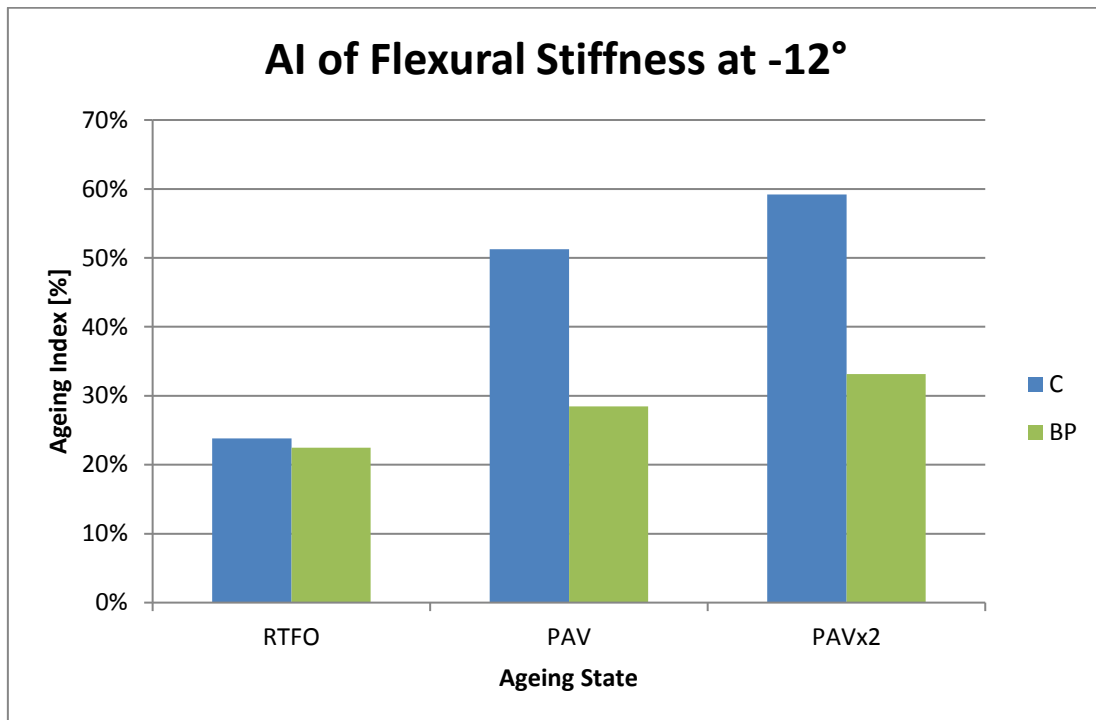


Figure IV-21. Ageing Index of Stiffness at -12°C

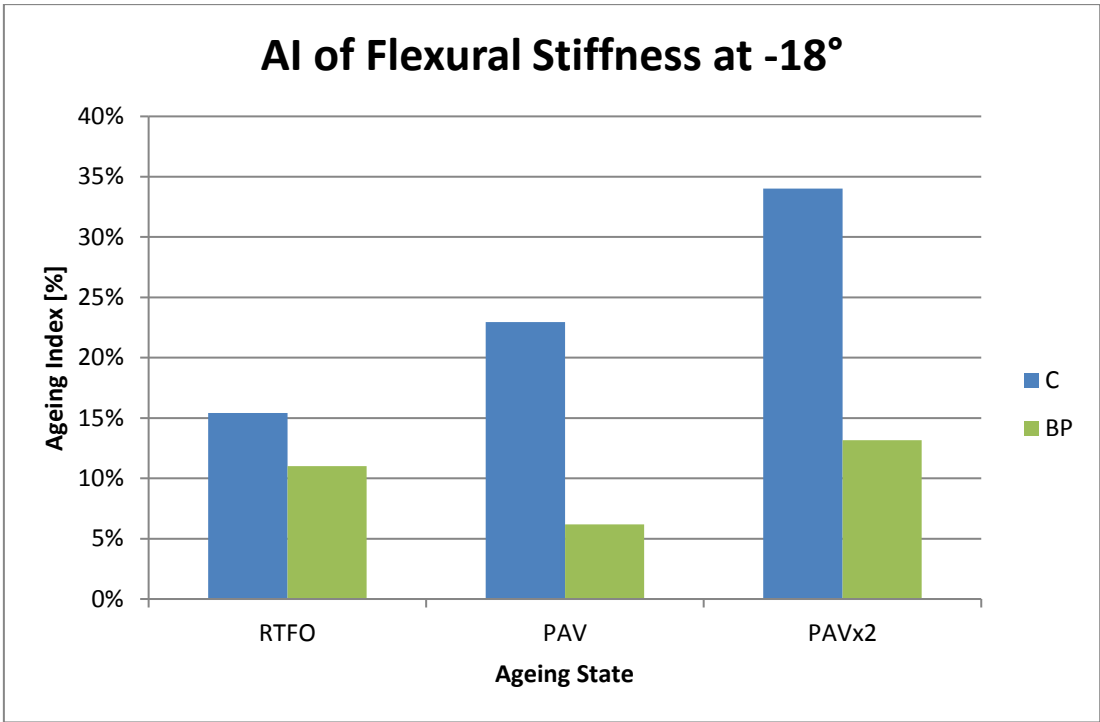


Figure IV-22. Ageing Index of Stiffness at -18°C

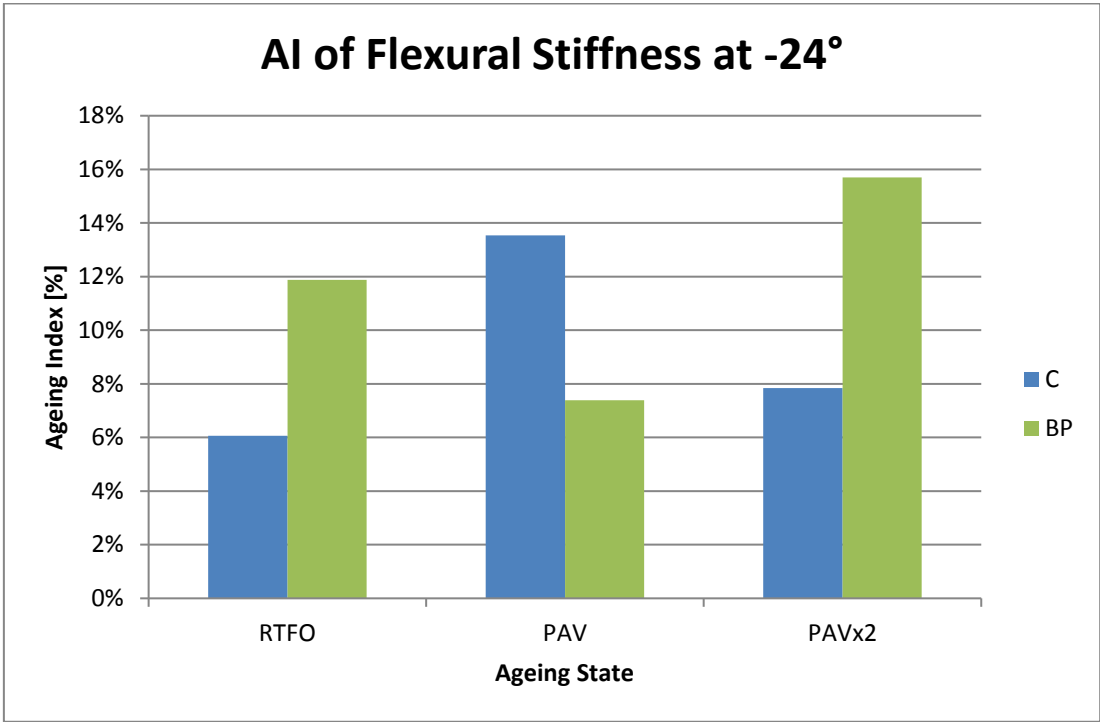


Figure IV-23. Ageing Index of Stiffness at -24°C

On the other hand, the m-value reflects the phase angle measured with the dynamic rheometer. In fact, its maximum value, equal to 0.5, represents a material that is completely viscous. Lower values move closer to elastic behaviour.

In addition, binder with larger values of m change stress much more readily with time. Therefore, as a pavement cools, the stress in the pavement relax and the pavement doesn't crack.

From the BBR's results, BioPhalt® appears more capable to relax stress, since BP's m is greater than the m-value of C for all levels of ageing at all temperatures [Table 4].

Table 4. Comparison of m-values

	m₆₀					
	-12°C		-18°C		-24°C	
	C	BP	C	BP	C	BP
Orig	0.420	0.575	0.316	0.432	0.236	0.286
RTFO	0.373	0.494	0.289	0.370	0.225	0.269
PAV	0.329	0.492	0.259	0.369	0.216	0.272
2xPAV	0.298	0.486	0.239	0.359	0.189	0.259

The good behaviour of BP at low T is confirmed also by $\delta(BP) > \delta(C)$ at high frequency, that means that BioPhalt is more viscous than C in those time-temperature conditions.

Another means of comparison is computing the Critical temperature T_c. It is the specific temperature at which an asphalt binder meets the specifications requirements. According to ASTM D6373 – 13, the T_c for the thermal cracking is the one at which correspond S=300 MPa and m=0.300 on a long term-aged sample (PAV), both measured at 60 seconds.

For these measurements, it's necessary to refer to PAV aged materials since the cracks is more sever when the bitumen is fragile.

The lower the temperature, the higher is the performance of the binder to thermal cracking. For samples aged at PAV, it has been obtained that the T_c for stiffness of BP is lower than the one of C Figure IV-24. According to this way

of proceeding, the cracking in BioPhalt® will occur at lower temperature. Thus, BP has more thermal resistance.

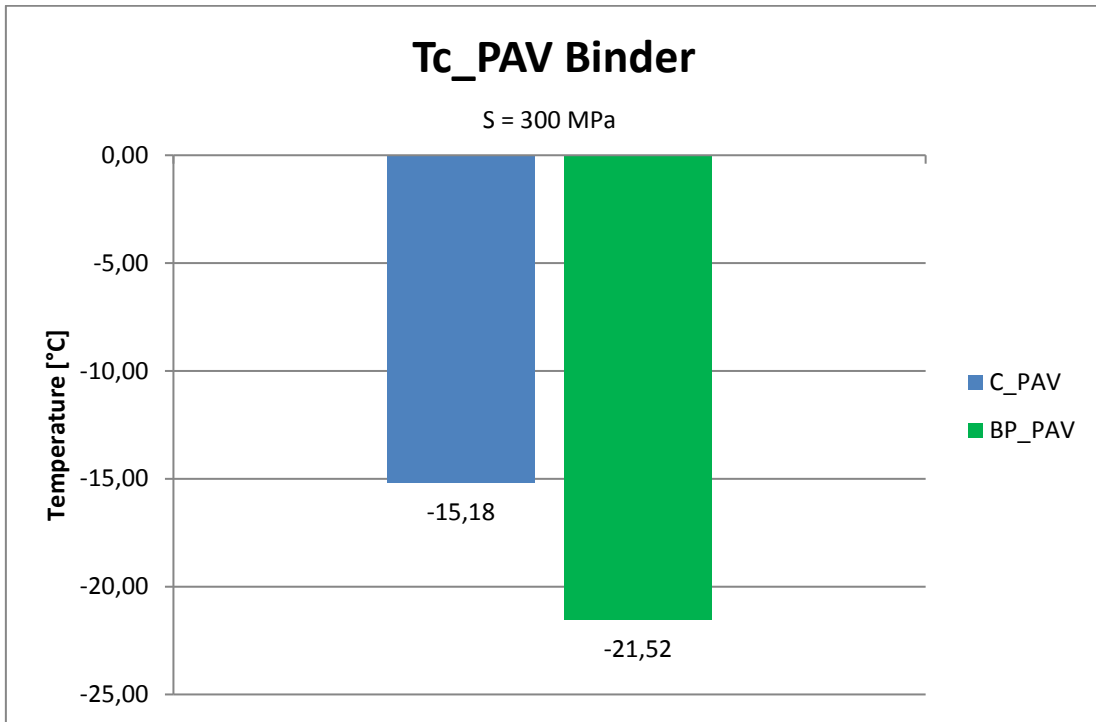


Figure IV-24. Critical Temperature for S

The same procedure has been repeated to find the critical temperature at which $m=0.300$. Figure IV-25 shows the results.

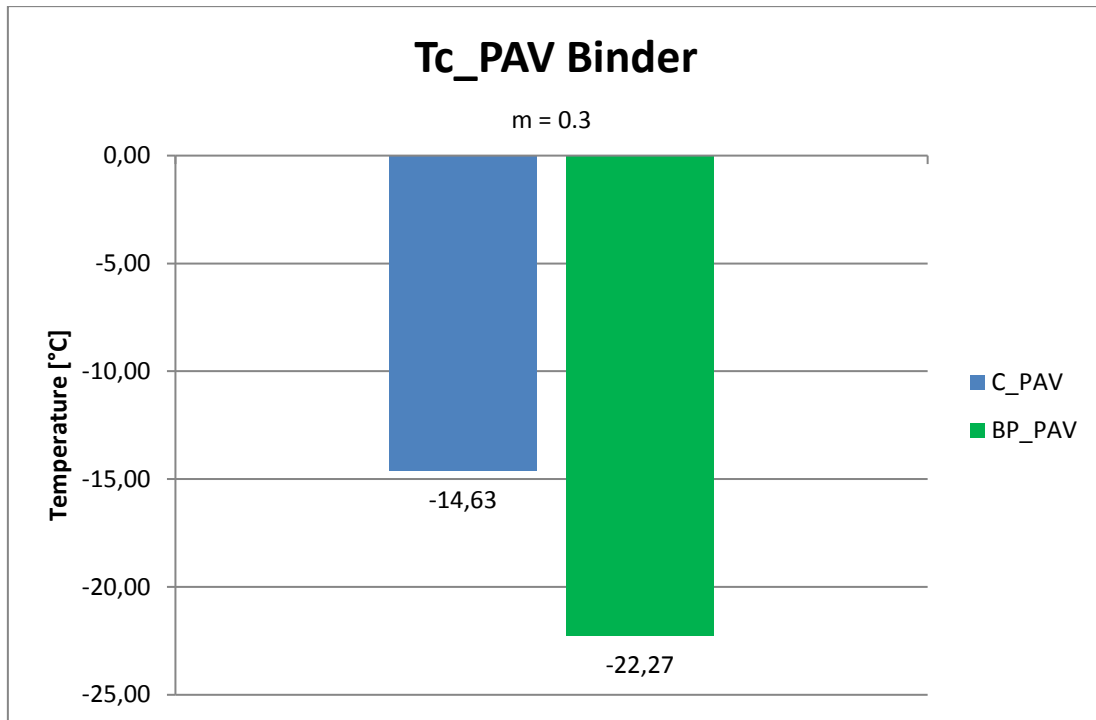


Figure IV-25. Critical Temperature for m-value

This plot confirms what already explained, that is that BioPhalt has greater resistance to thermal cracking with respect the 50/70 bitumen.

IV.3 Chemical Properties

In the chapter of the Literature Review there are several examples about the relation between the chemical structure of the bitumen and its rheological, physical and mechanical behaviour.

To totally govern the response of BioPhalt® at its original, RTFO, PAV and 2PAV aged state, the SARA analysis and the FTIR spectroscopy has been performed.

IV.3.1 SARA analysis

The SARA analysis allows to separate crude oil into fractions of saturates, aromatics, resins A, and asphaltenes or resins B (SARA) according to their solubility in solvents of differing polarity.

The results are expressed in terms of percentage of the four groups. The software draws four peaks, as shown in Figure IV-26.

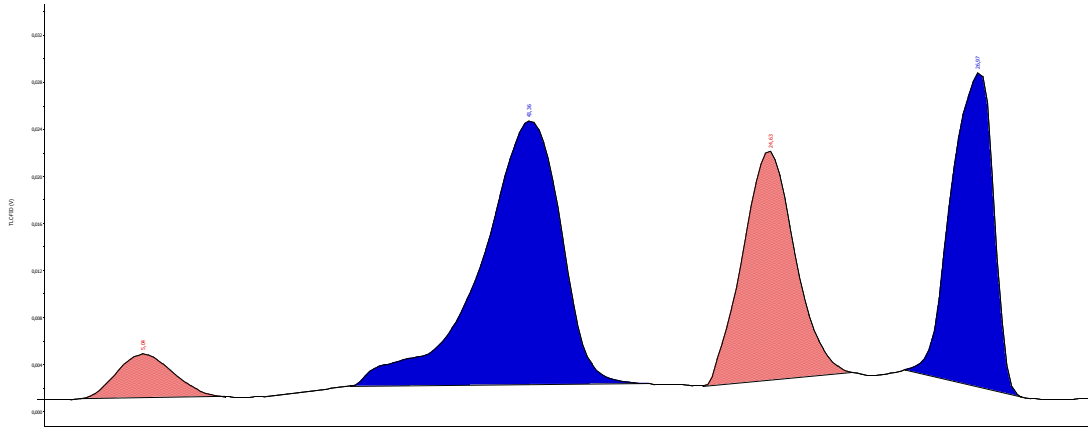


Figure IV-26. Example of SARA's results for standard bitumen

Respectively, these four peaks are: Saturates, Aromatics, Resins A and Resins B.

To represent them with a single factor, the colloidal index I_C has been calculated as follow:

$$I_C = \frac{As + S}{R + Ar}$$

Where:

- S are saturates, %;
- As are the asphaltenes or the resins B, %;
- R are resins A, %;
- Ar are aromatics, %.

The proportion of resins B and saturates to resins and aromatics governs the solution (SOL) or gelatinous (GEL) type character of the bitumen.

A GEL bitumen contains high asphaltenes/resins concentrations, leading to a network structure with high rigidity and elasticity (low δ), whereas a SOL bitumen possesses a low asphaltenes/resins ratio.

The percentages of fractions are affected by the ageing state and their value change with time.

It's generally known that the aged bitumens are harder and more brittle.

During ageing process, there is a migration of molecules from aromatics to resins and to asphaltenes.

In this way, there will be more asphaltenes that have a great molecular weight and so this make the bitumen hard. In addition, the initial hardening of the bitumen (short-term aging) is largely due to the evaporation of the lighter aromatics, that have smaller molecular weight.

Basically, with ageing: saturates are more or less stable, aromatics decrease whereas resins and asphaltenes increase.

For common binders, all the expectations are satisfied. In fact, the analysis of 50/70 binder shows that: saturates doesn't follow a specific trend, aromatics decrease and resins and asphaltenes increase. In Figure IV-27 it is possible to appreciate how the fractions change with ageing in binder C.

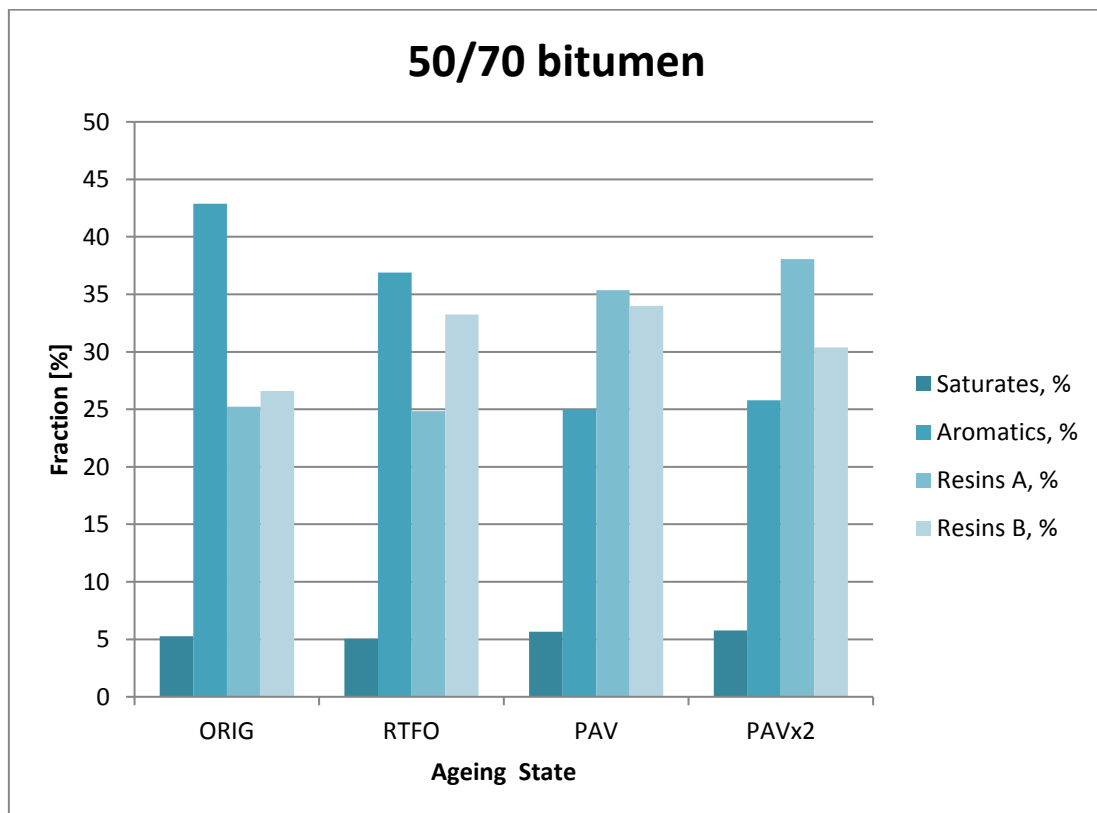


Figure IV-27. SARA analysis of 50/70 bitumen

In addition, for binder C, the index of colloidal structure changes with ageing according to the following values in Table 5.

Table 5. Colloidal Index for C

	C
Orig	0.47
RTFO	0.62
PAV	0.66
2PAV	0.57

Concerning the BioPhalt®, its SARA fractions were investigated and compared to their aged samples.

The analysis of BP has revealed very interesting results in terms of ageing and also in terms of chemical compositions.

Regarding the latter, it has been found that the BP is characterized by an unusual pattern of peaks: there are only three over four peaks. A deep analysis of the time in which the peaks are usually drawn (x-axis of the graph) has allowed to understand which the missed peak is: the one that represents saturates. Thus, the BioPhalt® doesn't have saturates in its chemical composition.

Figure IV-28 is an example of that.

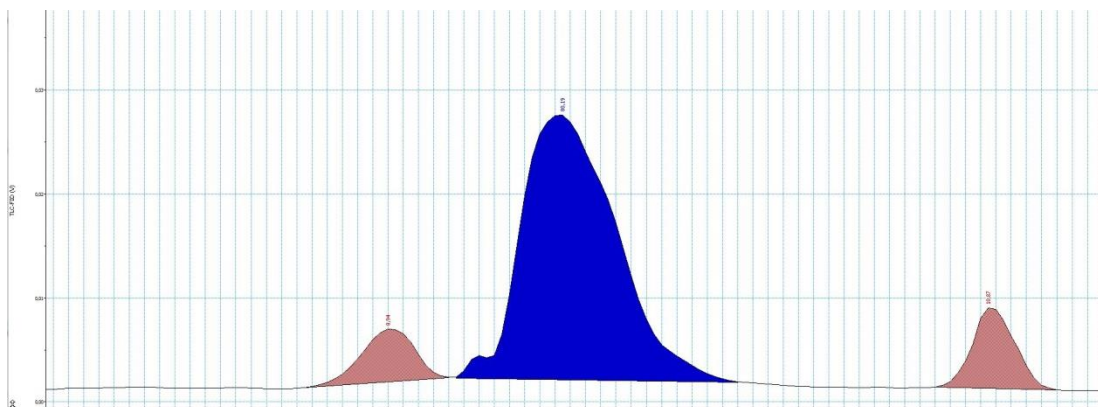


Figure IV-28. Example of BioPhalt analysis.

On the other hand, the peak with the biggest area is the one of the resins A.

As regards of the effect of ageing, the migration of the molecules doesn't follow a precise trend, so it doesn't happen as in the Control binder [Figure IV-29]. It is worth to take into account that BioPhalt® is a vegetable pitch and its chemical composition is different from standard bitumens.

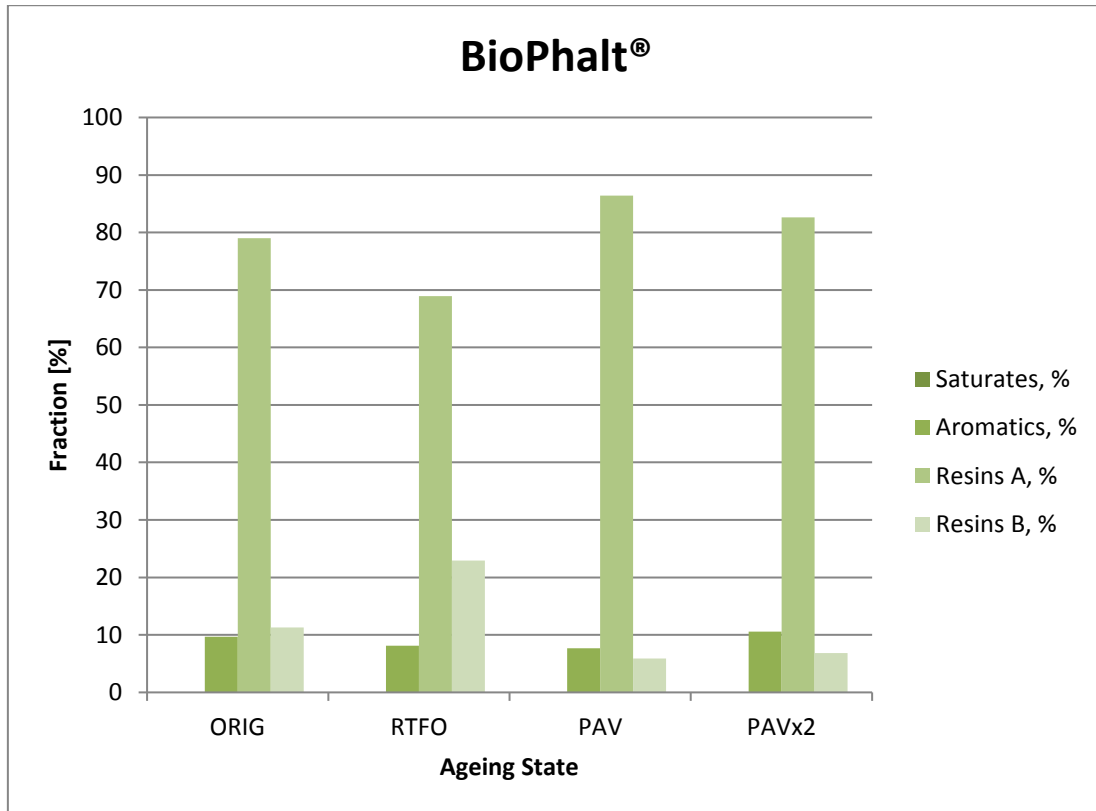


Figure IV-29. SARA analysis of BioPhalt®

The colloidal index I_C of BP reveals a strong change passing from the short term (RTFO) to long term ageing (PAV) [Table 6].

Table 6. Colloidal Index of BP

	BP
Orig	0.13
RTFO	0.30
PAV	0.06
2PAV	0.07

Plots for comparison between the materials are provided below.

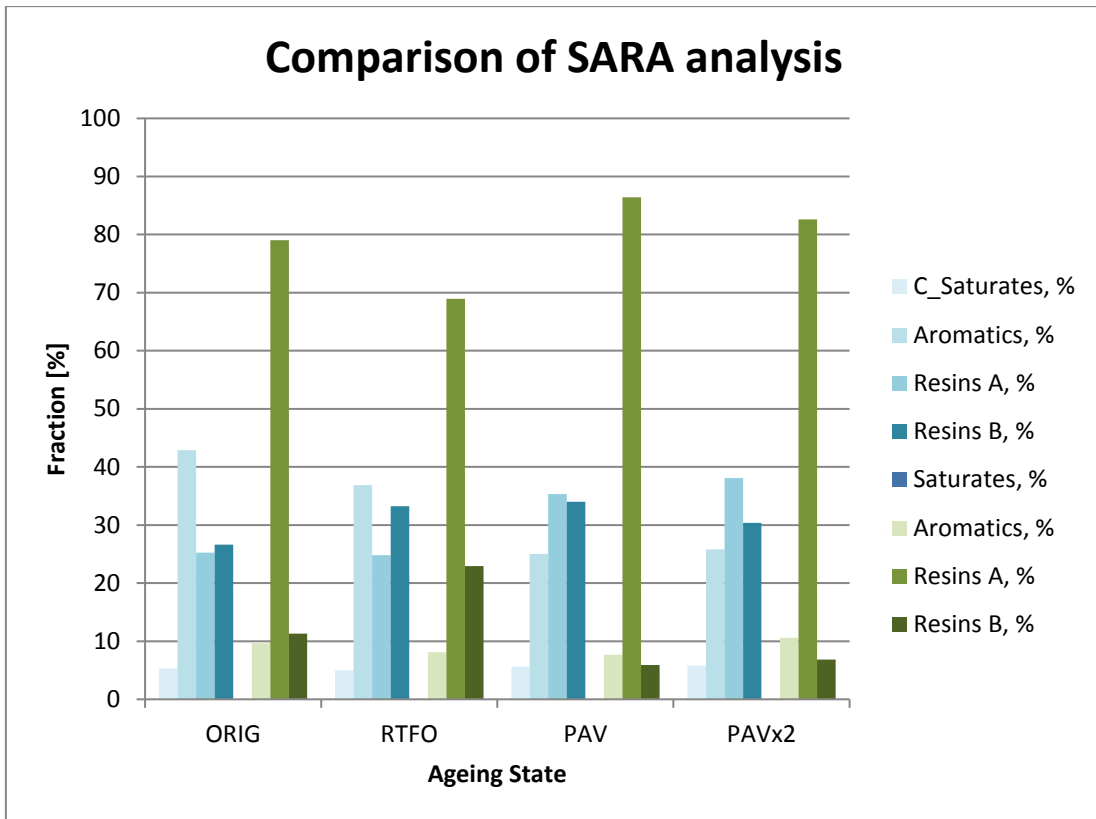


Figure IV-30. Comparison of SARA analysis

With Figure IV-30, it's possible to appreciate that:

- The first fraction of BP doesn't exist;
- The resins in BP play the biggest role and they are almost double of the C ones;
- The asphaltenes in BP are much lower than the ones in C.

In addition, I_C of BP is extremely lower than the one of C [Table 7]. Despite this, it's not possible to state that BP is a Newtonian fluid.

Table 7. Comparison of Colloidal Index

	C	BP
Orig	0.47	0.13
RTFO	0.62	0.30
PAV	0.66	0.06
2PAV	0.57	0.07

Ageing Indexes AI of all the fractions have been computed to investigate their developments with ageing.

AI represents the % of increase or decrease of parameters with respect to not-aged values. Results of C fractions, shown in Table 8, indicate that saturates slightly increase, aromatics decrease in favour of resins that increase, while asphaltenes decrease.

BioPhalt® presents different characteristics: no saturates and all other indexes don't follow a monotonic trend.

Table 8. Ageing Index for SARA analysis

Binder		AI of Saturates, %	AI of Aromatics, %	AI of Resins A, %	AI of Resins B, %
C	RTFO	-5%	-14%	-2%	25%
	PAV	7%	-42%	40%	28%
	2PAV	10%	-40%	51%	14%
BP	RTFO	-	-16%	-13%	103%
	PAV	-	-21%	9%	-48%
	2PAV	-	9%	5%	-40%

IV.3.2 FTIR Spectroscopy

In this research, FTIR spectroscopy has been accomplished to evaluate the change of chemical groups with ageing.

The resultant spectra have been analysed in both qualitative and quantitative ways.

Regarding the first, it was just a visual check. In Figure IV-31 and Figure IV-32 the effect of ageing on the two materials is represented as spectrum.

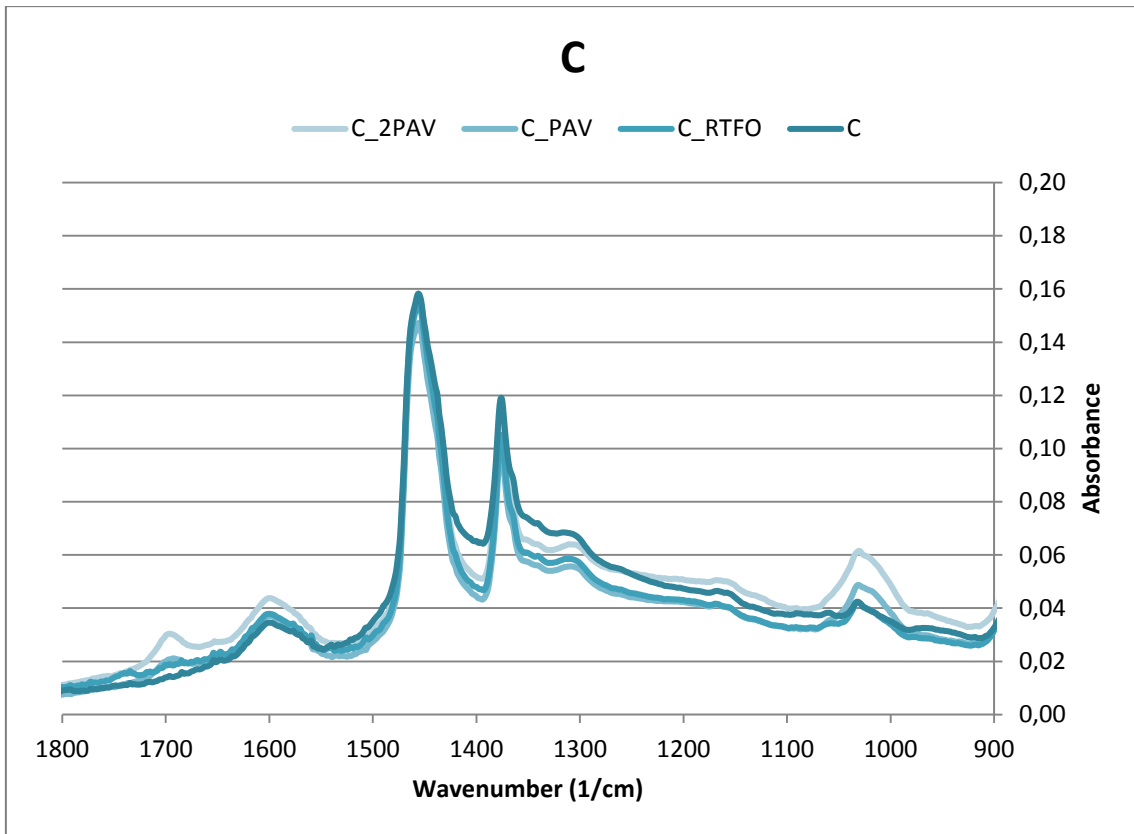


Figure IV-31. Spectrum of Control Binder at all ageing states

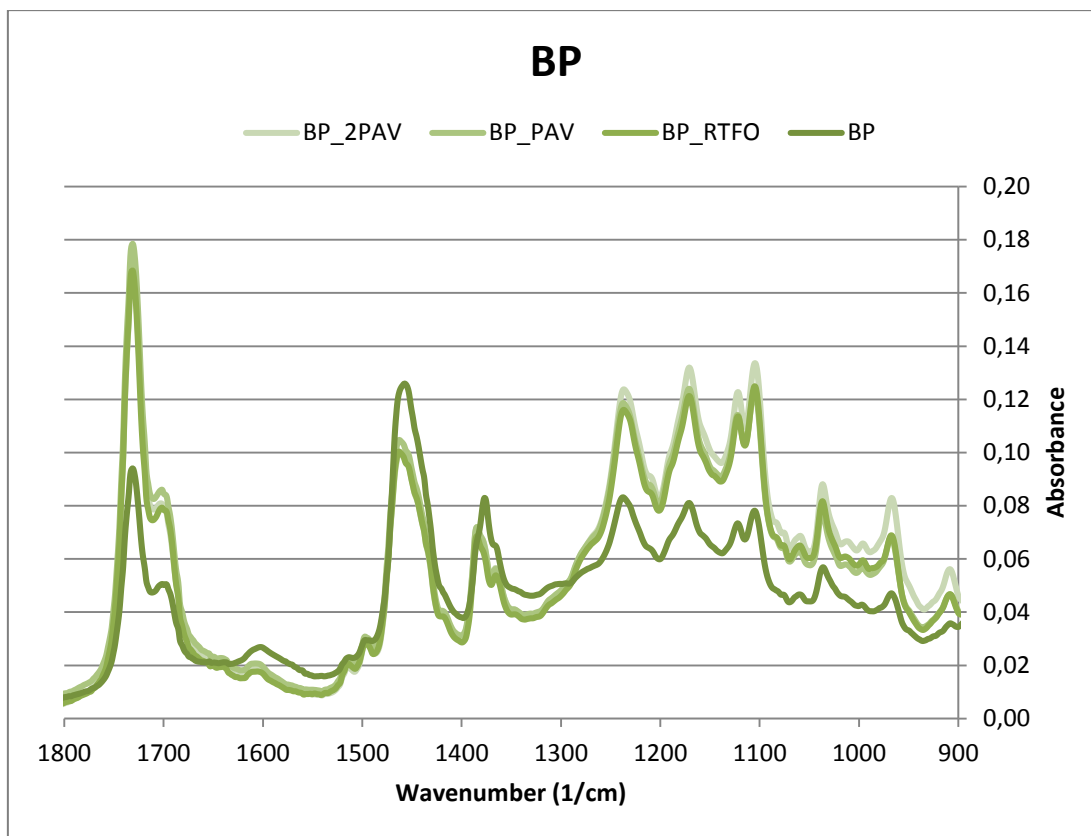


Figure IV-32. Spectrum of BioPhalt at all ageing states

As expected, it's noticeable a big difference between the functional groups that compose the two bitumens.

In this research, only few functional groups were evaluated. In particular:

- To 1700 cm^{-1} corresponds carbonyl structures;
- To 1030 cm^{-1} corresponds sulphoxide structures;
- 1460 and 1376 cm^{-1} represent the aliphatic structures;
- And at 1600 cm^{-1} there are the aromatics.

In the BioPhalt® there are some important groups that increase with ageing from wavelengths equal to 1100 to 1250 cm^{-1} , but they haven't been individuated.

For the quantitative analysis some indexes have been calculated:

- Carbonyl Index: $I_C = \frac{A_{1700}}{\Sigma A}$
- Sulphoxide Index: $I_S = \frac{A_{1030}}{\Sigma A}$
- Aliphatic Index: $I_B = \frac{(A_{1460} + A_{1376})}{\Sigma A}$

- Aromatic Index: $I_{Ar} = \frac{A_{1600}}{\sum A}$

Where $\sum A = (A_{2950} + A_{2920} + A_{2850}) + A_{1700} + A_{1600} + A_{1460} + A_{1377} + A_{1030} + A_{870} + A_{810} + A_{743} + A_{723}$.

One of the most important contribute to ageing is given by oxidation. Thus, chemical structures associated with oxidative aging have been in the focus of attention in this research. Carbonyl and Sulphoxide Indexes has been chosen because higher oxidation rate (or aging) leads to more carbonyl and sulphoxide groups. Generally, the creation of sulphoxide groups takes place in the materials aged at short term ageing, and so the Sulphoxide index I_s increases in the first stages of ageing. At long term ageing, the carbonyl structure become predominant and, this time, only the Index I_c increases.

The higher the indexes, the more susceptible to ageing the material is.

To compute the index, a prior normalization with respect the original spectrum is needed.

It has been obtained:

Table 9. FTIR indexes for C

CONTROL	I_s	I_c
Orig	2.28%	1.39%
RTFO	2.25%	1.85%
PAV	2.60%	1.76%
2PAV	3.31%	2.55%

Both Indexes increase with ageing, as expected.

The same indexes have been calculated for BioPhalt®:

Table 10. FTIR indexes for BP

BioPhalt®	I_s	I_c
Orig	4.49%	13.72%
RTFO	4.47%	12.61%
PAV	4.27%	13.66%
PAV40	3.83%	12.84%

The comparison among the indexes of the materials suggests that BP has more sulphoxide and carbonyl groups, but the Indexes don't have a monotonic increasing trend. Consequently, this could depend on its composition and not on its susceptibility to ageing.

To have a clear view of what said, Ageing Indexes AI of the chemical indexes have been introduced.

$$AI_{chemical\ group} = (Index_i - Index_{ORIG}) / (Index_{ORIG})$$

Where *i* could be either RTFO, PAV or 2PAV and Index refers to chemical structures that needs to be investigated.

Figure IV-33 shows two important aspects: the composition of BP is less subjected to the creation of Sulphoxide group and, moreover, the evolution of this group is negative. In fact, for Control binder there is a growth of Sulphoxide structures at each ageing state with respect the original one. On the contrary, in BioPhalt® there is a reduction of these groups.

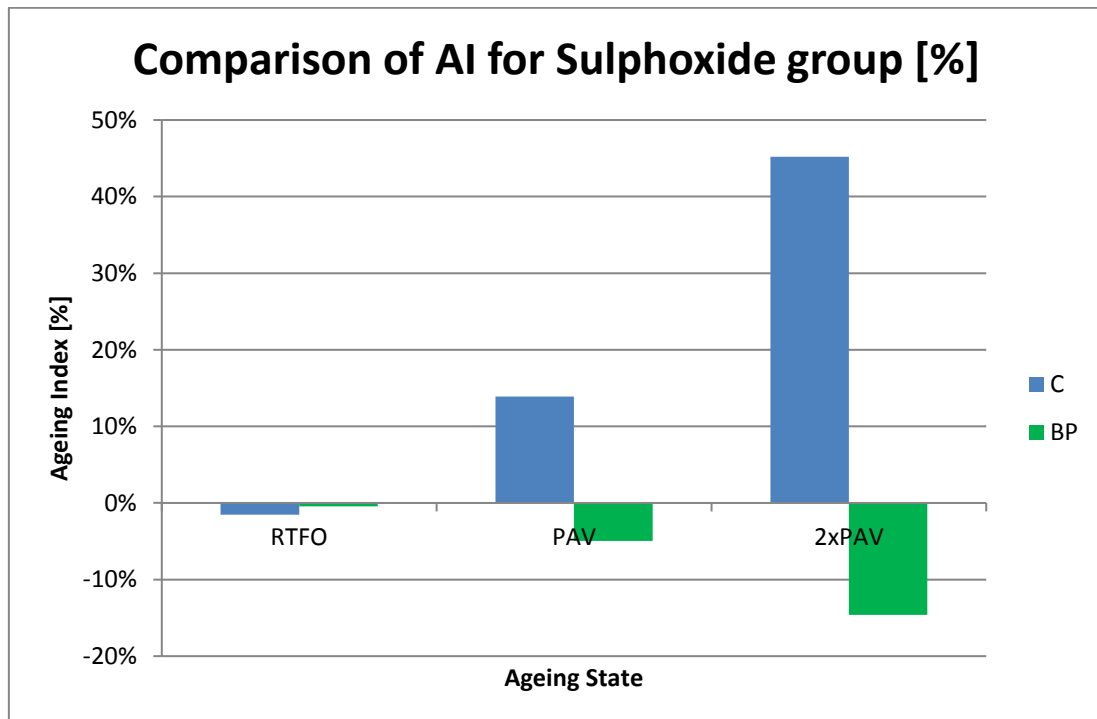


Figure IV-33. Comparison of Ageing Index for sulphoxide group

Thus, despite the fact that the sulphoxide group in BP is already abundant in the original state, it tends to decrease with respect the value at the original and so it doesn't develop new structures.

The same discussion needs to be done for the Carbonyl group I_c .

Comparing Table 9 with Table 10, it is found that the BioPhalt® has more carbonyl structures than the standard binder. Also in this case, this could depend on its composition.

To see the evolution of the groups' formation with ageing, it's necessary to resort to Ageing Index of I_c [Figure IV-34].

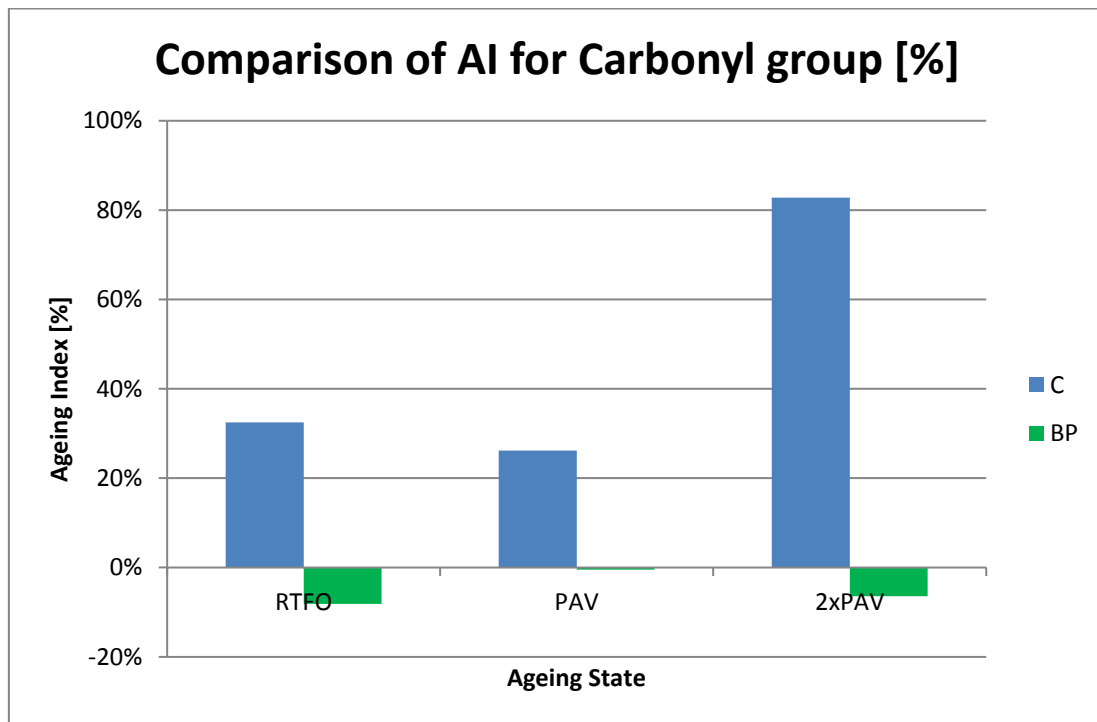


Figure IV-34. Comparison of Ageing Index of Carbonyl group

As just said, the carbonyl index is more representative of the long-term ageing and the trend of Control binder shows exactly this. There is a big jump from the RTFO state to 2xPAV.

On the other hand, BioPhalt® isn't affected by the development of this groups and so, also in this case, Control Binder is more subjected to oxidation and so to become brittle.

Another reason of this feeble reduction in BioPhalt® could be that the molecules are already saturated with oxygen since it has greater value of I_C and so there is no possibility to create new chemical bonds.

The FTIR results give the possibility to study other structural groups beyond the ones related to oxidation. For example, it has been computed the aliphatic index I_B and the Aromatic Index I_{Ar} , listed previously. These factors can be compared to SARA results. Tables with aliphatics and aromatics indexes are provided below:

Table 11. Aliphatics and Aromatics Index for C

CONTROL	I_b	I_{ar}
Orig	22.33%	2.51%
RTFO	20.08%	2.76%
PAV	19.05%	2.69%
2PAV	20.84%	3.21%

Table 12. Aliphatics and Aromatics Index for BP

BioPhalt®	I_b	I_{ar}
Orig	16.43%	1.65%
RTFO	15.49%	1.38%
PAV	16.29%	1.62%
PAV40	15.80%	1.46%

Table 11 and Table 12 suggest that aliphatics I_B and aromatics I_{Ar} are not affected by ageing since they don't follow a trend, neither for C or BP.

Ageing Indexes are displayed in Figure IV-35 and Figure IV-36.

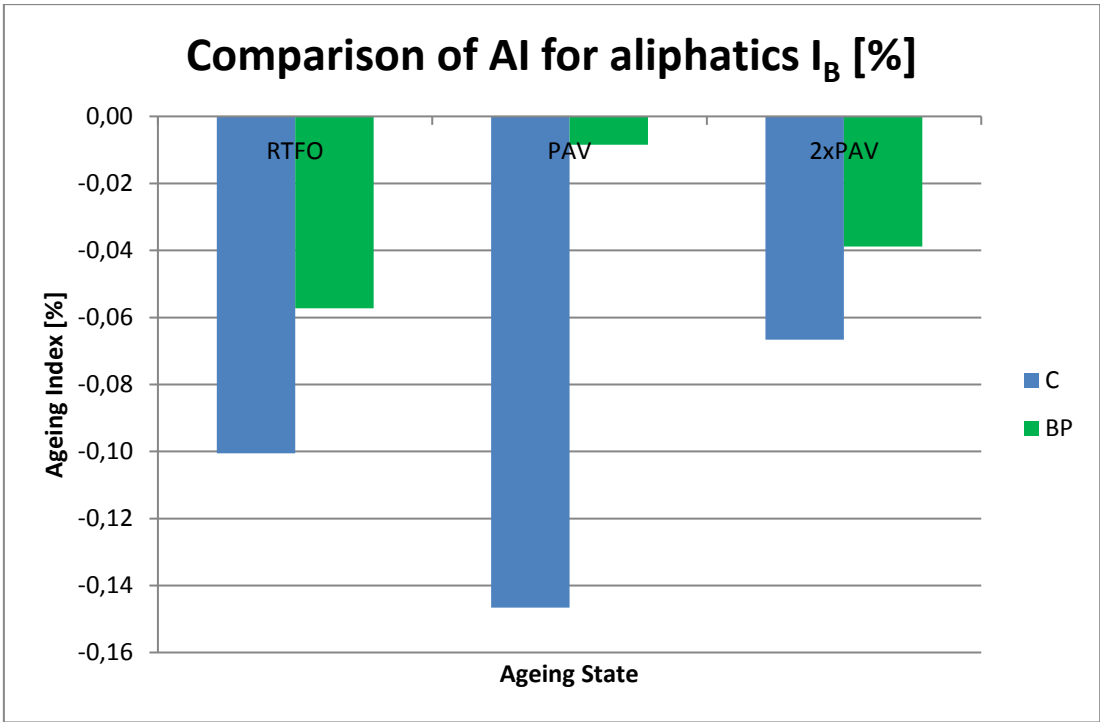


Figure IV-35 Comparison of AI for Aliphatics

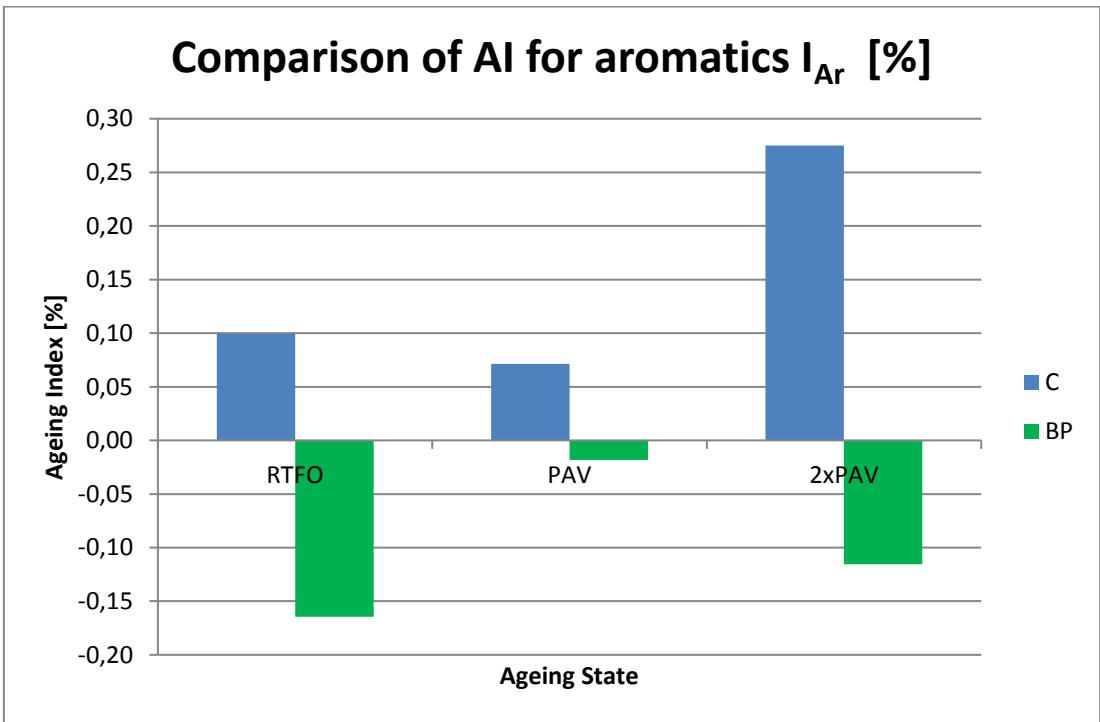


Figure IV-36. Comparison of AI for Aromatics

For the last one, SARA analysis shows a decrease of aromatics for C whereas FTIR results indicate a slight decrease of them and then an increase only at 2PAV state, that is not completely coherent. The results are acceptable since the variation is very small.

As seen from the SARA results, ageing index of aliphatics for both doesn't follow a specific trend and, in addition, these data are not totally comparable since SARA analysis includes all typologies of asphaltenes and not only the aliphatic one.

Chapter V

CONCLUSION AND RECOMMENDATIONS

Sustainability has become the key for a better future.

The utilization of non-petroleum binders for paving application have grown in the last decades. Studies have been focused on understanding and improving their characteristics. The main contribution of this research work is the evaluation of ageing effects on one of these environmental-friendly binders: the BioPhalt®.

It is a commercial product already used as pavement's surface, whose performances at long term need to be carefully investigated.

BioPhalt® was aged at both short and long-term ageing and tested to find rheological, performance-related and chemical characteristics. Result has been compared to a 50/70 neat binder, treated in the same way.

V.1 Rheological Findings

From the rheological point of view, parameters like G^* and δ were considered.

Summary of findings are provided below:

- The response of BioPhalt® to loads applied at low ω or at high temperature becomes more viscous with ageing. In fact, as G^* is more aged, it moves closer to the viscous asymptote. In addition, δ increases with ageing especially at low ω . Therefore, an unusual behaviour of BioPhalt® at high temperature is expected. The more aged the BioPhalt® is, the more viscous component there are.
- G^* of BP is generally lower than G^* of C, apart from the lower ω . This involves that the vegetable pitch is a softer bitumen.

- the viscous component of aged BP is prevalent on the elastic one since the curve of Phase angle is shifted to higher values of δ .
- At low ω , δ of BP is lower than C so the response of BP in those conditions is elastic, but δ increases with ageing and so the response to loads at low ω (high temperature) will get worse. The confirmation of that are the MSCR's results, presented in the following section.

V.2 Performance-related findings

The performance properties of binders are related to resistance to permanent deformations, to fatigue cracking and to thermal cracking.

In the first case the governing parameters are the non-recoverable creep compliance J_{nr} and the percent of recovery %R, obtained by MSCR test. The second distress is governed by the number of cycles to failure determined through a new test method: LAS test. The thermal cracking is monitored thanks the flexural stiffness S and the creep rate m , obtained with the BBR.

The results of the tests are:

- As expected, BP has a weird behaviour at high temperatures. In fact, the deformability due to accumulated deformations increases with ageing. In other words, J_{nr} of BP increases with ageing. BioPhalt® has a great capacity to recover deformations, with peaks that reach also $\approx 98\%$. In fact, the phase angle's plot, at high temperature and so low frequency, shows that BP has lower value of δ and so it is more elastic than C. Unluckily, these properties decreases with ageing. Thus, the material tends to recover less, thus to accumulate more. BP loses his elasticity with time and the viscous component is predominant. With these conditions, the problem of rutting get worse with time.

- Jnr of BioPhalt® is susceptible to ageing and it tends to increase, whereas %R of BP is more stable with ageing, but it will decrease.
- About the Fatigue cracking, Nf of BP is mostly greater than Nf of C at all levels of ageing, so it's easy stating that, at the same conditions, BP stands more than C during in-service life. The response of BioPhalt® at intermediate temperature is quite promising.
- At Low temperature, BioPhalt®'s flexural creep stiffness is more or less half the control's stiffness so it is less susceptible to ageing. From BBR's results, BioPhalt® appears to be more capable to relax stress. In fact, regarding the critical temperature, the cracking in BioPhalt® will occur at lower temperature than the C one. Thus, BP has more thermal resistance.

V.3 Chemical findings

The response of bitumen to load is related to its chemical composition. Studying the evolution with ageing of chemical properties makes the characterization of the material complete. In addition, it is an added value to the knowledge of these complex materials.

Briefly, this thesis reaches the following results:

- In BP, indexes related to oxidation, representing sulphoxide and carbonyl groups, are greater than in C. On the other hand, the Ageing Indexes don't increase with ageing. Thus, it's noticeable that they are not strongly dependent on the ageing state. Probably, those structures are already present in BP, since it is a vegetable pitch.
- The aliphatic and aromatic groups don't follow a monotonic trend with ageing, as expected. The point is that, in BioPhalt®, these groups are fewer with respect in control binder.

- SARA analysis of BioPhalt® leads to interesting results. Firstly, it has been found that BP has no saturate oil. The most abundant fraction in BP is resin whereas asphaltenes are present in a little quantity. In addition, in this vegetable pitch there is no migration among fractions during ageing.

V.4 Summary of findings and recommendations

This study has allowed to know the BioPhalt®'s behaviour well-round. From the performance findings it's possible deducing that:

- BioPhalt® has good resistance to thermal cracking at low temperatures. At those temperatures, also the PAV aged material is still viscous. The embrittlement occurs at very low temperatures, that is -21°C versus -15°C of the 50/70 binder. Thus, the material can be used in colder regions and it will resist in time.
- The number of cycles to failure of BioPhalt® are higher than the one of C, even at long term ageing. Thus, at intermediate temperatures, BP reacts better than C, also to continuous loadings.
- Some issues are observed at high temperatures for all ageing states. In fact, BioPhalt® is softer than C and its viscous component increases with ageing. So the problem of rutting will be important at both short and long term ageing. From the finding of this thesis, the utilization of BP in hot countries is discouraged.

All these results are coherent with and supported by both rheological and chemical outcomes.

V.5 Future Works

This study has been focused on the effect of ageing on non-bituminous binder, as BioPhalt®. Many areas are still needed to be further investigated. The following are the recommended areas of future researches:

- Investigate the behaviour of BioPhalt® in its non-linear viscoelastic field. From the MSCR test, a strong dependency to stress levels has been found.
- Test the material directly aged in-field and compare the results with the one from accelerated ageing to see if there are differences.
- It could be quite interesting an in-depth study of the SARA results, modifying the procedure.
- It has been found that the material preserves its viscous component at low temperatures. Another suggestion may be verifying the stability of this characteristic in time.
- Once bio-binder's results will be verified, it could be possible to go forward and study the mix-design. This new pavement will need the performance grade characterization. The last step of this process could be building a real-size road paved with different bio-binder mixtures and monitoring the evolution of its behaviour.

REFERENCES

- Yusoff, N. I. M., Jakarni, F. M., Nguyen, V. H., Hainin, M. R., & Airey, G. D. (2013). Modelling the rheological properties of bituminous binders using mathematical equations. *Construction and Building Materials*, *40*, 174–188. <https://doi.org/10.1016/j.conbuildmat.2012.09.105>
- Yusoff, N. I., Ginoux, M., Airey, G. D., & Hainin, M. R. (2012). Modelling the Linear Viscoelastic Rheological Properties of Base Bitumens. *THESIS - Nottingham University*, *22*(1), 22–37.
- Donald W. Christensen, JR., David A. Anderson, (1992). Interpretation of dynamic mechanical test data for paving grade asphalt cements. *Asphalt Paving Technology: Association of Asphalt Paving Technologists-Proceedings of the Technical Sessions* 61:67-116
- Zeng, M., Bahia, H. U., Zhai, H., Anderson, M. R., & Turner, P. (2001). Rheological modeling of modified asphalt binders and mixtures. *Proceedings of the Association of Asphalt Paving Technologists*, *70*, 403–441.
- Barco Carrión, A. J. del, Pérez-Martínez, M., Themeli, A., Lo Presti, D., Marsac, P., Pouget, S., ... Airey, G. D. (2017). Evaluation of bio-materials' rejuvenating effect on binders for high-reclaimed asphalt content mixtures. *Materiales de Construcción*, *67*(327), 1–11. <https://doi.org/10.3989/mc.2017.04516>
- Lu, X., & Isacsson, U. (2002). Effect of ageing on bitumen chemistry and rheology. *Construction and Building Materials*, *16*(1), 15–22. [https://doi.org/10.1016/S0950-0618\(01\)00033-2](https://doi.org/10.1016/S0950-0618(01)00033-2)
- Kamtornkiat Musiket; Mitchell Rosendahl; and Yunping Xi. (2016). Fracture of Recycled Aggregate Concrete under High Loading Rates. *Journal of Materials in Civil Engineering*, *25*(October), 864–870. [https://doi.org/10.1061/\(ASCE\)MT.1943-5533](https://doi.org/10.1061/(ASCE)MT.1943-5533)
- Wang, C., Wang, H., Zhao, L., & Cao, D. (2017). Experimental study on rheological characteristics and performance of high modulus asphalt binder with different modifiers. *Construction and Building Materials*, *155*, 26–36. <https://doi.org/10.1016/j.conbuildmat.2017.08.058>
- Mikhailenko, P., Bertron, A., & Ringot, E. (2016). Methods for analyzing the chemical mechanisms of bitumen aging and rejuvenation with FTIR spectrometry. *RILEM Bookseries*, *11*(February 2016), 203–214. https://doi.org/10.1007/978-94-017-7342-3_17

- Yut, I., & Zofka, A. (2011). Attenuated total reflection (ATR) fourier transform infrared (FT-IR) spectroscopy of oxidized polymer-modified bitumens. *Applied Spectroscopy*, 65(7), 765–770. <https://doi.org/10.1366/10-06217>
- Cong, P., Xu, P., & Chen, S. (2014). Effects of carbon black on the anti aging, rheological and conductive properties of SBS/asphalt/carbon black composites. *Construction and Building Materials*, 52, 306–313. <https://doi.org/10.1016/j.conbuildmat.2013.11.061>
- Kister, J. (2001). Comparison by Fourier transform infrared (FTIR) spectroscopy of different ageing techniques : Application to road bitumens Comparison by Fourier transform infrared (FTIR) spectroscopy of different ageing techniques : application to road bitumens, 80(MARCH), 483–488. [https://doi.org/10.1016/S0016-2361\(00\)00121-6](https://doi.org/10.1016/S0016-2361(00)00121-6)
- Murali Krishnan, J., & Rajagopal, K. (2003). Review of the uses and modeling of bitumen from ancient to modern times. *Applied Mechanics Reviews*, 56(2), 149. <https://doi.org/10.1115/1.1529658>
- Lu, X., & Isacsson, U. (2002). Effect of ageing on bitumen chemistry and rheology. *Construction and Building Materials*, 16(1), 15–22.
- Feng, Z. G., Wang, S. J., Bian, H. J., Guo, Q. L., & Li, X. J. (2016). FTIR and rheology analysis of aging on different ultraviolet absorber modified bitumens. *Construction and Building Materials*, 115, 48–53. <https://doi.org/10.1016/j.conbuildmat.2016.04.040>
- Mills-Beale, J., You, Z., Fini, E., Zada, B., Lee, C. H., & Yap, Y. K. (2014). Aging Influence on Rheology Properties of Petroleum-Based Asphalt Modified with Biobinder. *Journal of Materials in Civil Engineering*, 26(2), 358–366. [https://doi.org/10.1061/\(ASCE\)MT.1943-5533.0000712](https://doi.org/10.1061/(ASCE)MT.1943-5533.0000712)
- Hofko, B., Alavi, M. Z., Grothe, H., Jones, D., & Harvey, J. (2017). Repeatability and sensitivity of FTIR ATR spectral analysis methods for bituminous binders. *Materials and Structures/Materiaux et Constructions*, 50(3), 1–15. <https://doi.org/10.1617/s11527-017-1059-x>
- Canestrari, F., & Editors, M. N. P. (2014). *8th International RILEM Symposium on Testing and Characterization of Sustainable and Innovative Bituminous Materials, SIB 2015. International Journal of Pavement Research and Technology* (Vol. 7). <https://doi.org/10.1007/978-94-017-7342-3>
- Ksaibati, K., & Erickson, R. (2017). Khaled Ksaibati Ryan Erickson Dept . of Civil and Architectural Engineering P . O . Box 3295 University Station Laramie , Wyoming 82071-3295, (February).
- EN 14771. (2012). Bitumen and bituminous binders — Determination of the flexural creep stiffness — Bending Beam Rheometer (BBR), 21.

- AASHTO. (2014). Standard Method of Test for Estimating Damage Tolerance of Asphalt Binders Using the Linear Amplitude Sweep Standard Method of Test for Estimating Damage Tolerance of Asphalt Binders Using the Linear Amplitude Sweep, *12*(August).
- Jafari, M., & Babazadeh, A. (2016). Evaluation of polyphosphoric acid-modified binders using multiple stress creep and recovery and linear amplitude sweep tests. *Road Materials and Pavement Design*, *17*(4), 859–876.
<https://doi.org/10.1080/14680629.2015.1132631>
- Ameri, M., Nowbakht, S., Molayem, M., & Mirabimoghaddam, M. H. (2016). A study on fatigue modeling of hot mix asphalt mixtures based on the viscoelastic continuum damage properties of asphalt binder. *Construction and Building Materials*, *106*, 243–252. <https://doi.org/10.1016/j.conbuildmat.2015.12.066>
- Subhy, A., & Presti, D. Lo. (2017). Fatigue and Healing Properties of Low Environmental Impact Rubberized Bitumen for Asphalt Pavement. *Coatings*, *7*(5), 66. <https://doi.org/10.3390/coatings7050066>
- Subhy, A. (2017). Advanced analytical techniques in fatigue and rutting related characterisations of modified bitumen: Literature review. *Construction and Building Materials*, *156*, 28–45.
<https://doi.org/10.1016/j.conbuildmat.2017.08.147>
- Xu, G., Wang, H., & Zhu, H. (2017). Rheological properties and anti-aging performance of asphalt binder modified with wood lignin. *Construction and Building Materials*, *151*, 801–808.
<https://doi.org/10.1016/j.conbuildmat.2017.06.151>
- ASTM-D7405. (2015). Standard Test Method for Multiple Stress Creep and Recovery (MSCR) of Asphalt Binder Using a Dynamic Shear Rheometer, *i*, 7–10. <https://doi.org/10.1520/D7405-15.2>
- D'Angelo, J. A. (2009). The relationship of the mscr test to rutting. *Road Materials and Pavement Design*, *10*(2009), 61–80.
<https://doi.org/10.1080/14680629.2009.9690236>
- Subhy, A. (2017). Advanced analytical techniques in fatigue and rutting related characterisations of modified bitumen: Literature review. *Construction and Building Materials*, *156*(December), 28–45.
<https://doi.org/10.1016/j.conbuildmat.2017.08.147>
- Luo, W., Zhang, Y., & Cong, P. (2017). Investigation on physical and high temperature rheology properties of asphalt binder adding waste oil and polymers. *Construction and Building Materials*, *144*, 13–24.
<https://doi.org/10.1016/j.conbuildmat.2017.03.105>

- Yang, S. H., & Suciptan, T. (2016). Rheological behavior of Japanese cedar-based biobinder as partial replacement for bituminous binder. *Construction and Building Materials*, *114*, 127–133. <https://doi.org/10.1016/j.conbuildmat.2016.03.100>
- Yang, X., & You, Z. (2015). High temperature performance evaluation of bio-oil modified asphalt binders using the DSR and MSCR tests. *Construction and Building Materials*, *76*, 380–387. <https://doi.org/10.1016/j.conbuildmat.2014.11.063>
- Zhang, J., Simate, G. S., Hu, X., Souliman, M., & Walubita, L. F. (2017). Impact of recycled asphalt materials on asphalt binder properties and rutting and cracking performance of plant-produced mixtures. *Construction and Building Materials*, *155*, 654–663. <https://doi.org/10.1016/j.conbuildmat.2017.08.084>
- Zhang, J., Walubita, L. F., Faruk, A. N. M., Karki, P., & Simate, G. S. (2015). Use of the MSCR test to characterize the asphalt binder properties relative to HMA rutting performance - A laboratory study. *Construction and Building Materials*, *94*, 218–227. <https://doi.org/10.1016/j.conbuildmat.2015.06.044>
- Zeng, M., Pan, H., Zhao, Y., & Tian, W. (2016). Evaluation of asphalt binder containing castor oil-based bioasphalt using conventional tests. *Construction and Building Materials*, *126*, 537–543. <https://doi.org/10.1016/j.conbuildmat.2016.09.072>
- Wen, H., Bhusal, S., & Wen, B. (2012). Laboratory evaluation of waste cooking oil-based bioasphalt as sustainable binder for hot-mix asphalt. *Alternative Binders for Sustainable Asphalt Pavements, Transportation Research Circular, No. E-C165, Transportation Research Board, National Academies, Washington, DC*, *25*(10), 49–60. [https://doi.org/10.1061/\(ASCE\)MT.1943-5533.0000713](https://doi.org/10.1061/(ASCE)MT.1943-5533.0000713)
- Shirodkar, P., Mehta, Y., Nolan, A., Dahm, K., Dusseau, R., & McCarthy, L. (2012). Characterization of creep and recovery curve of polymer modified binder. *Construction and Building Materials*, *34*, 504–511. <https://doi.org/10.1016/j.conbuildmat.2012.02.018>
- BSI Standards Publication Bitumen and bituminous binders — Sampling bituminous binders. (2012).
- ASTM D 6373. (1999). Standard Specification for Performance Graded Asphalt Binder. *Annual Book of ASTM Standards*, *04*, 3–5. <https://doi.org/10.1520/D6373-13.2>
- Weigel, S., & Stephan, D. (2017). Relationships between the chemistry and the physical properties of bitumen. *Road Materials and Pavement Design*, *0*(0), 1–15. <https://doi.org/10.1080/14680629.2017.1338189>

- Bissada, K. K. A., Tan, J., Szymczyk, E., Darnell, M., Mei, M., & Zhou, J. (2016). Group-type characterization of crude oil and bitumen. Part I: Enhanced separation and quantification of saturates, aromatics, resins and asphaltenes (SARA). *Organic Geochemistry*, *95*, 21–28. <https://doi.org/10.1016/j.orggeochem.2016.02.007>
- Handle, F., Harir, M., Füssl, J., Koyun, A. N., Grosseegger, D., Hertkorn, N., ... Grothe, H. (2017). Tracking Aging of Bitumen and Its Saturate, Aromatic, Resin, and Asphaltene Fractions Using High-Field Fourier Transform Ion Cyclotron Resonance Mass Spectrometry. *Energy and Fuels*, *31*(5), 4771–4779. <https://doi.org/10.1021/acs.energyfuels.6b03396>
- Selucky, M. L. (1983). Quantitative-Analysis of Coal-Derived Liquids by Thin-Layer Chromatography with Flame Ionization Detection. *Analytical Chemistry*, *55*(1), 141–143. <https://doi.org/10.1021/ac00252a036>
- Airey, G. D., Singleton, T. M., & Collop, A. C. (2002). Properties of Polymer Modified Bitumen after Rubber-Bitumen Interaction. *Journal of Materials in Civil Engineering*, *14*(4), 344–354. [https://doi.org/10.1061/\(ASCE\)0899-1561\(2002\)14:4\(344\)](https://doi.org/10.1061/(ASCE)0899-1561(2002)14:4(344))
- Borghi, A., Jiménez del Barco Carrión, A., Lo Presti, D., & Giustozzi, F. (2017). Effects of Laboratory Aging on Properties of Biorejuvenated Asphalt Binders. *Journal of Materials in Civil Engineering*, *29*(10), 04017149. [https://doi.org/10.1061/\(ASCE\)MT.1943-5533.0001995](https://doi.org/10.1061/(ASCE)MT.1943-5533.0001995)